

**Modulations of Receptor Activity of
Orphan G Protein-coupled Receptor
Mas by C-terminal GFP Tagging and
Expression Level**

SUN, Jingxin

**A Thesis Submitted in Partial Fulfillment
of the Requirements for the Degree of
Doctor of Philosophy
In
Biochemistry (Medicine)**

April 2009

UMI Number: 3392256

All rights reserved

INFORMATION TO ALL USERS

The quality of this reproduction is dependent upon the quality of the copy submitted.

In the unlikely event that the author did not send a complete manuscript and there are missing pages, these will be noted. Also, if material had to be removed, a note will indicate the deletion.



UMI 3392256

Copyright 2010 by ProQuest LLC.

All rights reserved. This edition of the work is protected against unauthorized copying under Title 17, United States Code.



ProQuest LLC
789 East Eisenhower Parkway
P.O. Box 1346
Ann Arbor, MI 48106-1346

Thesis/Assessment Committee

Chair of Committee

Professor Wan Chi-Cheong

Thesis Supervisor

Professor Cheung Wing-Tai

Committee Member

Professor Wan Chi-Cheong

Professor Ko Wing-Hung

External Examiner

Professor Yung Kin-Lam

Abstract

Orphan G protein-coupled receptor (GPCR) mas was initially isolated from a human epidermal carcinoma. Previous study from our lab identified a surrogate ligand---MBP7 (mas binding peptide 7) for mas, and suggested that GFP tagging might affect the receptor activity of mas. In this project, three stable CHO cell lines expressing native mas, mas-GFP and mas-(Gly₁₀Ser₅)-GFP were used to characterize receptor activity of mas.

In a phage binding assay, phage clone (3p5A190) expressing a surrogate mas ligand displayed punctate binding and were internalized in cell expressing native mas and GFP-tagged variants. However, the number of bound and internalized phages in cells expressing mas-GFP was substantially less than the cells expressing mas-(Gly₁₀Ser₅)-GFP and native mas. In parallel, biotinylation experiment quantitatively showed that the extent of mas-(Gly₁₀Ser₅)-GFP translocation was higher than that of mas-GFP. Consistently, cells expressing mas-(Gly₁₀Ser₅)-GFP and native mas showed a rapid and sustained increase of intracellular calcium levels upon MBP7 stimulation. By contrast, cells expressing mas-GFP only response to higher concentration of MBP7 challenge and showed a delayed increase of intracellular calcium level. Moreover, cells expressing native mas had a higher proportion (80%) of cells responsive to MBP7 stimulation; in contrast to only 10~20% of cells expressing mas fusion proteins.

MBP7-like motif was identified in human facilitative GLUT1 and GLUT7 indicating that mas might interact with glucose transporter (GLUT) and regulate cellular glucose uptake. GLUT4 was found to be expressed endogenously in the CHO cell by RT-PCR, but expression of insulin receptor was not detectable. Although no statistical difference was detected in basal glucose uptake among control cells Vc0M80 and cells with different levels of mas expression, cells expressing mas-(Gly₁₀Ser₅)-GFP showed a high glucose uptake in response to insulin. Furthermore, basal 2-DOG uptake in Mc0M80 cells was not affected by pretreatment with various kinase inhibitors or transient expression of Rho variants. By contrast, MBP7 was found to induce a significant elevation of glucose uptake specifically in Mc0M80 cells transiently transfected with GLUT1.

To summarize, direct GFP tagging at the C-terminus of mas decreased its interactions with ligand and downstream signaling molecules. Partial recovery of mas receptor activity by adding a peptide linker was confirmed by phage binding, membrane fusion protein translocation and calcium response. In addition, mas was possibly coupled with GLUT1 to affect cellular glucose uptake via signaling pathways yet to be fully characterized.

摘要

寡 G 蛋白偶聯受體 (GPCR) mas 於人表皮癌中首次分離得到。以往本實驗室研究獲得一個 mas 代用配體---MBP7 (mas 結合配體 7) 並發現 GFP 標記可能會影響 mas 的受體活性。為進一步研究 mas 的受體活性，本實驗應用了 CHO 細胞構建的三條穩定細胞系, 其分別表達 mas, mas-GFP 和 mas-(Gly₁₀Ser₅)-GFP。

在噬菌體結合實驗中，表達 mas 代用配體的噬菌體克隆 (3p5A190) 與表達 mas 或者 GFP 標記的不同 mas 融合蛋白的細胞發生點狀結合並被內在化。但是，在表達 mas-GFP 的細胞中結合和內在化的噬菌體量比在表達 mas-(Gly₁₀Ser₅)-GFP 或者 mas 的細胞中要少。同時，生物素實驗定量檢測到 MBP7 引起的細胞膜 mas-(Gly₁₀Ser₅)-GFP 轉移比 mas-GFP 要多。此外，表達 mas 或者 mas-(Gly₁₀Ser₅)-GFP 的細胞受到 MBP7 刺激之後可產生迅速及持續的細胞內鈣離子濃度升高。而表達 mas-GFP 的細胞僅對高濃度的 MBP7 刺激有反應；由此引起的細胞內鈣離子濃度升高比較緩慢。此外，表達 mas 的細胞相對於表達 mas 融合蛋白的細胞有更高的反應率，達到 80%；而後者僅為 10%到 20%。

MBP7 的類似蛋白基序在人糖轉運蛋白 1 和糖轉運蛋白 7 中被發現提示 mas 有可能與糖轉運蛋白發生作用並調節細胞糖攝取。RT-PCR 結果顯示 CHO 細胞表達糖轉運蛋白 4, 但是卻未發現胰島素受體表達。儘管針對基礎糖攝取量的統計學分析並未在對照組細胞 Vc0M80 和 mas 表達量不同的細胞中發現顯著性差異，表達 mas-(Gly₁₀Ser₅)-GFP 的細胞系在胰島素刺激下的糖攝入量有顯著升高。此外，Mc0M80

的基礎糖攝取量並不受各種激酶抑制劑預處理或者不同 RhoA 質粒瞬間轉染的影響。2-DOG 攝取實驗還意外發現 MBP7 可以特異性升高暫態轉染糖轉運蛋白 1 的 Mc0M80 細胞的糖攝取量。

綜上所述，GFP 直接在 mas 的 C 端標記會減少 mas 與其配體及其下游信號傳導分子的相互作用。而加入肽連接體可以恢復 mas 活性，並由噬菌體結合，膜融合蛋白轉運及鈣釋放實驗證明之。mas 可能與糖轉運蛋白 1 藕聯而影響細胞糖攝取，且其信號傳導通路尚有待進壹步確定。

Acknowledgement

After writing up the thesis, I recall the memory of three and a half years of study and life in Hong Kong, in sc194 with my supervisor and dear friends. Firstly, I would like to express my deepest and most sincere gratitude to my supervisor Prof. Cheung Wing-Tai. I still bear in mind how carefully he revised my abstracts and slides for departmental seminar and how thoroughly he trained me up for good presentation in public. To be honest, I learn a lot from Prof. Cheung Wing-Tai as to be a genuine researcher and scientist which are comprehensive planning for experiments, cautious interpretation on data and so on.

I am also very thankful to my colleagues in sc194 such as Lin Wen Zhen, Sherman Cheng, Zhao Qi, Gladys Teng, Stone Zhu, Li Zhou Fang, Jiang Li Li, Wang Da Kui, Qi Wei, Shirley Chan and Elaine Chan. They constantly support and encourage me making me feel at home. Here, I'm especially grateful to Gladys Teng who shared with me a lot of personal experience on molecular experiments. I'm also very appreciated with the technical support from Prof. Ko Wing-Hung and Wallace Yip in intracellular calcium ion concentration ($[Ca^{2+}]_i$) measurement and Prof. Ho Yuan-Yuan as well as Peggy Law in 2-deoxy-D-glucose uptake assay. I should also thank for the generous gift of Prof. Wong Yung-Hou for Rho constructs and Prof. Yousuke Ebina for GLUT constructs.

I would like to thank Prof. Ko Wing-Hung and Prof. Wan Chi-Cheong of the Chinese University of Hong Kong, as well as Prof. Yung Kin-Lam of Hong Kong Baptist University for thesis review and constructive suggestion.

I would like to express my thanks to financial support of Chinese University of Hong Kong which made my study and life here without burden.

Last but not the least, I wish to give my greatest loving thankfulness to my parents and my husband Tian Feng. Their continuous love and support are the most powerful strength in my pursuing of PhD degree. Thanks again to my beloved Tian Feng for his consideration and forgiveness in my study and life.

Table of contents

| | |
|----------------------------------|------|
| Thesis/Assessment Committee..... | i |
| Abstract (English)..... | ii |
| Abstract (Chinese)..... | iv |
| Acknowledgement..... | vi |
| Table of contents..... | viii |
| List of Tables..... | xii |
| List of Figures..... | xiii |
| List of Abbreviations..... | xv |

Chapter 1 General Introduction

| | |
|--|----|
| 1.1 Characterization of GPCR | 1 |
| 1.2 Identification of mas oncogene..... | 4 |
| 1.3 Cell and tissue distribution of mas..... | 4 |
| 1.4 Mas homology among species..... | 5 |
| 1.5 Putative structure of mas..... | 13 |
| 1.6 GPCR signaling pathway..... | 13 |
| 1.7 Candidates of mas ligand..... | 19 |
| 1.8 Interaction of GPCR and glucose transporter..... | 20 |
| 1.9 Aims of study..... | 22 |

Chapter 2 Construction and Expression of Mas-(Gly₁₀Ser₅)-GFP Fusion Protein

| | |
|-----------------------|----|
| 2.1 Introduction..... | 24 |
|-----------------------|----|

| | | |
|-------|--|----|
| 2.1.1 | Green fluorescent protein..... | 24 |
| 2.1.2 | mas-(Gly ₁₀ Ser ₅)-GFP chimeras..... | 24 |
| 2.2 | Materials and Methods..... | 25 |
| 2.2.1 | Materials | 25 |
| 2.2.2 | Methods..... | 27 |
| 2.3 | Results..... | 41 |
| 2.3.1 | Preparation of mas-oligo-GFP construct | 41 |
| 2.3.2 | DNA and protein sequences of mas-(Gly ₁₀ Ser ₅)-GFP | 42 |
| 2.3.3 | Confocal microscopy analysis | 49 |
| 2.3.4 | Immunoprecipitation and Western Blot analysis..... | 49 |
| 2.4 | Discussion | 53 |

Chapter 3 Functional Characterization of Mas Protein

| | | |
|-------|--|----|
| 3.1 | Introduction..... | 55 |
| 3.2 | Materials and Methods..... | 55 |
| 3.2.1 | Materials | 55 |
| 3.2.2 | Methods..... | 57 |
| 3.3 | Results..... | 63 |
| 3.3.1 | Phage binding assay..... | 63 |
| 3.3.2 | Biotinylation assay..... | 66 |
| 3.3.3 | Intracellular calcium ion concentration ([Ca ²⁺] _i) measurement..... | 73 |
| 3.4 | Discussion | 89 |
| 3.4.1 | Phage binding assay..... | 89 |

| | | |
|-------|---|----|
| 3.4.2 | Biotinylation assay | 90 |
| 3.4.3 | Calcium ion concentration ($[Ca^{2+}]_i$) measurement | 91 |

Chapter 4 Cellular Glucose Uptake in Mas expressing cells

| | | |
|-------|--|-----|
| 4.1 | General introduction | 96 |
| 4.1.1 | Glucose Transporter (GLUT) type and tissue distribution | 96 |
| 4.1.2 | Classification of GLUTs | 96 |
| 4.1.3 | Function of GLUTs..... | 97 |
| 4.1.4 | Purpose of study..... | 97 |
| 4.2 | Materials and Methods..... | 100 |
| 4.2.1 | Materials | 100 |
| 4.2.2 | Methods..... | 101 |
| 4.3 | Results..... | 113 |
| 4.3.1 | Screening of GLUT type in CHO cells..... | 113 |
| 4.3.2 | Examination of IR in CHO cells..... | 120 |
| 4.3.3 | Standardization of working condition for 2-DOG uptake assay..... | 120 |
| 4.3.4 | Glucose uptake in Vc0M80, Mc0M80 and CHO cells expressing mas fusion variants..... | 124 |
| 4.3.5 | Evaluation of mas effect on glucose uptake | 127 |
| 4.3.6 | RhoA effect on mas regulated glucose uptake..... | 127 |
| 4.3.7 | Pathways involved in glucose uptake of Mc0M80 cells..... | 132 |
| 4.3.8 | Effect of mas on GLUT1-mediated glucose uptake | 135 |
| 4.4 | Discussion | 139 |

| | | |
|--|---|------------|
| 4.4.1 | Screening of GLUT and IR in CHO cells..... | 139 |
| 4.4.2 | Standardization of 2-DOG uptake assay..... | 140 |
| 4.4.3 | Glucose uptake in the absence or presence of mas | 140 |
| 4.4.4 | RhoA effect on mas-MBP7 regulated glucose uptake..... | 142 |
| 4.4.5 | Kinase inhibitors effect on mas-MBP7 mediated glucose uptake .. | 142 |
| 4.4.6 | Mas effect on GLUT1-mediated glucose uptake | 143 |
| Chapter 5 General Discussion..... | | 144 |
| Reference | | 150 |

Appendices

| | | |
|------------|--------------------------------------|-----|
| Appendix 1 | Composition of media | 172 |
| Appendix 2 | Composition of buffer solutions..... | 174 |
| Appendix 3 | Bacterial Strain..... | 179 |
| Appendix 4 | Sequences of primers | 180 |
| Appendix 5 | Sequences of constructs | 181 |
| Appendix 6 | Published abstract..... | 184 |

List of Tables

| | | |
|-----------|--|-----|
| Table 1.1 | Organ distribution of mas mRNA..... | 6 |
| Table 1.2 | Proteins that shared homology with the mas-binding consensus motif 1..... | 21 |
| Table 4.1 | Chromosomal localization and distribution of GLUT..... | 98 |
| Table 4.2 | Tissue distribution and function of GLUT..... | 99 |
| Table 4.3 | Information of GLUT and IR primers for screening | 103 |
| Table 4.4 | PCR condition for GLUT and IR screening | 105 |

List of Figures

| | | |
|------------|---|----|
| Figure 1.1 | Classifications of GPCR using phylogenetic analysis..... | 3 |
| Figure 1.2 | Multiple sequence alignment of the rat, mouse and human mas DNA sequences..... | 8 |
| Figure 1.3 | Multiple sequence alignment of rat, mouse and human mas amino acid sequences..... | 12 |
| Figure 1.4 | Predicted secondary structure of mas proto-oncogene..... | 16 |
| Figure 1.5 | GPCR signaling pathway..... | 18 |
| Figure 2.1 | Construction of mas-(Gly ₁₀ Ser ₅)-GFP by overlapping PCR..... | 29 |
| Figure 2.2 | Vector map of pEGFP-N1..... | 30 |
| Figure 2.3 | Overlapping PCR for mas-oligo-GFP..... | 43 |
| Figure 2.4 | Multiple sequence alignment of mas-oligo-GFP..... | 44 |
| Figure 2.5 | Protein sequence of mas-(Gly ₁₀ Ser ₅)-GFP..... | 48 |
| Figure 2.6 | Intracellular localization of GFP, mas-(Gly ₁₀ Ser ₅)-GFP and mas-GFP fusion proteins..... | 51 |
| Figure 2.7 | Stable expressions of different mas fusion proteins..... | 52 |
| Figure 3.1 | Biotinylation strategy 1 using sulfo-NHS-biotin reagent..... | 60 |
| Figure 3.2 | Biotinylation strategy 2 using sulfo-NHS-SS-biotin reagent..... | 61 |
| Figure 3.3 | Phage binding assay..... | 65 |
| Figure 3.4 | Biotinylation assay..... | 69 |
| Figure 3.5 | Intracellular calcium ion concentration ([Ca ²⁺] _i) measurement for cells expressing mas fusion proteins or native mas | 75 |
| Figure 3.6 | Quantification of calcium assay for cells expressing | |

| | | |
|-------------|--|-----|
| | mas fusion proteins or native mas..... | 78 |
| Figure 3.7 | Responsive ratios in calcium ion concentration ($[Ca^{2+}]_i$) measurement | 81 |
| Figure 3.8 | Intracellular calcium ion concentration ($[Ca^{2+}]_i$) measurement on cells with various mas transcription levels..... | 83 |
| Figure 3.9 | Quantification of calcium assay for cells with various mas expression levels..... | 86 |
| Figure 3.10 | Fractions of cells responsive to MBP7..... | 88 |
| Figure 3.11 | GPCR activated increase of $[Ca^{2+}]_i$ | 93 |
| Figure 4.1 | Vector map of pcDNA 3.1+ RhoA plasmid variants..... | 111 |
| Figure 4.2 | Vector map of pCX 2-Glut1 myc..... | 112 |
| Figure 4.3 | Positive control of GLUT fragment amplification..... | 114 |
| Figure 4.4 | GLUT screening in non-transfected CHO-K1 cell..... | 115 |
| Figure 4.5 | Multiple alignment of PCR products with rat GLUT4..... | 117 |
| Figure 4.6 | Multiple alignment of PCR products with rat GLUT1..... | 119 |
| Figure 4.7 | Insulin receptor (IR) screening in native CHO cell..... | 121 |
| Figure 4.8 | Standardization of working conditions for 2-DOG uptake assay..... | 122 |
| Figure 4.9 | Normalization of 2-DOG uptake with protein amount..... | 123 |
| Figure 4.10 | 2-DOG uptake in Vc0M80, Mc0M80 and CHO cells expressing mas fusion variants | 126 |
| Figure 4.11 | Glucose uptake in cells of various mas expression levels | 130 |
| Figure 4.12 | RhoA effect on glucose uptake in Mc0M80 cells..... | 131 |

| | | |
|-------------|--|-----|
| Figure 4.13 | Effect of protein kinase on glucose uptake in Mc0M80 cells..... | 134 |
| Figure 4.14 | Peptide sequence alignment of human facilitative GLUT1 and GLUT7..... | 136 |
| Figure 4.15 | GLUT1-mediated glucose uptake..... | 138 |

List of Abbreviations

| | |
|-------------------|---------------------------------------|
| APS | Ammonium persulfate |
| BCA | Bi-cinchoninic acid |
| BCPIP | 5-bromo-4-cholor-3-indolyl-phosphate |
| BSA | Bovine serum albumin |
| bp | Base pair |
| CaCl ₂ | Calcium chloride |
| CHO | Chinese hamster ovary cell |
| CMV | Cytomegalovirus |
| CO ₂ | Carbon dioxide |
| Dhfr | Dihydrofolate reductase |
| DMEM | Dulbecco's modified eagle medium |
| DMSO | Dimethylsulfoxide |
| DNA | Deoxyribonucleic acid |
| dNTP | Deoxynucleotide triphosphate |
| DTT | Dithiothreitol |
| EB | Ethidium bromide |
| EDTA | Ethylenediaminetetraacetic acid |
| EGFP | Enhanced green fluoresenct proteins |
| EXPASY | Exptert protein analysis system |
| FBS | Fetal bovine serum |
| FITC | Fluorescien isothyocyanate |
| FRET | Fluorescent resonance energy transfer |

| | |
|-------------------|--|
| GAPDH | Glyceraldehyde-3-phosphate dehydrogenase |
| GPCR | G protein-coupled receptor |
| GFP | Green fluorescent protein |
| HT | Hypoxanthine thiamine |
| IMDM | Iscove's modified DMEM medium |
| kDa | Kilodalton |
| LB | Luria Bertani medium |
| MBP7 | Mas binding peptide 7 |
| Mc0M0 | CHO Dhfr ⁻ cells clone number 0 stably expressing pFRSV-mas |
| Mc0M80 | CHO Dhfr ⁻ cells clone number 0 stably over-expressing pFRSV-mas in the presence of 80 μ M MTX |
| Mc7M0 | CHO Dhfr ⁻ cells clone number 7 stably expressing pFRSV-mas |
| Mc7M80 | CHO Dhfr ⁻ cells clone number 7 stably over-expressing pFRSV-mas in the presence of 80 μ M MTX |
| Mc35M0 | CHO Dhfr ⁻ cells clone number 35 stably expressing pFRSV-mas |
| Mc35M4 | CHO Dhfr ⁻ cells clone number 35 stably over-expressing pFRSV-mas in the presence of 4 μ M MTX |
| Mc35M80 | CHO Dhfr ⁻ cells clone number 35 stably over-expressing pFRSV-mas in the presence of 80 μ M MTX |
| MgCl ₂ | Magnesium chloride |
| MCS | Multiple cloning site |
| Mrg | Mas-related gene |
| MTX | Metotrexate |

| | |
|----------|---|
| NaCl | Sodium chloride |
| NBT | Nitroblue tetrazolium chloride |
| NHS | N-Hydroxysuccinimide |
| P/S | Penicillin and Streptomycin |
| PAGE | Polyacrylamide gel electrophoresis |
| PBS | Phosphate buffer saline |
| PCR | Polymerase chain reaction |
| PEG/NaCl | Polyethyleneglycol/sodium chloride |
| PMSF | Phenyl methyl sulphonyl fluoride |
| RNA | Ribonucleic acid |
| RNase | Ribonuclease |
| SDS | Sodium dodecyl sulfate |
| SOBAG | SOB agar with ampicillin and glucose |
| TAE | Tris acetate EDTA buffer |
| TEMED | N,N,N,N,-Tetramethyl ethylene diamine |
| Vc0M80 | CHO Dhfr ^r cells clone number 0 stably over-expressing pFRSV in the presence of 80 μ M MTX |

Chapter 1

General Introduction

G proteins are guanine nucleotide binding proteins. They are consisted of three heterotrimeric subunits--- α , β and γ (Marrari et al., 2007). G protein-coupled receptors (GPCRs) are a huge family of proteins which couple to G proteins to transfer the downstream signals in cells. They share a structure of seven trans-membrane regions with an extracellular N terminus and an intracellular C terminus (Baldwin, 1993). Mas protein is a proto-oncogene which also belongs to the GPCR family (Young et al., 1986).

1.1 Characterization of GPCR

The G protein-coupled receptors (GPCRs) form one of the largest protein families in the mammalian genome (Lander et al., 2001; Venter et al., 2001). There are two main characteristics for GPCR. The first one is that they contain seven α -helices that span across the cell membrane in a counter-clockwise manner. The second characteristic is that GPCRs transfer the downstream signaling via interaction with G proteins. The GPCR superfamily is classified into five main groups based on phylogenetic analysis on human genome. They are glutamate, rhodopsin, adhesion, frizzled/taste2, and secretin (Figure 1.1). Among them, rhodopsin family is the largest one and divided into four sub-groups with thirteen branches (Fredriksson et al., 2003). Mas and mas-related receptors are included in the δ -group of rhodopsin receptors and show high homology with each other (Dong et al., 2001).

Figure 1.1 Classifications of GPCR using phylogenetic analysis. GPCRs are divided into five main groups: glutamate, rhodopsin, adhesion, frizzled/taste2, and secretin. The rhodopsin family is further divided into α , β , γ and δ subgroups. Mas together with mas-related receptors constituted the largest branch of rhodopsin family. The location of mas in the phylogenetic tree was highlighted in blue color [compiled and modified from (Fredriksson et al., 2003)]

1.2 Identification of mas oncogene

Mas was identified as a proto-oncogene from human epidermoid carcinoma (Young et al., 1986), leukemia (Janssen et al., 1988) and ovarian carcinoma (van 't Veer et al., 1988). It was predicted to encode a membrane protein of 325 amino acids with a molecular mass of 38 kDa. It contains seven putative hydrophobic trans-membrane helices. Both the amino- and the carboxyl- ends are hydrophilic (Young et al., 1986).

In a tumorigenicity assay, mas could induce tumor formation in the nude mice. In a foci formation assay, NIH 3T3 cells transfected with mas formed the foci which appears as excessively high cell density island (van 't Veer et al., 1988). Analysis on mas sequence indicated that there is a 5'-upstream rearrangement of mas gene, but no mutation in the coding regions (Young et al., 1986).

1.3 Cell and tissue distribution of mas

In situ hybridization detected high expression level of mas mRNA in rat neuronal cells in the forebrain regions (Table 1.1) such as dentate gyrus, piriform cortex, hippocampus and olfactory as well as a relatively weak expression in neocortex, thalamus and frontal lobe (Janssen et al., 1988; van 't Veer et al., 1988; Bunnemann et al., 1990; Hanley et al., 1990; Kumar et al., 1996; Dong et al., 2001). Mas was also found in the retinal pigment epithelial (RPE) cells of rhesus macaque (Xu et al., 2000; Chalmers & Behan, 2002). Apart from the expression in nervous system and retina, mas was detected in Leydig and

Sertoli cells in mouse testis aging from 18 days old to 6 months, which indicated a possible role of mas in testis maturation and function (Alenina et al., 2002).

Mas gene is located in different chromosomal positions in different species. In rat, mas gene is located between the region of 1q11 and 1q12 while in mouse its position ranges from 17a to 17c. In human, mas is mapped between q24 to q27 of chromosome 6 which is often rearranged in its distal end in malignant cells, implying that mas may involve in the pathogenesis of some tumors (Rabin et al., 1987; Lander et al., 2001; Venter et al., 2001). Both in mouse and rat, mas lies closely to a gene with the name of insulin-like growth factor 2 receptor (IGF2R) which is lost in 70% of human hepatocellular tumors (Andrawis et al., 1992).

1.4 Mas homology among species

Mas sequence is highly conserved among various species. There are over 84% and 88% homologies in DNA and amino acid sequences, respectively, of mas among rat, mouse and human (Figure 1.2 & Figure 1.3).

Table 1.1 Organ distribution of mas mRNA

| | In situ Hybridization | RNase Protection assay | Young rat | Adult rat |
|----------------------|------------------------------|-------------------------------|------------------|------------------|
| Forebrain | Detectable | +++++ | +++++ | +++++ |
| Cerebrum | Detectable | +++++ | +++++ | ++ |
| Testis | NA | ++++ | ++ | +++++ |
| Heart | NA | + | ++ | + |
| <i>Kidney</i> | NA | + | ++ | + |

“+” to “+++++” indicated increased transcription levels of mas mRNA. “NA” meant no available data. [Compiled from (Bunnemann et al., 1990; Metzger et al., 1995)]

Figure 1.2 Multiple sequence alignment of the rat, mouse and human mas DNA sequences. The open reading frames of rat and mouse mas sequences contain 975 nucleotides while human mas has 978 with additional "CTG" at position 56. NCBI accession numbers of rat, mouse and human mas DNA sequence are J03823, AK 030261 and BC069142 respectively. * represented identical nucleotide.

Rat TATCTGCTGACAGCCATCAGTGTGGAGAGATGCCTTTTCAGTCCTCTACCCCATCTGGTAC 417

Mouse TATCTGCTGACAGCCATCAGTGTGGAGAGGTGCCTATCGGTCCTCTACCTATATGGTAC 417

Human TATCTGCTGACGGCCATTAGTGTGGAGAGGTGCCTGTCAGTCCTTTACCCCATCTGGTAC 420

***** * * * * *

Rat AGATGTCACCGCCCCAAGCACCAGTCGGCATTTCGTCTGTGCCCTCCTGTGGGCACTTTCA 477

Mouse ACTAGCCACCGCCCCAAGCACCAGTCAGCATTTCGTCTGTGCCCTTCTGTGTGCACTTTTCG 477

Human CGATGCCATCGCCCCAAGTACCAGTCGGCATTGGTCTGTGCCCTTCTGTGGGCTCTTTCT 480

* * * * *

Rat TGCTTGGTGACCACCATGGAGTACGTCATGTGTATTGACAGCGGAGAAGAGAGTCACTCT 537

Mouse TGCTTGGTGACCACCATGGAGTATGTCATGTGTATTGACAGCGGAGAAGAGAGTCACTCT 537

Human TGCTTGGTGACCACCATGGAGTATGTCATGTGCATCGACAGAGAAGAAGAGAGTCACTCT 540

***** * * * * *

Rat CAGAGTGACTGTCGGGCGGTATCATCTTCATAGCCATCCTCAGCTTCTTGGTCTTCACT 597

Mouse CGGAGTGACTGCCGGGCGGTATCATCTTCATAGCCATCCTCAGCTTCTTGGTCTTCACT 597

Human CGGAATGACTGCCGAGCAGTATCATCTTTATAGCCATCCTGAGCTTCTTGGTCTTCACT 600

* * * * *

Rat CCGCTCATGTTAGTGTCCAGCACCATCTTGGTGGTGAAGATACGGAAGAACACATGGGCC 657

Mouse CCGCTCATGTTAGTGTCCAGCTCCATCTTGGTGGTGAAGATACGGAAGAACACGTGGGCC 657

Human CCCCTCATGCTGGTGTCCAGCACCATCTTGGTCGTGAAGATCCGGAAGAACACGTGGGCT 660

** * * * * *

Rat TCCATTCTTCGAAGCTGTACATCGTCATCATGGTCACCATTATCATATTCCTCATCTTT 717

Mouse TCCATTCTTCGAAGCTGTACATTGTCATCATGGTCACCATTATCATATTCCTCATCTTT 717

Human TCCATTCTTCGAAGCTTTACATAGTCATCATGGTCACCATTATATTCCTCATCTTC 720

***** * * * * *

Rat GCCATGCCCATGCGGGTCCTCTACCTGTTGTATTACGAGTACTGGTCAACCTTTGGGAAC 777

Mouse GCCATGCCCATGCGGGTCCTCTACTTGCTGTACTACGAGTACTGGTCAGCCTTTGGGAAC 777

Human GCTATGCCCATGAGACTCCTTTACCTGCTGTACTATGAGTATTGGTCGACCTTTGGGAAC 780

** ***** * ***** ** ***** ***** *****

Rat CTGCATAACATCTCCTTGCTTTTCTCCACCATCAATAGCAGCGCCAACCCTTTCATCTAC 837

Mouse CTGCATAACATCTCCTTGCTTTTCTCCACCATCAACAGCAGCGCCAACCCTTTCATCTAC 837

Human CTACACCACATTTCCCTGCTCTTCTCCACAATCAACAGTAGCGCCAACCCTTTCATTTAC 840

** ** ***** ** ***** ***** ***** ** *****

Rat TTTTTTGTGGGCAGCAGTAAGAAGAAGCGCTTCAGGGAGTCCTTAAAAGTGGTCCTGACC 897

Mouse TTTTTTGTGGGCAGCAGTAAGAAGAAGCGCTTCAGGGAGTCCTTAAAAGTCGTCTGACC 897

Human TTCTTTGTGGGAAGCAGTAAGAAGAAGAGATTCAAGGAGTCCTTAAAAGTTGTTCTGACC 900

** ***** ***** * ***** ***** *****

Rat AGAGCTTTCAAAGACGAGATGCAACCTAGGCGTCAGGAGGGCAATGGCAACACTGTATCC 957

Mouse AGGGCTTTCAAAGATGAAATGCAACCCAGGCGCCAGGAGGGCAACGGCAACACTGTATCC 957

Human AGGGCTTTCAAAGATGAAATGCAACCTCGGCGCCAGAAAGACAATTGTAATACGGTCACA 960

** ***** ** ***** ***** ** *****

Rat ATTGAGACTGTGGTCTGA 975

Mouse ATTGAGACTGTGGTCTGA 975

Human GTTGAGACTGTCGTCTAA 978

***** ***** *

Figure 1.3 Multiple sequence alignment of rat, mouse and human mas amino acid sequence. Mas of rat and mouse have 324 amino acids while human mas has 325 amino acids with an additional “glycine” at position 20. The mouse mas protein shares around 97% and 91% of homology with rat and human mas, respectively. NCBI accession number of rat, mouse and human mas sequences were P12526, P30554 and NP_002368 respectively. * and : represented the identical amino acid residues in three or two protein sequences.

1.5 Putative structure of mas

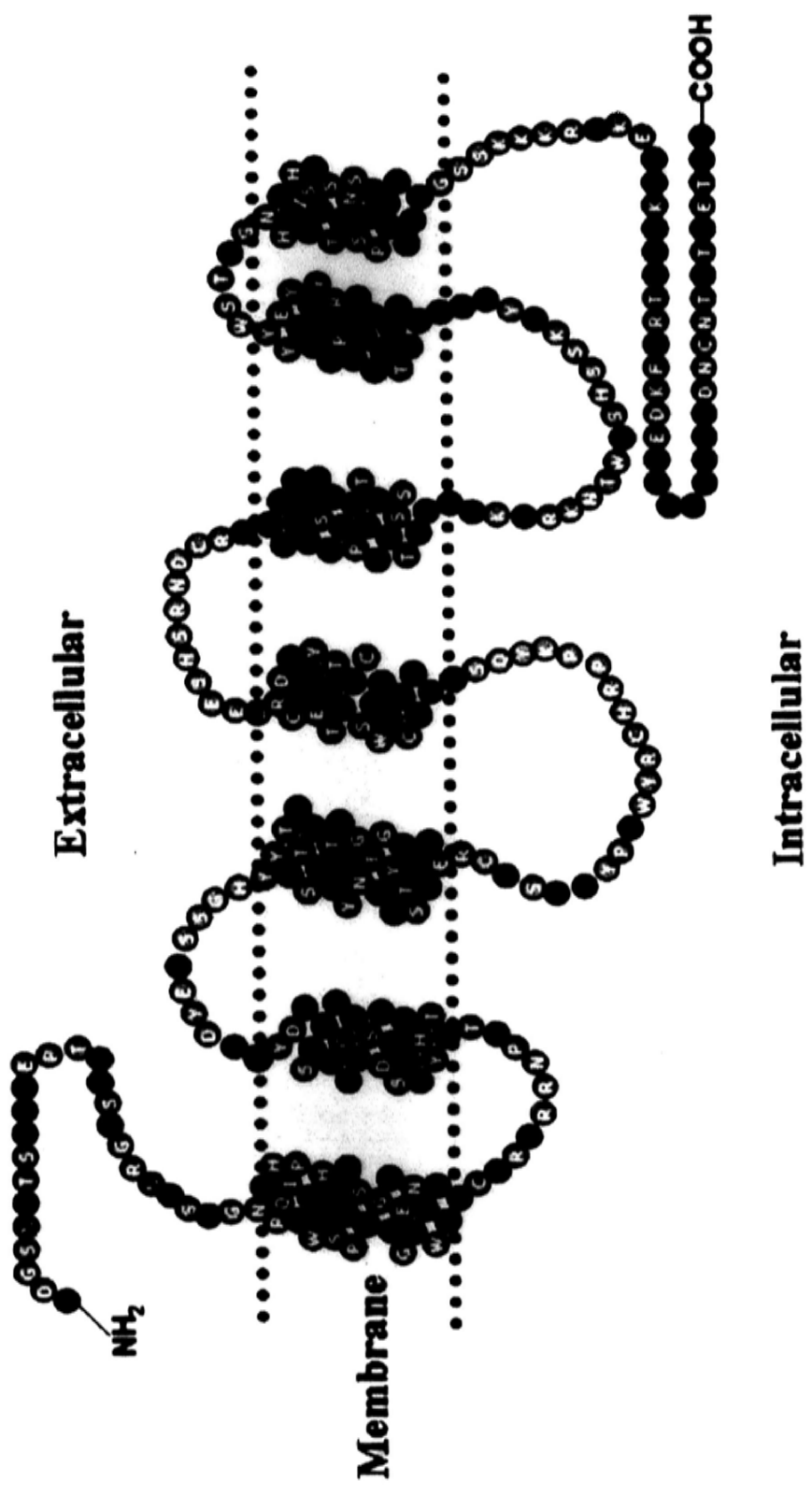
As a member of GPCR family, mas has a tertiary structure of seven putative trans-membrane segments linked by extracellular and intracellular loops. The N- and C-terminus are located in the extracellular and cytoplasmic space, respectively. Several N-glycosylation sites are found in the N-terminus of mas (Figure 1.4).

1.6 GPCR signaling pathway

Endogenous ligands for some of the GPCRs are neurotransmitters, hormones, phospholipids, photons, ordants and purine nucleotides and so on (Dohlman et al., 1987). The interaction between GPCR and ligand usually triggers activation of heterotrimeric G proteins which are located in the intracellular surface of the cell membrane (Figure 1.5) (Onrust et al., 1997). The G proteins are composed of α , β and γ subunits (Downes & Gautam, 1999; Cabrera-Vera et al., 2003; Malbon, 2005). The $G\alpha$ subunit binds guanine nucleotides. In the absence of GPCR ligand, the three subunits conjugate together and the $G\alpha$ subunit binds GDP. Upon ligand binding, GPCR functions as a guanine nucleotide exchange factor (GEF) to catalyze the exchange of GDP with GTP on the $G\alpha$ subunit which is then dissociated with $G\beta$ and $G\gamma$ subunit. The GDP and GTP form of G protein represent inactive and active state, respectively. Upon dissociation, $G\alpha$ and $G\beta\gamma$ activate different downstream effectors in the signaling pathway (Coleman et al., 1994; Lambright et al., 1994; Rens-Domiano & Hamm, 1995; Wall et al., 1995; Sprang, 1997; Hamm, 1998). The downstream signaling pathways that are activated by $G\alpha$ protein

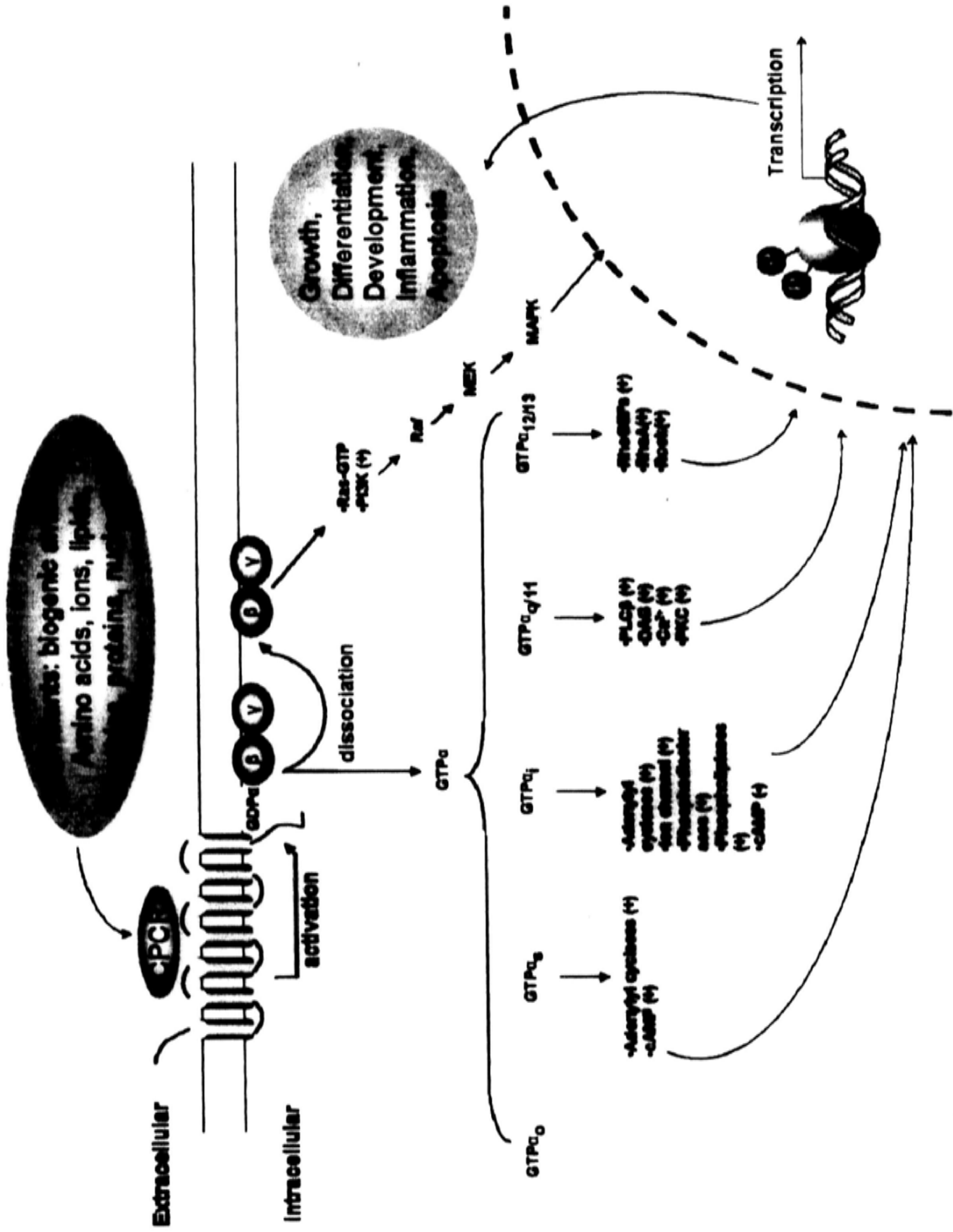
included $G\alpha_o$, $G\alpha_s$, $G\alpha_i$, $G\alpha_q$ and $G\alpha_{12}$ while activation on $G\beta\gamma$ triggers Ras-GFP to Raf, MEK and MAPK signalings (Figure 1.5).

Figure 1.4 Predicted secondary structure of mas proto-oncogene. In trans-membrane segments are linked by three extracellular and intracellular loops following with a long cytoplasmic tail. The purple and blue spots represented hydrophobic and hydrophilic amino acids, respectively. The oranges spots showed potential N-glycosylation sites. (Adapted and modified from(Hanley et al., 1990)



- Hydrophobic AA residues
- N-glycosylation sites
- Hydrophilic AA residues

Figure 1.5 GPCR signaling pathway. Stimulants that activate GPCR include biogenic amines, amino acids, ions, lipids, proteins and so on. The dissociated G α and G $\beta\gamma$ subunits transfer different downstream signals. Activation of different protein kinases bring changes on cell proliferation, migration and survival etc. [Modified from TRENDS in Pharmacological Sciences]



1.7 Candidates of mas ligand

Angiotensin was once considered as a mas ligand from an enhanced angiotensin responsiveness in mammalian cells transfected with mas (Jackson et al., 1988; Dean & Boynton, 1990; Von Bohlen und Halbach et al., 2000; Walther et al., 2000; Canals et al., 2006). However, mas was found only to increase cellular responses of the endogenous angiotensin II receptor (Kostenis et al., 2005). The angiotensin inhibitor or antagonist had no effect on the growth of mas-transfected cells (Han et al., 2002). Recently, angiotensin-(1-7) was proposed to be a potential mas ligand for its binding with mas-transfected CHO cells (Santos et al., 2003; Hellner et al., 2005; Tallant et al., 2005). However, it showed no homology with the putative peptide ligand identified in the phage-displayed library. In addition, Mc0M80 cells didn't response to Ang-(1-7) to accumulate inositol phosphate in the cytoplasm (Bikkavilli et al., 2006). A surrogate ligand for mas was identified using phage-displayed peptide library and named as MBP7 (mas binding peptide 7). MBP7 had high affinity and punctate binding to membrane mas receptor transfected and stably expressed in CHO cell. Moreover, MBP7 induced a significant accumulation of intracellular [³H]-inositol phosphate and calcium mobilization specifically in mas expressing cells (Bikkavilli et al., 2006).

The amino acid sequences of the two consensus motifs derived from the mas-binding peptides showed similarities with several kinds of protein after multiple alignments with NCBI database (Table 1.2). Among them, the putative monosaccharide transporter 1 and the intestinal facilitative glucose transporter 7 were noted to be homologous to motif 1 of MBP7, implying potential interaction between mas and glucose transporter (GLUT).

1.8 Interaction of GPCR and glucose transporter

Several GPCRs were known to interact with GLUTs. ET-1 triggered GLUT4's translocation to cell surface through ET_A receptor in differentiated 3T3-L1 cells via tyrosine kinase activation (Roettger et al., 1995). fMLP (formyl-methionyl-leucyl-phenylamine) and PAF (platelet activating factor) stimulated GLUT1 membrane trafficking in CHO cells (Sorkin & Von Zastrow, 2002). Type II diabetes patients might experience blockade of glucose uptake from due to chronic desensitization of purinergic P2Y receptors (Tsao et al., 2001). GLP-2 enhanced intestinal glucose transporter activity through glucagon-like peptide-2 receptor (GLP-2R) (Lefkowitz et al., 1998). However, the underlined mechanism that couples GPCR to glucose transporter is still an open question.

Table 1.2 Proteins that shared homology with the mas-binding consensus motif 1

| Protein class | Consensus motif 1(<i>RQALRLLRRGL</i>) | |
|---------------------------------|--|------------------|
| | Protein | Accession number |
| Membrane proteins | Putative monosaccharide transporter 1 | XP_466377.1 |
| | Intestinal facilitative glucose transporter 7 | NP_997303.1 |
| G protein-coupled receptors | Olfactory receptor 19 | NP666447.1 |
| | Olfactory receptor MOR256-16 | XP_605585 |
| | CC chemokine receptor 10 | NP_057686.1 |
| | G protein-coupled receptor 2 | AAF72871.1 |
| Enzymes and regulatory proteins | Kidney and liver proline oxidase | XP_541686.1 |
| | Fe-S oxidoreductase | NP_614215.1 |
| | Pristinamycin I synthetase | CAA67140.1 |
| | Superfamily II DNA and RNA helicases | ZP_00270322.1 |
| | ATP-dependent DNA helicase | YP_147039.1 |
| | Putative acyltransferase | YP_145344.1 |

Modified from (Bikkavilli et al., 2006)

1.9 Aims of study

Previous data from our laboratory indicated that GFP-tagged mas protein partially lost the competency of translocation after binding with MBP7, suggesting C-terminus of mas protein might be very important for mediating downstream signaling.

Mas protein was reported to be constitutively active (Canals et al., 2006). But in our laboratory, elevation of intracellular calcium level was only detected after MBP7 activation on mas (Bikkavilli et al., 2006). In parallel, bioinformatic approaches suggested a possible linkage between mas and glucose transporter (Bikkavilli et al., 2006). Hence, in the present study, the endogenous receptor activity of mas and its possible interaction with glucose transporter were characterized.

To assess the importance of mas C-terminus in receptor activity, different mas fusion constructs were established (Chapter 2). The expression and cellular distributions of various mas fusion proteins were confirmed by Western blot and confocal microscopy. Furthermore, binding affinity and MBP7 induced translocation of mas fusion variants were examined by phage binding assay and cell surface biotinylation assay (Chapter 3).

To determine the receptor activity of mas, MBP7-induced calcium mobilization was examined in different cell clones expressing different mas fusion variants and in cells expressing different levels of native mas (Chapter 3).

In Chapter 4, cellular glucose uptake in the basal condition and upon stimulations of insulin or MBP7 was examined in CHO cells stably expressing mas. Basal glucose uptake and cellular response to stimulations from cells expressing native mas, mas fusion variants and vector control were compared as well.

The significance of current findings and future applications were discussed in Chapter 5.

Chapter 2

Construction and Expression of

Mas-(Gly₁₀Ser₅)-GFP Fusion Protein

2.1 Introduction

Tagging GPCR with green fluorescent protein (GFP) is a convenient way to study localization and translocation of receptor in a real time manner in living cells. For example, the trafficking of thyrotropin-releasing hormone (Drmota et al., 1998), vasopressin V₂ receptor (Schulein et al., 1998), cholestykinin CCK₁ receptor (Tarasova et al., 1997) and other GPCRs were studied as GFP fusion proteins.

2.1.1 *Green fluorescent protein*

Green fluorescent protein (GFP) was firstly discovered in an ocean jellyfish, *Aequoria Victoria*, in 1992. It is an autofluorescent protein containing 238 amino acid residues and characterized with a molecular mass of about 25 kDa. GFP has been engineered and resulted mutant is an enhanced version of GFP (EGFP) which emits stronger fluorescence with higher stability. The wavelength for maximal excitation and emission of EGFP are 488 nm and 577 nm, respectively (Prasher et al., 1992). Anti-GFP antibodies have been widely used for immunoprecipitation and Western blot analysis with GFP. Besides, orange, yellow and cyan fluorescent protein were derived from GFP (Shaner et al., 2007). The creation of different colored fluorescent proteins facilitates studies on protein co-localization via fluorescence resonance energy transfer (FRET) (Pollok & Heim, 1999).

2.1.2 *mas-(Gly10Ser5)-GFP chimeras*

Although widely used, some proteins were reported to have altered receptor activities after GFP tagging. For example, adrenoreceptor and cAMP1 receptor when fused with

GFP underwent auto-phosphorylation after ligand binding (Barak et al., 1997; Xiao et al., 1997).

As for mas, binding affinity and translocation upon MBP7 were partially decreased after direct tagging of GFP at its C terminus. However, another protein closely related to mas named mas-related gene (MRG) showed no defect in ligand binding and translocation (Milasta et al., 2006). Comparison of the C terminus between mas and MRG indicated that C terminus of MRG was 18 amino acids longer than that of mas. So it was assumed that mas C terminus was relatively short. Direct tagging of GFP at its C terminus might block the interaction of mas with cellular proteins and consequently impaired the downstream signaling. A 15-amino acid peptide linker was designed and inserted between mas and GFP in frame to separate mas and GFP further away from each other without affecting normal expression and localization of mas.

2.2 Materials and Methods

2.2.1 *Materials*

2.2.1.1 Chemicals

Iscove's modified DMEM medium, F12-Nutrient Mixture (Ham), fetal bovine serum, penicillin/streptomycin, HT supplement, TRIzolTM reagent, Lipofactamine 2000, all DNA primers, dNTP, 1kb DNA markers, agarose (electrophoresis grade) and BenchMarkTM Pre-stained Protein Ladder were from Invitrogen (Carlsbad, CA, USA). QIAquick gel extraction kit, Qiagen plasmid midi and maxi kits were from Qiagen (Hilden, Germany).

G418 were from Merck Biosciences (Whitehouse Station, NJ, USA). Nitroblue tetrazolium chloride (NBT) and 5-bromo-4-chloro-3-indolylyl-phosphate-4-toluidine salt (BCPIP) were from Roche (Roche Diagnostics Corporation, IN, USA). Nitrocellulose transfer membrane was from Whatman (Hahnstrabe 3, D-37586 Dassel, Germany). All other chemicals and reagents were of molecular grade and from Sigma-Aldrich (St. Louis, MO, USA).

2.2.1.2 Enzyme

SuperScript™ II reverse transcriptase, T4 DNA ligase, trypsin were from Invitrogen Corporation (Carlsbad, CA, USA). PFU ultra high fidelity DNA polymerase was from Stratagene (Cedar Creek, TX, USA). All the restriction enzymes were from New England BioLabs (Beverly, MA, USA).

2.2.1.3 Antibodies

Mouse monoclonal anti-GFP antibody was from Clontech (Mountain View, CA, USA). Rabbit anti-mas was raised against a peptide antigen which derived from mas (Bikkavilli et al., 2006). Anti-GFP serum was a gift from Dr. C. C. Wan, and the serum was raised against purified GFP protein in rabbit. AP-conjugated goat anti-mouse antibody was from Zymed Laboratories (San Francisco, CA, USA).

2.2.2 *Methods*

2.2.2.1 **Preparation of mas-(Gly₁₀Ser₅)-GFP constructs**

Mas-(Gly₁₀Ser₅)-GFP was constructed by overlapping PCR. Firstly, overlapped fragments of mas-linker and linker-GFP were prepared by PCR with primers encoding part of the (Gly₁₀Ser₅) linkers. Then a mas forward and a GFP reverse primer were used for the overlapping PCR (Figure 2.1). The PCR product was then cloned into pEGFP-N1 vector (Figure 2.2).

2.2.2.1.1 Construction of mas-linker fragment

The full-length of mas cDNA was amplified from pFRSV-mas vector with forward primer Rmas-EcoR I-F5 (5' CCG GAA TTC ATG GAC CAA TCA AAT ATG AC 3') and reverse primer Rmas-Kpn I-oligo-R1034 (5' AGA ACC GCT GCC TGA ACC GCC TCC ACC ACT CGG TAC CCC TCC TCC GAC CA 3'). The underlined nucleotides segments were EcoR I and Kpn I restriction cutting sites in the corresponding primers. An oligonucleotide fragment encoding ten glycines and five serines was added to the reverse primer Rmas-Kpn I-oligo-R1034. The PCR amplification was performed in a buffer containing 10x PFU buffer (2.5 µl), 10 µM primer (each 1 µl for forward and reverse), pFRSV-mas cDNA (2 ng), 10 mM dNTP (0.5 µl) and nano pure water making up a volume to 24.5 µl. The 10x cloned PFU buffer was consisted of 200 mM Tris-HCl (pH 8.8), 100 mM (NH₄)₂SO₄, 100 mM KCl, 1 mg/ml nuclease-free BSA and 1% Triton X-100. The PCR reaction was initialized using hot start program in Applied Biosystems

Elmer Gene Amp 9700 PCR machine. After denaturing at 94°C for 3 minutes, 0.5 µl of PFU DNA polymerase (2.5 U/ µl) was added to the reaction mixture and heated up for

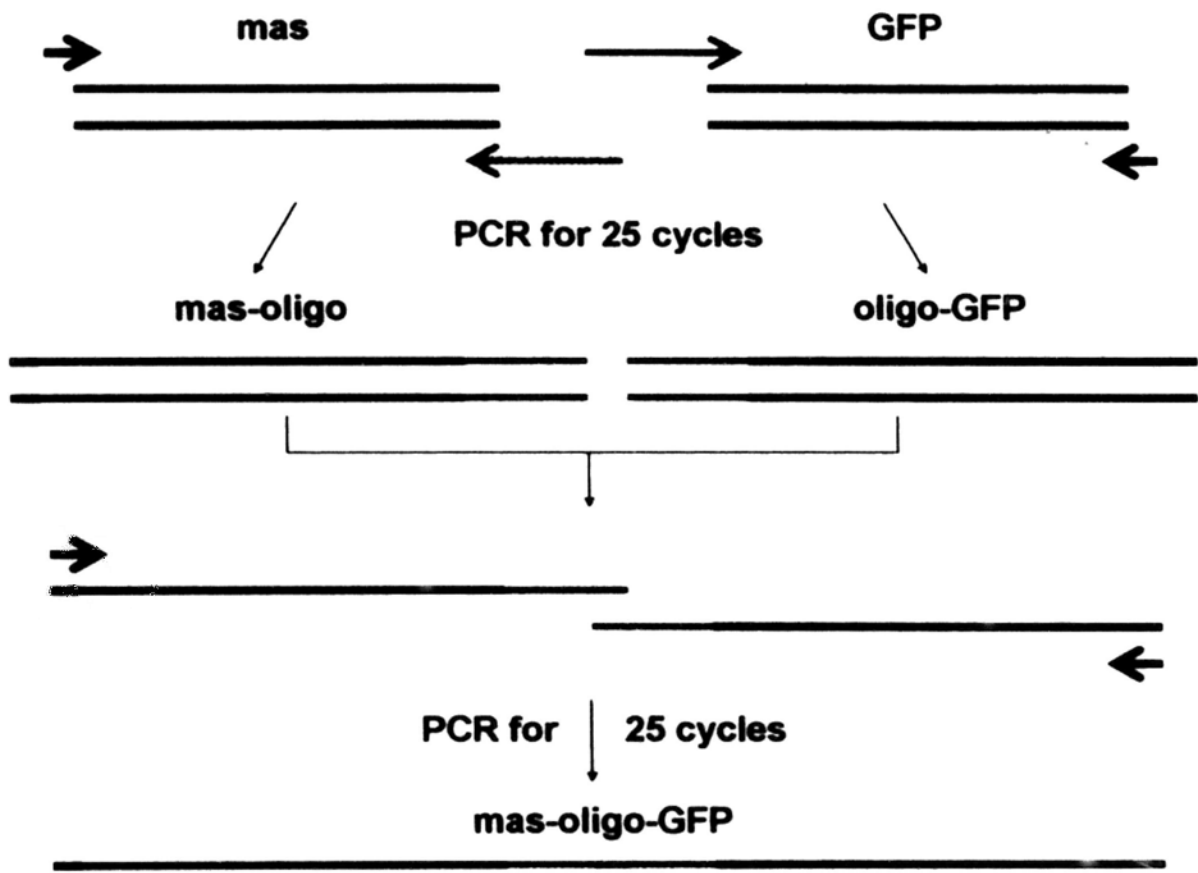


Figure 2.1 Construction of mas-(Gly₁₀Ser₅)-GFP by overlapping PCR. Mas-oligo and oligo-GFP fragments were constructed separately by PCR amplification with individual primers. Both in the 3' end of mas-oligo and in the 5' end of oligo-GFP there were 30-nucleotide fragments which were complementary to each other for 15 nucleotides. The mixture of mas-oligo and oligo-GFP was used as template for construction of mas-(Gly₁₀Ser₅)-GFP by overlapping PCR with the forward primer of mas-oligo and reverse primer of oligo-GFP.

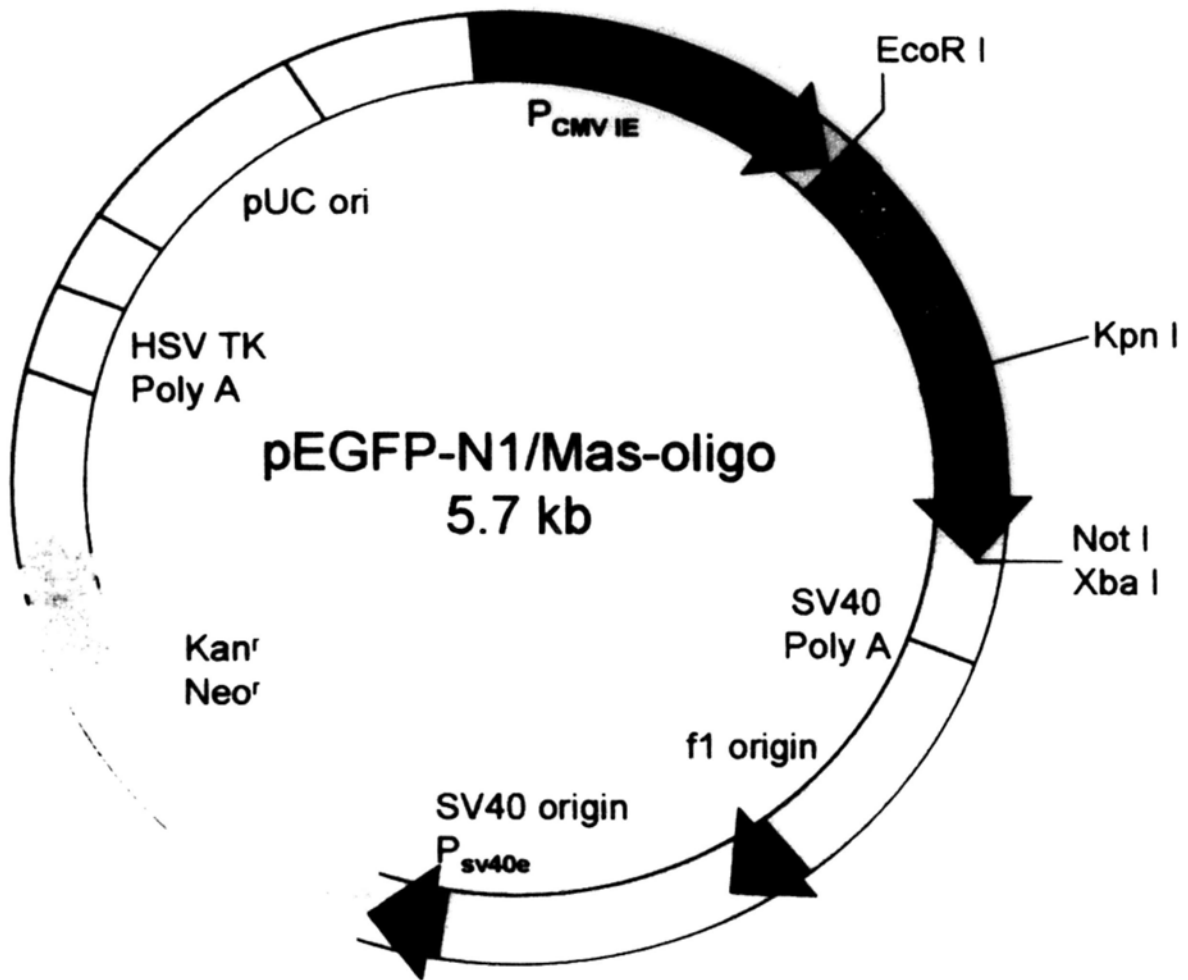


Figure 2.2 Vector map of pEGFP-N1. The full length of EGFP in the mammalian expression vector pEGFP-N1 (4.7 kb) was digested out in EcoR I/ Not I cutting sites. The full length of mas-(Gly₁₀Ser₅)-GFP construct was ligated into the multiple cloning site at the Kpn I and Not I cutting sites. The open reading frame of mas-(Gly₁₀Ser₅)-GFP was cloned downstream of a constitutive CMV promoter and expressed as a whole fusion protein. The expression vector encoded kanamycin and neomycin resistant genes for selection in bacterial or mammalian hosts. The vector map was modified from the website: <http://www.pasteur.ac.ir/researchDepartment/GeneBank/Plasmid.htm>.

two more minutes. After that, PCR reaction was running for 25 cycles with a denature temperature of 94°C for 30 seconds, an annealing temperature of 65°C for 30 seconds and an extension temperature of 72°C for 60 seconds. Following it, an extended incubation of 7 minutes at 72°C was added.

2.2.2.1.2 Construction of linker-GFP fragment

The open reading frame of GFP was amplified from pEGFP-N1 using oligo-EGFP-F1033 (5' TCA GGC AGC GGT TCT AGC GGC GGT GGC GGA CCG GTC GCC ACC ATG GTG AG 3') as the forward primer and Xba I-Not I-EGFP-R1037 (5' TGA TCT AGA GTC GCG GCC GCT TTA CTT GTA 3') as the reverse one. The two underlined nucleotide sequences were Xba I and Not I restriction cutting sites respectively. The PCR reaction mixture and running program were similar to previous one in section 2.2.2.1.1 except that the template was pEGFP-N1 plasmid (2 ng).

2.2.2.1.3 Construction of mas-(Gly₁₀Ser₅)-GFP by overlapping PCR

Overlapping PCR was carried out using 1 µl of mas-oligo and 1 µl of oligo-GFP together as templates. Rmas-EcoR I-F5 (10 µM, 1µl) and Xba I-Not I-EGFP-R1037 (10 µM, 1µl) were used as forward and reverse primers. The concentration of all the other components in the PCR reaction system (total volume of 24.5 µl) was the same as that described in section 2.2.2.1.1 and 2.2.2.1.2. The PCR reaction was running for 25 cycles using hot start program except that the extension time was elongated to 120 seconds. PFU DNA polymerase (0.5 µl) was added after pre-heating for three minutes. To prepare mas-

(Gly₁₀Ser₅)-GFP in large scale, the PCR reaction was increased to a volume of 50 µl and five PCR samples were pooled together for gel purification.

2.2.2.1.4 Agarose gel electrophoresis

PCR products of mas-oligo, oligo-GFP and mas-(Gly₁₀Ser₅)-GFP were mixed with 6x orange loading dye and performed electrophoresis in 1% agarose gel [agarose (w)/ 1x TAE buffer (v)] containing 0.5 µg/ml EB (ethidium bromide) at 100V constant voltages until the dye arrived to 2/3 of the gel. The electrophoresis buffer was 1x TAE which contained 40 mM Tris-Acetic acid and 1 mM EDTA. Specific bands were visualized by UV exposure in Multimage™ Light Cabinet.

2.2.2.1.5 Gel extraction of PCR products

Mas-(Gly₁₀Ser₅)-GFP in the gel was extracted with the Gel Extraction Kit according to manufacturer's instruction. The putative band in agarose gel was excised by a clean blade. The weight of each gel piece was measured and three folds (v/w) of Buffer QG were added to the gel piece. Then the mixture was heated up to 50°C for 10 minutes until a homogenous state was formed. The mixture was transferred to a QIAquick spin column above an eppendorf tube. The column and the tube were centrifuged at 13000 rpm for 1 minute at room temperature to make DNA bind to the column. Then the column was washed with 0.75 ml of buffer PE for twice and the waste was removed by centrifugation at 13000 rpm for 1 minute. To rescue DNA, the column was transferred to a new eppendorf tube and was incubated with appropriate volume of nano water for 1 minute at

room temperature. The eluted DNA was collected by centrifugation at 13000 rpm for 1 minute.

2.2.2.1.6 Restriction enzyme digestion

Purified mas-oligo-GFP (~10 µg) after gel extraction was digested in a mixture containing 10 µl of 1x NEBuffer III, 1µl of EcoR I (20 U/µl), 2 µl of Not I (10 U/µl) in a volume of 100 µl. The digestion was carried out at 37°C overnight and confirmed by agarose gel electrophoresis. pEGFP-N1 (10 ug) vector was digested by the same step as described above.

2.2.2.1.7 Purification of DNA by ethanol precipitation

Solution mixture containing phenol chloroform and isoamyl alcohol in a ratio of 25: 24:1 was added to the digested sample with an equal volume. The mixture was vortexed vigorously and centrifuged down at 13000 rpm for 1 minute. Two layers were formed while the upper aqueous one contained DNA. The supernatant was transferred to a new tube and added with 2.5 volume of pure ethanol and 0.1 volume of 3 M sodium acetate to precipitate DNA at 4°C overnight. Next day, the mixture was centrifuged at 13000 rpm for 10 minutes to pellet DNA. After washing the pellet once with 75% ethanol, the purified DNA was dissolved in nano pure water.

2.2.2.1.8 Ligation of mas-oligo-GFP to pEGFP-N1 vector

The EcoR I-Not I restricted pEGFP-N1 vector and mas-oligo-GFP insert were ligated at three different quantity ratios (1:1, 1:3 and 1:5). For instance, the size of mas-oligo-GFP and EcoR I-Not I restricted pEGFP-N1 after GFP being digested out were 1.7 kb and 4.0 kb (GFP was ~0.7 kb), respectively. So the quantity of 100 ng of linearized pEGFP-N1 was equal to the quantity of 42.5 ng, 127.5 ng and 212.5 ng of digested mas-oligo-GFP when the ratio was 1:1, 1:3 and 1:5, respectively. The vector and insert were mixed at anyone of the three ratios and incubated with 5x T4 DNA ligase buffer (4 μ l), T4 DNA ligase (2 μ l, 400 U/ μ l) and pure nano water in a final volume of 20 μ l. The T4 DNA ligase buffer was composed of 250 mM Tris-HCl (pH 7.5), 50 mM MgCl₂, 5 mM ATP, 50 mM DTT and 125 μ g/ml BSA. The ligation was performed at 16°C water bath overnight.

2.2.2.1.9 Preparation of competent cells

DH5 α *E. coli* were thawed from -70°C stock and streaked on a sterile Luria-Bartani (LB) agar plate. After overnight growing at 37°C, single colonies were picked and grown in 2 ml of LB culture medium with shaking at 250 rpm overnight. Half of the culture was added to a flask containing 100 ml of fresh LB medium and shook at 37°C at 250 rpm until the absorbance in OD_{600 nm} reached 0.3 to 0.4. Then the bacteria were centrifuged down at 4000 rpm for 10 minutes at 4°C. After discarding the supernatant, the bacteria pellet was resuspended and incubated with ice-cold 0.1 M CaCl₂ (20 ml) at 4°C for 10 minutes and then centrifuged at 4000 rpm for another 10 minutes at 4°C. The competent cells were resuspended in 2.5 ml of ice-cold CaCl₂ (0.1 M) containing 16% glycerol and stored with aliquots (200 μ l) at -70°C.

2.2.2.1.10 Bacterial transformation

Ligated product (10 μ l) and DH5 α competent cells (200 μ l) were co-incubated on ice for 30 minutes. Then the mixture was heat-shocked at 42°C for 90 seconds and quickly inserted on ice for 5 minutes. The transformed cells were added with LB medium (0.8 ml) and shook at 37°C at 250 rpm for 1 hour. Recovered cells were pelleted at 3000 g for 5 minutes at 4°C and resuspended in 400 μ l of LB medium. The resuspension was spread evenly on LB agar plate containing 50 μ g/ml kanamycin and grown at 37°C overnight.

2.2.2.1.11 Minipreparation of mas-oligo-pEGFP N1 vector

The vector of mas-(Gly₁₀Ser₅)-pEGFP N1 was prepared in mini scale following the instruction of QIAprep Spin Miniprep Kit. A single colony from transformed bacteria containing mas-(Gly₁₀Ser₅)-pEGFP N1 was picked and grown in 5 ml of LB medium with 50 μ g/ml kanamycin. After shaking at 250 rpm overnight, the bacteria were pelleted by 4000 rpm centrifugation for 10 minutes at room temperature and lysed in 250 μ l of buffer P1 (with 100 mg/ml RNase A). The lysate was mixed with buffer in the order of P2 and then P3 by gently inverting the tube up and down for five times. After that, the mixture was centrifuged at 14000 rpm for 10 minutes at 4°C and the transparent phase was taken to a spin column. The vector DNA bound to the column by centrifugation at 13000 rpm for 1 minute at room temperature. The column was washed once with 0.75 ml of buffer PE followed by centrifugation at 13000 rpm for 1 minute at room temperature.

The column was incubated with 50 μ l of nano pure water for 1 minute at room temperature. The vector DNA was rescued by centrifugation at 13000 rpm for 1 minute.

2.2.2.1.12 Quantification of vector DNA

DNA has maximal absorbance at OD_{260 nm} and one absorbance unit at OD₂₆₀ equals to 50 μ g/ml DNA. Nano pure water was set as blank and DNA concentration was measured in 1:100 and 1:50 dilutions consecutively. Average of the two determinants was used to calculate DNA concentration. The absorbance ratio of OD_{260 nm} to OD_{280 nm} reflected the DNA purity and a theoretic value of 2 for pure DNA.

2.2.2.1.13 DNA sequencing

The purified plasmid DNA was sequenced by a custom sequencing company (Macrogen, Korea) to confirm the nucleotides sequence.

2.2.2.2 **Stable expression of mas-(Gly₁₀Ser₅) in CHO cells**

To establish cell clones stably expressing mas-(Gly₁₀Ser₅)-GFP fusion protein, CHO cells were transfected with pEGFP-N1/Mas-(Gly₁₀Ser₅) construct using lipid transfectants, and then selected against 1 mg/ml G418.

2.2.2.2.1 Cell culture

Chinese Hamster Ovary cell (CHO) was cultured in 100 mm culture plate with 10 ml of Ham's F-12 complete medium containing 10% (v/v) fetal bovine serum (FBS, qualified) and 1% (v/v) penicillin/ streptomycin (P/S). Cells were subcultured after reaching 70~80% confluence. Following removal of medium, 0.05% (w/v) trypsin solution (1 ml) (Sigma) was added to detach cells from the plate bottom. The digestion was stopped by adding 1 ml of medium. Cells were then pelleted by centrifugation at 800 rpm for 3 minutes. The cell pellet was resuspended in 10 ml of medium and subcultured at a ratio of 1: 10.

2.2.2.2.2 Linearization of vector

pEGFP-N1 and mas-oligo-pEGFP N1 (30 µg) were linearized with Sfi I enzyme in a reaction system containing 1x NEBuffer 2 (10 mM Tris-HCl, 10 mM MgCl₂, 50 mM NaCl and 1 mM dithiothrietol, pH 7.9), 1mg/ml BSA and 100 units of Sfi I in a final volume of 200 µl. The whole reaction system was incubated at 50°C overnight. The linearized plasmid DNA was purified by ethanol precipitation as described in section 2.2.2.1.7.

2.2.2.2.3 Transfection by Lipofectamine 2000

CHO cells (1×10^5) were seeded in 35 mm culture plate and grown for 24 hours at 37°C, 5% CO₂. Linearized plasmid DNA (4 µg) and lipofectamine 2000 (12 µl) were incubated separately in 100 µl of serum free DMEM for 5 minutes and then mixed at room temperature for another 15 minutes. The mixture together with 800 µl of serum free

DMEM were added to the CHO cells after removal of the complete medium. After 5 hours of incubation at 37°C, 5% CO₂, medium was changed back to F-12 complete medium.

2.2.2.2.4 Selection of stably transfected cells

Two days after the transfection, cells containing the plasmid were selected against 1 mg/ml G418 in Ham's F-12 complete medium. The selection medium was refreshed every 3 days to remove dead cells and allowed resistant cells growing. After one week, well-isolated colonies were observed and picked using cloning rings. Briefly, the colonies were marked at the bottom of the plate. Sterile cloning rings were paced over the marked colony with vacuum grease around the rings' edge. Trypsin (100 µl) was added into the cloning cylinder and digestion was going on for 3 minutes. Cells from each colony were transferred to a well containing 1 ml of selection medium in a 24-well plate. Until confluence, 1/4 well of cells was seeded on the coverslips in a new 24-well plate for confocal microscopy analysis. The rest was for stable clone maintenance. Colonies with high expression were further purified using limiting dilution. Cells were seeded in 96-well plates at two different concentrations: 0.1 cell/well and 0.01 cell/well. Single cell-derived cell colonies in the 96-well plates were subcultured consecutively in 24-well plates, 6-well plates and 100 mm culture dishes.

2.2.2.2.5 Confocal microscopy

Cells grown on coverslips were assembled into a perfusion chamber (Model PH-2, Warner Instrument Corporation) and covered with 1 ml of selection medium. GFP was excited at 488 nm by an Ar/Kr laser and detected with a 525±50 bandpass filter in a Leica TCSNT Confocal Microscope. Fluorescent and transmission images were captured in separate channels and merged to create overlay images.

2.2.2.2.6 Immunoprecipitation

Cells were grown in 150 cm² sterile culture flask. Until 80% confluence, cells were scraped from the flask bottom and centrifuged at 1800 rpm for 3 minutes. Each cell pellet was lysed in 2 ml of RIPA buffer and passed through a 1 ml of syringe for 10 times to increase protein solvency. The content of RIPA buffer was 0.1 M Tris-HCl (pH 7.4), 150 mM NaCl, 1% Na deoxycholate, 1% Triton[®] X-100, 5mM EDTA and 40 µl/ml protease inhibitor cocktail. The lysate was centrifuged at 10000 rpm for 10 minutes at 4°C to remove debris. Well dissolved protein in the rescued supernatant was quantified using bicinchoninic Acid (BCA) protein assay kit (Pierce). Serial diluted BSA in the concentration of 2 mg/ml, 1 mg/ml, 0.5 mg/ml, 0.25 mg/ml, 0.125 mg/ml and 0.0625 mg/ml were used as protein standards. BSA standards and cell lysate were added to 96-well plate (10 µl per well). Solution A and solution B were mixed in a ratio of 50:1. The protein standards and samples were incubated with the solution mixture of A and B (80 µl/well) at 37°C for 5 minutes. The protein concentration was determined by endpoint absorbance at 562 nm with a µQuant microplate reader (Bio-Tek Instruments Inc, Winnoski, VT, USA) and analyzed using a KCjunior software (Bio-Tek Instruments Inc, Winnoski, VT, USA). Protein (1mg) from each sample was mixed with 1:250 (v/v) anti-

mas serum or anti-GFP serum and incubated for 8 hours at 4°C. Protein A agarose beads (50 µl) was added to precipitate the immune complex at 4°C overnight. Immunoprecipitated protein was cleaned with washing buffer I (50 mM Tris-HCl, pH 7.5; 150 mM NaCl; 1% Nonidet P40 and 0.5% Na deoxycholate), washing buffer II (50 mM Tris-HCl, pH 7.5; 500 mM NaCl; 0.1% Nonidet P40 and 0.05% Na deoxycholate) and washing buffer III (50 mM Tris-HCl, pH 7.5; 0.1% Nonidet P40 and 0.05% Na deoxycholate) each for twice. Every washing lasted for 15 minutes. The cleaned beads in each eppendorf tube was mixed thoroughly with 40 µl of 2x sample buffer (4% SDS, 20% glycerol and 20 µl/ml β-mercaptoethanol in 2x Tris-HCl, pH6.8) and boiled at 100°C for 15 minutes to dissociate protein from the beads. After being cooled down at room temperature, 40 µl urea lysis buffer (2% SDS, 8% urea, 100 mM EDTA, 20 mM Tris-HCl, pH 7.4 and 40 µl/ml protease inhibitor cocktail) was mixed with each sample. The totally denatured protein sample in the aqueous mixture was separated in Western Blot.

2.2.2.2.7 Western Blot analysis

The HOEFER SE 600 SERIES VERTICAL SLAB GEL UNIT was used to run SDS-PAGE. Protein sample (80 µl/well) was separated in 12% PAGE gel in a running buffer (25 mM Tris, 192 mM glycine and 0.1% SDS, pH 8.3) at 70 V constant voltage overnight. The separated proteins were transferred to nitrocellulose membrane in transferring buffer (25 mM Tris, 192 mM glycine and 10% methanol) in the HOEFER TE SERIES TRANSPHOR ELECTROPHORESIS UNIT at a constant voltage of 70 V for 3 hours. Protein binding sites in the nitrocellulose membrane was blocked by incubation with an

immuno-blotting buffer (5% skimmed milk, 0.05% Tween[®]20, 150 mM NaCl and 10 mM Tris-HCl, pH 7.5) for 1 hour at room temperature to prevent non-specific protein binding. Specific proteins for mas-GFP fusion proteins were probed by 1:5000 (v/v) monoclonal anti-GFP antibody as primary antibody in the immno-blotting buffer with gentle shaking at 4°C overnight. After removal of the unbound primary antibody, the protein blot was probed with 1:2000 (v/v) AP-conjugated anti-mouse secondary antibody with gentle shaking at room temperature for 2 hours. Unbound secondary antibody was removed by washing the blot with the immuno-blotting buffer for 3 times. Specific proteins were visualized by incubating the blot with 0.5 mg/ml NBT and 0.1895 mg/ml BCPIP in a developing buffer (0.1 M MgCl₂, 0.05 M NaCl and 0.1 M Tris-HCl, pH 9.5).

2.3 Results

2.3.1 *Preparation of mas-oligo-GFP construct*

To construct the mas-linker-GFP fusion proteins, the stop codon of rat mas was mutated to glycine (⁹⁷⁵TGA→⁹⁷⁵GGA). To prepare mas-(Gly₁₀Ser₅)-GFP, an overlapping PCR reaction was performed using mas-oligo and oligo-GFP as templates (Figure 2.2). The pEGFP-N1 plasmid and gel extracted mas-(Gly₁₀Ser₅)-GFP product were digested with EcoR I and Not I at 37°C overnight. The digested pEGFP-N1 and mas-(Gly₁₀Ser₅)-GFP were ligated in different ratios after purification by ethanol precipitation.

2.3.2 DNA and protein sequences of mas-(Gly₁₀Ser₅)-GFP

Ligation products were transformed to competent bacteria cell DH5α and grown at 37°C overnight. Mas-(Gly₁₀Ser₅)-GFP construct in the positive clones was selected and prepared in mini scale for sequencing. The sequencing results were aligned with GFP and rat mas sequence using Clustalx software (European Molecular Biological Laboratory). The nucleotide sequence and translated protein sequence of mas-(Gly₁₀Ser₅)-GFP was identical to that of mas and GFP (Figure 2.3 & Figure 2.4)

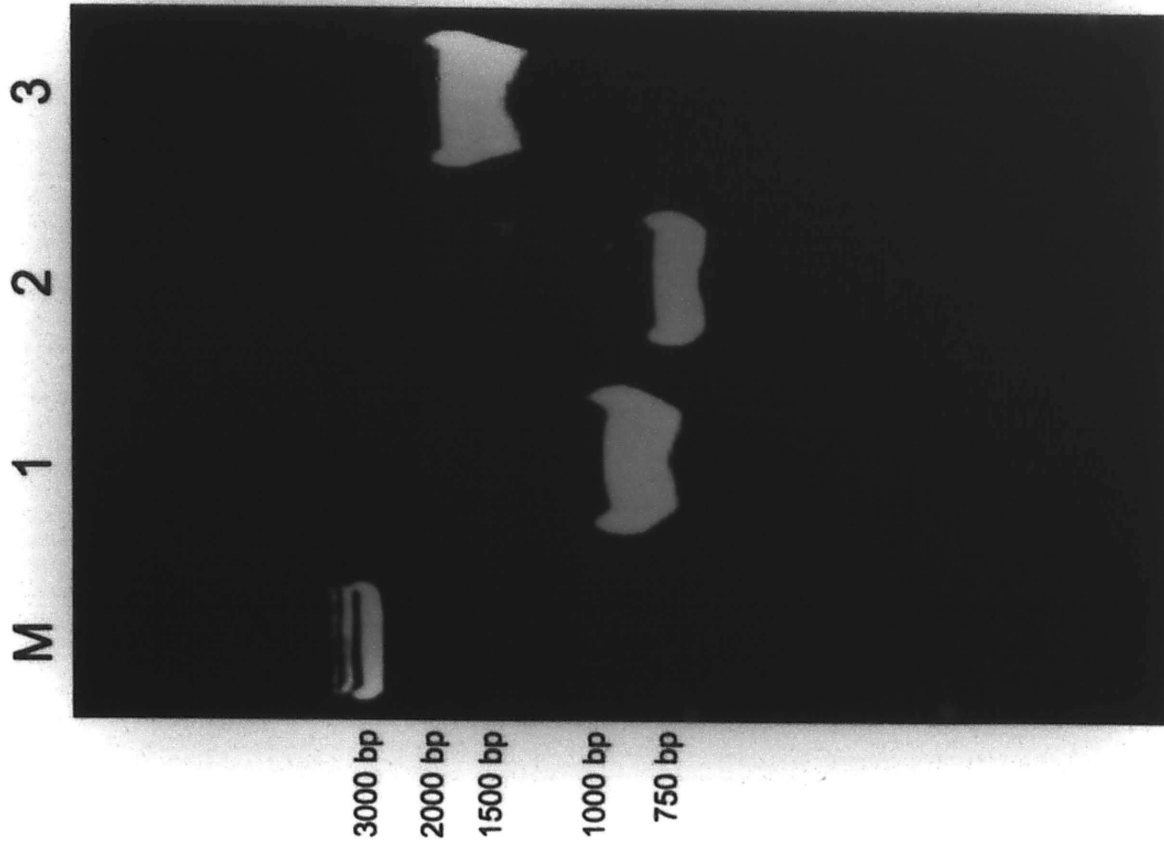


Figure 2.3 Overlapping PCR for mas-(Gly₁₀Ser₅)-GFP. Mas-oligo and oligo-GFP fragments were prepared by PCR using pFRSV-mas and pEGFP-N1 as templates, respectively. Mas-(Gly₁₀Ser₅)-GFP was amplified by overlapping PCR using the above PCR products as templates. PCR products of the three fragments were separated in 1% agarose gel electrophoresis and visualized by UV exposure in MultiImage™ Light Cabinet. The marker was Fermentas™ 1kb DNA ladder. Lane 1 to lane 3 were PCR amplification of mas-oligo fragment, oligo-GFP fragment and mas-(Gly₁₀Ser₅)-GFP which contained 975 bp, 725 bp and 1770 bp, respectively.

mas - (Gly₁₀Ser₅) -GFP ██████GACCAATCAAATATGACATCCTTTGCTGAGGAGAAAAGCCATGAATACCTCCAGCAGA 60

Mas ██████GACCAATCAAATATGACATCCTTTGCTGAGGAGAAAAGCCATGAATACCTCCAGCAGA 60

mas - (Gly₁₀Ser₅) -GFP AATGCCTCCCTGGGGACTTCACACCCACCCATTCCCATAGTGCCTGGGTTCATCATGAGC 120

Mas AATGCCTCCCTGGGGACTTCACACCCACCCATTCCCATAGTGCCTGGGTTCATCATGAGC 120

mas - (Gly₁₀Ser₅) -GFP ATCTCTCCTCTCGGCTTTGTGGAGAACGGGATCCTCCTCTGGTTCCTTTGCTCCGGATG 180

Mas ATCTCTCCTCTCGGCTTTGTGGAGAACGGGATCCTCCTCTGGTTCCTTTGCTCCGGATG 180

mas - (Gly₁₀Ser₅) -GFP AGGAGAAATCCCTTCACGGTCTATATCACCCACTTGTCCATTGCTGACATCTCCCTCCTG 240

Mas AGGAGAAATCCCTTCACGGTCTATATCACCCACTTGTCCATTGCTGACATCTCCCTCCTG 240

mas - (Gly₁₀Ser₅) -GFP TTCTGTATTTTATTCTGTCCATCGACTATGCTTTAGACTATGAACTCTCTTCTGGCCAT 300

Mas TTCTGTATTTTATTCTGTCCATCGACTATGCTTTAGACTATGAACTCTCTTCTGGCCAT 300

mas - (Gly₁₀Ser₅) -GFP TACTACACAATCGTGACGTTATCGGTGACTTTTCTATTTGGCTACAACACAGGCCTCTAT 360

Mas TACTACACAATCGTGACGTTATCGGTGACTTTTCTATTTGGCTACAACACAGGCCTCTAT 360

mas - (Gly₁₀Ser₅) -GFP CTGCTGACAGCCATCAGTGTGGAGAGATGCCTTTTCGGTCTCTACCCCATCTGGTACAGA 420

Mas CTGCTGACAGCCATCAGTGTGGAGAGATGCCTTTTCGGTCTCTACCCCATCTGGTACAGA 420

mas - (Gly₁₀Ser₅) -GFP TGTCACCGCCCCAAGCACCAGTCGGCATTTCGTCTGTGCCCTCCTGTGGGCACCTTTCATGC 480

Mas TGTCACCGCCCCAAGCACCAGTCGGCATTTCGTCTGTGCCCTCCTGTGGGCACCTTTCATGC 480

mas - (Gly₁₀Ser₅) -GFP TTGGTGACCACCATGGAGTACGTATGTGTATTGACAGCGGAGAAGAGAGTCACTCTCAG 540
Mas TTGGTGACCACCATGGAGTACGTATGTGTATTGACAGCGGAGAAGAGAGTCACTCTCAG 540

mas - (Gly₁₀Ser₅) -GFP AGTGA CTGTCGGGCGGT CATCATCTTCATAGCCATCCTCAGCTTCTTGGTCTTCACTCCG 600
Mas AGTGA CTGTCGGGCGGT CATCATCTTCATAGCCATCCTCAGCTTCTTGGTCTTCACTCCG 600

mas - (Gly₁₀Ser₅) -GFP CTCATGTTAGTGTCCAGCACCATCTTGGTGGTGAAGATACGGAAGAACACATGGGCCTCC 660
Mas CTCATGTTAGTGTCCAGCACCATCTTGGTGGTGAAGATACGGAAGAACACATGGGCCTCC 660

mas - (Gly₁₀Ser₅) -GFP CATTCTTCGAAGCTGTACATCGTCATCATGGTCACCATTATCATATTCTCATCTTCGCC 720
Mas CATTCTTCGAAGCTGTACATCGTCATCATGGTCACCATTATCATATTCTCATCTTCGCC 720

mas - (Gly₁₀Ser₅) -GFP ATGCCCATGCGGGTCTCTACCTGTTGTATTACGAGTACTGGTCAACCTTTGGGAACCTG 780
Mas ATGCCCATGCGGGTCTCTACCTGTTGTATTACGAGTACTGGTCAACCTTTGGGAACCTG 780

mas - (Gly₁₀Ser₅) -GFP CATAACATCTCCTTGCTTTTCTCCACCATCAATAGCAGCGCCAACCTTTTCATCTACTTT 840
Mas CATAACATCTCCTTGCTTTTCTCCACCATCAATAGCAGCGCCAACCTTTTCATCTACTTT 840

mas - (Gly₁₀Ser₅) -GFP TTTGTGGGCAGCAGTAAGAAGAAGCGCTTCAGGGAGTCCTTAAAAGTGGTCTTGACCAGA 900
Mas TTTGTGGGCAGCAGTAAGAAGAAGCGCTTCAGGGAGTCCTTAAAAGTGGTCTTGACCAGA 900

mas - (Gly₁₀Ser₅) -GFP GCTTTCAAAGACGAGATGCAACCTAGGCGCCAGGAGGGCAATGGCAACACTGTATCCATT 960
Mas GCTTTCAAAGACGAGATGCAACCTAGGCGCCAGGAGGGCAATGGCAACACTGTATCCATT 960

mas - (Gly₁₀Ser₅) -GFP GAGACTGTGGTCGGAGGAGGGGTACCGAGTGGTGGAGGCGGTTTCAGGCAGCGGTTCTAGC 1020

Mas GAGACTGTGGTCTGA 975

***** **

mas - (Gly₁₀Ser₅) -GFP GGCGGTGGCGGACCGGTGCGCCACC[REDACTED]GTGAGCAAGGGCGAGGAGCTGTTACCCGGGGTG 1080

GFP [REDACTED]GTGAGCAAGGGCGAGGAGCTGTTACCCGGGGTG 36

mas - (Gly₁₀Ser₅) -GFP GTGCCCATCCTGGTCGAGCTGGACGGCGACGTAAACGGCCACAAGTTCAGCGTGTCCGGC 1140

GFP GTGCCCATCCTGGTCGAGCTGGACGGCGACGTAAACGGCCACAAGTTCAGCGTGTCCGGC 96

mas - (Gly₁₀Ser₅) -GFP GAGGGCGAGGGCGATGCCACCTACGGCAAGCTGACCCTGAAGTTCATCTGCACCACCGGC 1200

GFP GAGGGCGAGGGCGATGCCACCTACGGCAAGCTGACCCTGAAGTTCATCTGCACCACCGGC 156

mas - (Gly₁₀Ser₅) -GFP AAGCTGCCCGTGCCCTGGCCACCCTCGTGACCACCCTGACCTACGGCGTGCAGTGCTTC 1260

GFP AAGCTGCCCGTGCCCTGGCCACCCTCGTGACCACCCTGACCTACGGCGTGCAGTGCTTC 216

mas - (Gly₁₀Ser₅) -GFP AGCCGCTACCCCGACCACATGAAGCAGCAGACTTCTTCAAGTCCGCCATGCCCGAAGGC 1320

GFP AGCCGCTACCCCGACCACATGAAGCAGCAGACTTCTTCAAGTCCGCCATGCCCGAAGGC 276

mas - (Gly₁₀Ser₅) -GFP TACGTCCAGGAGCGCACCATCTTCTTCAAGGACGACGGCAACTACAAGACCCGCGCCGAG 1380

GFP TACGTCCAGGAGCGCACCATCTTCTTCAAGGACGACGGCAACTACAAGACCCGCGCCGAG 336

mas - (Gly₁₀Ser₅) -GFP GTGAAGTTCGAGGGCGACACCCTGGTGAACCGCATCGAGCTGAAGGGCATCGACTTCAAG 1440

GFP GTGAAGTTCGAGGGCGACACCCTGGTGAACCGCATCGAGCTGAAGGGCATCGACTTCAAG 396

```

mas - (Gly10Ser5) - GFP GAGGACGGCAACATCCTGGGGCACAAGCTGGAGTACAACACTACAACAGCCACAACGTCTAT 1500
GFP GAGGACGGCAACATCCTGGGGCACAAGCTGGAGTACAACACTACAACAGCCACAACGTCTAT 456
*****

mas - (Gly10Ser5) - GFP ATCATGGCCGACAAGCAGAAGAACGGCATCAAGGTGAACTTCAAGATCCGCCACAACATC 1560
GFP ATCATGGCCGACAAGCAGAAGAACGGCATCAAGGTGAACTTCAAGATCCGCCACAACATC 516
*****

mas - (Gly10Ser5) - GFP GAGGACGGCAGCGTGCAGCTCGCCGACCACTACCAGCAGAACACCCCCATCGGCGACGGC 1620
GFP GAGGACGGCAGCGTGCAGCTCGCCGACCACTACCAGCAGAACACCCCCATCGGCGACGGC 576
*****

mas - (Gly10Ser5) - GFP CCCGTGCTGCTGCCCGACAACCACTACCTGAGCACCCAGTCCGCCCTGAGCAAAGACCCC 1680
GFP CCCGTGCTGCTGCCCGACAACCACTACCTGAGCACCCAGTCCGCCCTGAGCAAAGACCCC 636
*****

mas - (Gly10Ser5) - GFP AACGAGAAGCGCGATCACATGGTCCTGCTGGAGTTCGTGACCGCCGCCGGGATCACTCTG 1740
GFP AACGAGAAGCGCGATCACATGGTCCTGCTGGAGTTCGTGACCGCCGCCGGGATCACTCTG 696
*****

mas - (Gly10Ser5) - GFP GAAATGGACATGGACGAGCTGTACAAG 1770
GFP GAAATGGACATGGACGAGCTGTACAAG 726
*****

```

Figure 2.4 Multiple alignment of DNA sequence of mas-(Gly₁₀Ser₅)-GFP. The sequencing result of mas-(Gly₁₀Ser₅)-GFP was in 100% agreement with rat mas and GFP. The start codons and stop codons were highlighted with red and blue color, respectively. The stop codon of mas in mas-(Gly₁₀Ser₅)-GFP construct was mutated from TGA to GGA which was highlighted in the yellow color. Between mas and GFP there was an oligo sequence containing 45 nucleotides. The nucleotide numbers of the rat mas, GFP and mas-oligo-GFP were 975 bp, 726 bp and 1770 bp, respectively.

MDQSNM TSFA EEKAMNTSSR NASLGTSHPP IPIVHWVIMS ISPLGEYENG ILLWFLCFRM 60
 RRNPFTVYIT HLSIADISLL FCIFILSIDY ALDYELSSGH YYTIVTLSVT FLFGYNTGLY 120
 LLTAISVERC LSVLYPIWYR CHRPKHQSAF VCALLWALSC LVTTMEYVMC IDSGEESH SQ 180
 SDCRAVIIFI AILSFLVFTP LMLVSSTILV VKIRKNTWAS HSSKLYIVIM VTIIIFLIFA 240
 MPMRVLYLLY YEYWSTFGNL HNISLLFSTI NSSANPFIYF FVGSSKKKRF RESLKVVLTR 300
 AFKDEMQPRR QEGNGNTVSI ETVVGGSGSS GGGGSGSGSS GGGGSGSGSS MV SKGEELFTGV 360
 VPILVELDGD VNGHKFSVSG EGECDATY GK LTLKFICTTG KLPVPWPTLV TTLTYGVQCF 420
 SRYPDHMKQH DFFKSAMPEG YVQERTIFFK DDGNYKTRAE VKFEGDTLVN RIELKGIDFK 480
 EDGNILGHKL EYNYNSHNVY IMADKQKNGI KVNFKIRHNI EDGSVQLADH YQNTPIGDG 540
 PVLLPDNHYL STQSALS KDP NEKRDH MVLL E FVTAAGITL EMDMDELYK* 590

Figure 2.5 Protein sequence of mas-(Gly₁₀Ser₅)-GFP. Amino acid residues in blue and purple colors represented protein sequence of rat mas or GFP. The stop codon of mas in the fusion protein was mutated to glycine (G). The fifteen green colored amino acid residues containing ten glycines and five serines formed the peptide linker. The orange colored eight amino residues outside the two ends of peptide linker were originated from the multiple cloning sites in pEGFP-N1 vector. The rat mas, GFP and mas-(Gly₁₀Ser₅)-GFP fusion protein respectively contained 325 aa, 240 aa and 590 aa, respectively.

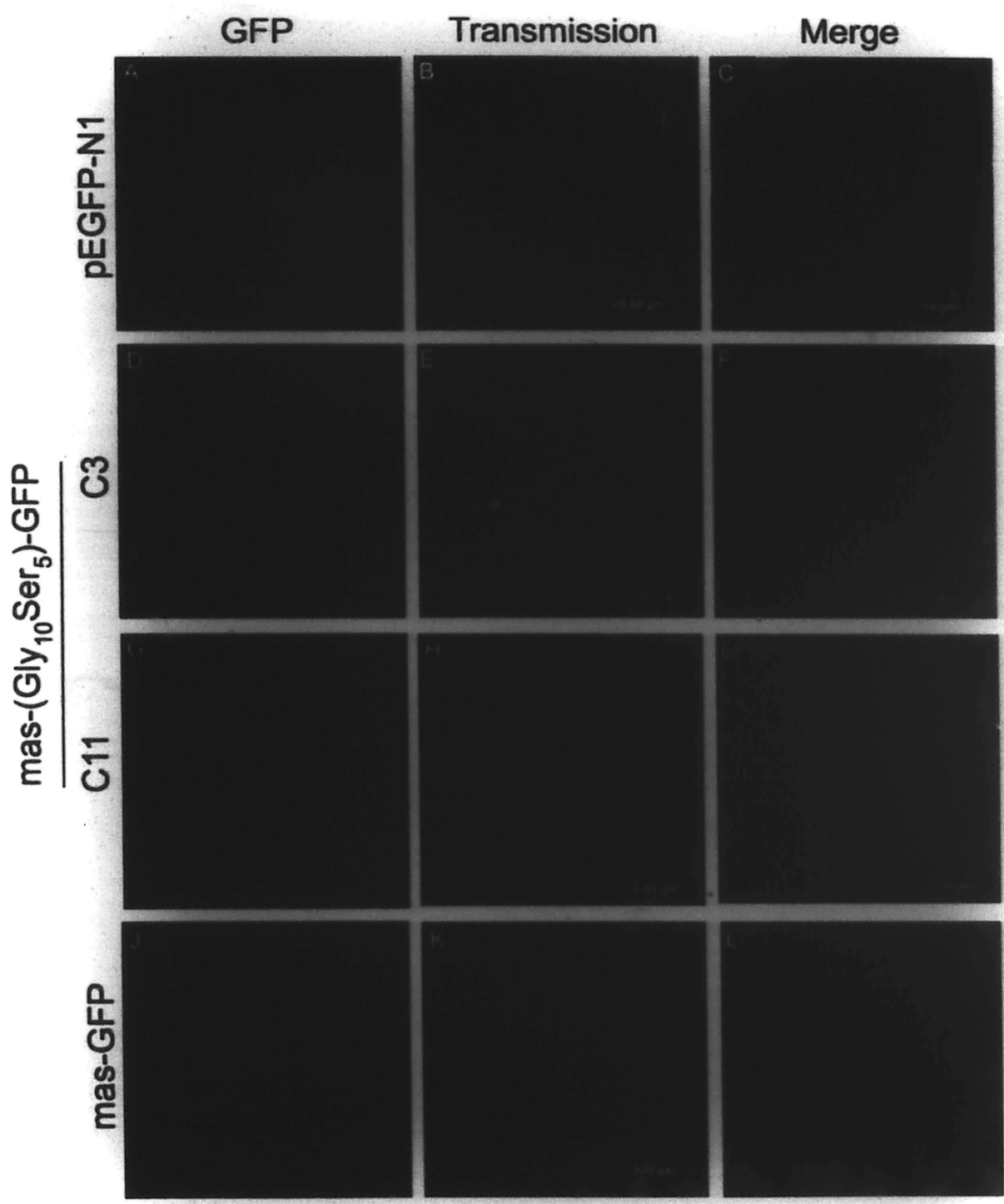
2.3.3 Confocal microscopy analysis

Cells stably expressing GFP, mas-(Gly₁₀Ser₅)-GFP and mas-GFP were subjected to confocal microscopy analysis for examination of intracellular distribution. GFP was excited at 488 nm by an Ar/Kr laser and green fluorescence was captured with a 525±50 bandpass filter. Fluorescence image and transmission image were captured separately and merged together to form overlay images. Green fluorescence in cells expressing GFP distributed evenly in the cytosolic spaces while that from mas fusion proteins was displayed sharply in the cell surface (Figure 2.6).

2.3.4 Immunoprecipitation and Western Blot analysis

Mas fusion proteins in cells stably expressing mas-(Gly₁₀Ser₅)-GFP and mas-GFP were immunoprecipitated with a polyclonal anti-GFP serum at 1:250 dilution. In addition, our lab raised an anti-mas serum against a peptide antigen. The anti-mas serum was shown to work for immunostaining but not for Western analysis (Bikkavilli et al., 2006). For further confirmation, mas-GFP and mas-(Gly₁₀Ser₅)-GFP fusion proteins were also immunoprecipitated using the anti-mas serum at 1:250 dilution and then Western analyzed by anti-GFP antibody. Cell line expressing pEGFP-N1 was used as the vector control. GFP had a size of about 24 kDa. Mas fusion proteins were characterized with a molecular weight of 64 to 82 kDa using anti-GFP serum for immunoprecipitation. By contrast, only a sharp protein band of 80 kDa was detected using anti-mas serum for immunoprecipitation (Figure 2.7).

Figure 2.6 Intracellular localization of GFP, mas-(Gly₁₀Ser₅)-GFP and mas-GFP fusion proteins. Green fluorescence from cells stably expressing GFP, mas-(Gly₁₀Ser₅)-GFP and mas-GFP were excited at 488 nm by an Ar/Kr laser and fluorescent images were captured with a 525±50 bandpass filter using a Leica TCSNT Confocal microscope. Fluorescent and transmission images were collected separately and merged to form overlay image. The experiments were repeated with at least three times independently.



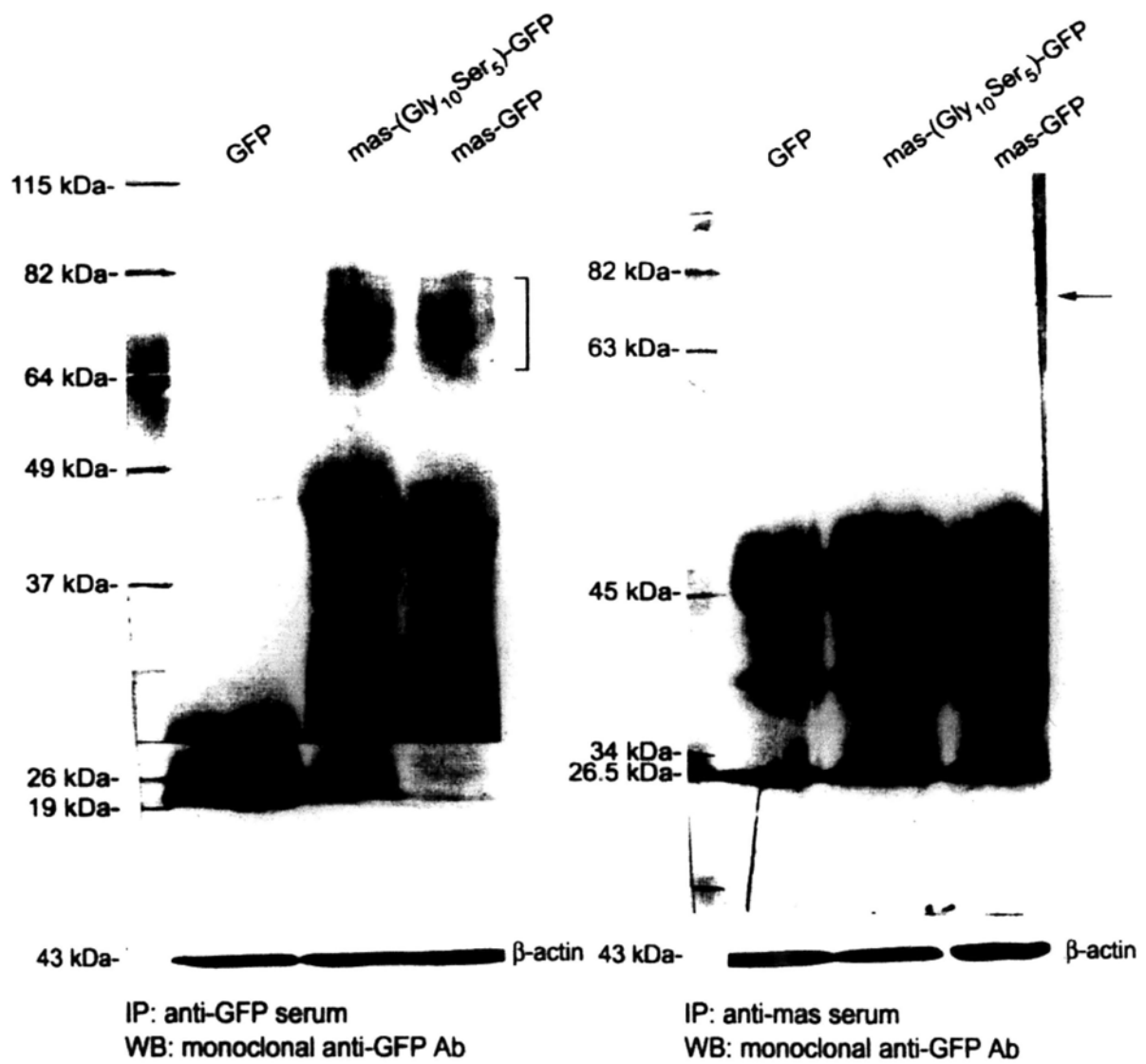


Figure 2.7 Stable expressions of different mas fusion proteins. Cells stably expressing GFP or mas fusion proteins were lysed with RIPA buffer followed by immunoprecipitation with anti-GFP (left) or anti-mas (right) serum. Immunoprecipitated GFP or mas fusion proteins were separated in 12% SDS-PAGE and then transferred to the nitrocellulose membrane. GFP (~25 kDa) and mas fusion proteins (64~82 kDa) were probed with anti-GFP monoclonal antibody. Blot of β -actin was the internal control and data shown was a representative of two separate experiments with similar results.

2.4 Discussion

GPCR-GFP fusion construct was a convenient way to trace GPCR localization and transportation in a real-time manner (Kallal & Benovic, 2000). Among GPCR family, β_2 -adrenoreceptor-GFP was studied most thoroughly. Translocation and membrane trafficking of the receptor after binding with the ligand were indicated by the migration of green fluorescence (Milligan, 1999). But GFP was too large to some proteins. As a tag, it might partially affect GPCRs' receptor activity.

The N-terminus and C-terminus of mas were predicted to locate in the extracellular and intracellular space, respectively. Since GFP was a cytosolic protein, it could be covalently tagged at the C-terminus of mas. Previous data from confocal microscopy analysis showed that direct tagging of GFP at the C-terminus might inhibit MBP7-triggered mas translocation. But this didn't happen on native mas. To alleviate GFP tagging effect, mas-(Gly₁₀Ser₅)-GFP construct was prepared. The molecular weight and intracellular distribution of the new construct was compared with native mas and mas-GFP. The fragment of forty-five oligo nucleotides expressing ten glycines and five serines were constructed derived from a peptide linker used in single chain variable fragment (scFv) in our lab. To minimize spatial hindrance, amino acid residues in the peptide linker were characterized with smaller size and fewer charges. The (Gly₁₀Ser₅) peptide linker was artificially fused in frame with mas and GFP. So mas-(Gly₁₀Ser₅)-GFP was expressed as a whole protein.

The molecular mass of mas and GFP were 40 kDa and 25 kDa, respectively. The peptide linker containing ten glycines and five serines with a predicted molecular mass of 1.8 kDa didn't make a significant difference between the size of mas-GFP and mas-(Gly₁₀Ser₅)-GFP. As expected, both the two mas fusion proteins showed a molecular weight between 64 kDa and 82 kDa in the blots.

It was of interest to note that a broad band (64~82 kDa) was obtained when anti-GFP was used for immunoprecipitation. The broad band might represent the difference in the glycosylation of mas. By contrast, a sharp band of ~80 kDa was obtained when anti-mas serum was used for immunoprecipitation. The difference might be attributed to the affinity difference between the two serums. Anti-GFP is a polyclonal serum against purified GFP while anti-mas is a polyclonal serum against a peptide antigen. Hence, it was predicted that anti-GFP had high avidity than anti-mas for immunoprecipitation, and it was likely only one of the major glycosylated mas was immunoprecipitated by the anti-mas serum.

In the confocal microscopy analysis, the distribution of mas-GFP and mas-(Gly₁₀Ser₅)-GFP were similar to that of native mas. They always displayed a membrane localization pattern. So GFP tagging and peptide linker between GFP and mas didn't alter the intracellular localization of mas protein.

In general, mas-(Gly₁₀Ser₅)-GFP was successfully constructed and expressed in CHO cells.

Chapter 3

Functional Characterization

of Mas Protein

3.1 Introduction

Investigation on β -adrenergic receptor showed that GPCRs were translocated to the cell surface or internalized into the cytosolic space upon ligand binding. Activation of GPCR was reported to stimulate secondary signaling pathways, such as calcium-dependent downstream reactions and so on.

Since mas was an orphan GPCR, all the functional assays on mas were performed using the surrogate ligand identified using phage displayed peptide library (Bikkavilli et al., 2006). Ligand binding to native mas or mas fusion proteins was visualized by co-localization of mas and phages expressing surrogate ligand using immunocytochemistry. The translocation of mas fusion proteins after MBP7 treatment was quantified with biotinylation assay. Downstream signaling of activated mas or mas fusion protein was determined by calcium ion concentration ($[Ca^{2+}]_i$) measurement.

3.2 Materials and Methods

3.2.1 *Materials*

3.2.1.1 *Chemicals*

Iscove's modified DMEM medium, F12-Nutrient Mixture (Ham), fetal bovine serum, penicillin/streptomycin, HT supplement and BenchMark™ pre-stained protein ladder were from Invitrogen (Carlsbad, CA, USA). G418 were from Merck Biosciences (Whitehouse Station, NJ, USA). Bacto™ Yeast Extract and Bacto™ Tryptone were from

Becton, Dickinson and Company (Sparks, MD, USA). EZ-Link sulfo-NHS-biotin reagents, sulfo-NHS-SS-biotin and immobilized streptavidin were from Pierce (Rockford, IL, USA). MBP7 (KAQLRRLS) peptide was synthesized in-house using Fmoc solid-phase technique with an Applied Biosystems 433A peptide synthesizer (Applied biosystems, Foster City, CA, USA). Fura-2 AM^{*} was from Molecular Probes Inc (Eugene, OR, USA). Nitrocellulose transfer membrane was from Whatman (Hahnstrabe 3, D-37586 Dassel, Germany). Nitroblue tetrazolium chloride (NBT) and 5-bromo-4-chloro-3-indolylyl-phosphate-4-toluidine salt (BCPIP) were from Roche (Roche Diagnostics Corporation, IN, USA). All the other chemicals and reagents were of molecular grade from Sigma-Aldrich (St. Louis, MO, USA).

3.2.1.2 Antibodies

Mouse monoclonal anti-GFP antibody was from Clontech (Mountain View, CA, USA). Rabbit anti-mas polyclonal serum was raised against a peptide antigen derived from the putative C-terminus of mas protein in our laboratory (Bikkavilli et al., 2006). M13KO7 helper phage and anti-M13 monoclonal antibody were from GE Healthcare (Piscataway, NJ, USA). Cy³-conjugated goat anti-mouse antibody, FITC-conjugated goat anti-rabbit antibody and AP-conjugated goat anti-mouse antibody were from Zymed Laboratories (San Francisco, CA, USA).

3.2.2 Methods

3.2.2.1 Phage binding assay

3.2.2.1.1 Preparation of phages

Phage clone 3p5A190 (enriched sequence of consensus motif 2, FLVTLTRTWAIR) which expressed surrogate ligand of mas was chosen for phage binding assay. Bacterial stock of it was spread on the SOBAG plate and grown at 30°C overnight. Single colony was picked and gently shaken in 5 ml of 2x YT medium containing 100 µg/ml ampicillin and 2% glucose for 5 hours at 37°C. Aliquot of 100 µl of the above culture were inoculated into 1 ml of 2x YT medium containing 2% glucose, 5 mM MgCl₂ and 100 µg/ml ampicillin. M13KO7 helper phages (2.5×10^{11} pfu) were added to the mixture and shaken for two hours at 37°C to let helper phages enter the bacteria. The bacteria containing the whole target phages were concentrated with centrifugation at 4000 rpm for 10 minutes at 4°C. Bacteria pellet from every 1 ml of the above culture was resuspended in every 10 ml of 2x YT medium containing 100 µg/ml ampicillin and 50 µg/ml kanamycin and grown at 37°C overnight for package of the whole phages. The bacteria pellets were obtained by spin down at 4000 rpm for 5 minutes at room temperature. Phages released into the supernatant were precipitated by co-incubation with 1/5th volume of PEG/NaCl (20% polyethylene glycol 8000 in 2.5 M NaCl solution) and incubated on ice for at least 1 hour. Precipitated phages were collected by centrifugation at 10000 rpm for 15 minutes at 4°C. The concentrated phages were resuspended in appropriate volume of IMDM complete medium.

3.2.2.1.2 Phage immunocytochemistry

Cells (2.5×10^4) were seeded on coverslips in a 24-well plate and grown for 16 hours at 37°C, 5% CO₂. After discarding the medium, cells were incubated with IMDM complete medium (1 ml per well) containing freshly prepared phages (1×10^{11}) for 1 hour at 37°C, 5% CO₂. The unbound phages were removed by washing with 1x PBS for 5 minutes for 3 times. Cells were then fixed with freshly prepared 4% paraformaldehyde in PBS for 10 minutes and permeabilized with 0.1% Triton[®] X-100 for another 10 minutes at room temperature. Fixed and permeabilized cells were incubated with IMDM complete medium (250 µl per well) containing (1:250, v/v) mouse anti-M13 monoclonal antibody at 37°C, 5% CO₂ for 3 hours. Rabbit anti-mas serum (1:250, v/v) was added Mc0M80 or Vc0M80 cells. Unbound anti-M13 antibody was removed by washing with PBS as described above. The bound phages to mas or mas fusion proteins were detected by Cy³-conjugated sheep anti-mouse antibody (1/250, v/v) or FITC-conjugated goat anti-rabbit antibody (1/250, v/v) in IMDM complete medium (250 µl per well) for 2 hours at 37°C, 5% CO₂. The excess secondary antibodies were washed out with 1x PBS and air-dried in the dark. Finally cells on the coverslips were mounted with anti-fade mounting medium (2.3% 1,4-diazabicyclo-[2,2,2]-octane, 90% glycerol, 0.02% sodium azide and 0.1 M Tris-HCl, pH 8.0) and sealed with nail polish. GFP and FITC were excited at 488 nm and detected with a 525±50 bandpass filter. Red fluorescence from Cy³ was excited at 568 nm and detected with a 590 nm longpass filter.

3.2.2.2 Biotinylation assay

Surface proteins were covalently labeled with water-soluble, membrane impermeable biotin reagents and isolated with immobilized streptavidin. Changes in the amount of surface proteins before and after ligand stimulation were quantitatively evaluated by band intensity. Two strategies using different biotin reagents were used to examine the change of membrane fusion proteins. The detailed working flows were shown schematically in **Figure 3.1** and **Figure 3.2**. Briefly, cells were collected by trypsinization (0.05%) from 150 cm culture flask. For strategy 1, equal numbers of cells were divided into control group and treatment group. After incubation for 15 minutes with medium in the absence or presence of 100 μ M MBP7, cells were incubated with 1 mg/ml sulfo-NHS-biotin at room temperature for 30 minutes. Biotin-labeled cells were then lysed and precipitated with immobilized streptavidin and finally probed with anti-GFP antibody. For strategy 2, cells were firstly incubated with sulfo-NHS-ss-biotin at room temperature for 30 minutes before divided into two groups. Cells with equal number in the control or treatment group were incubated with medium in the absence or presence of 100 μ M MBP7 for 15 minutes. Cells were then treated with reducing reagent to remove biotin from membrane protein by cleaving the disulfide bond in the biotin reagent in the cell surface. After lysis, biotin-labeled proteins in the lysate were precipitated with immobilized streptavidin and detected with an anti-GFP antibody. The differences of band intensities in the absence or presence of MBP7 treatment were quantified using the UN-SCAN-IT software (Silk Scientific, Utah, USA). Statistical significance of quantified data was analyzed with SigmaStat 3.0 program (SPSS Inc, IL, USA).

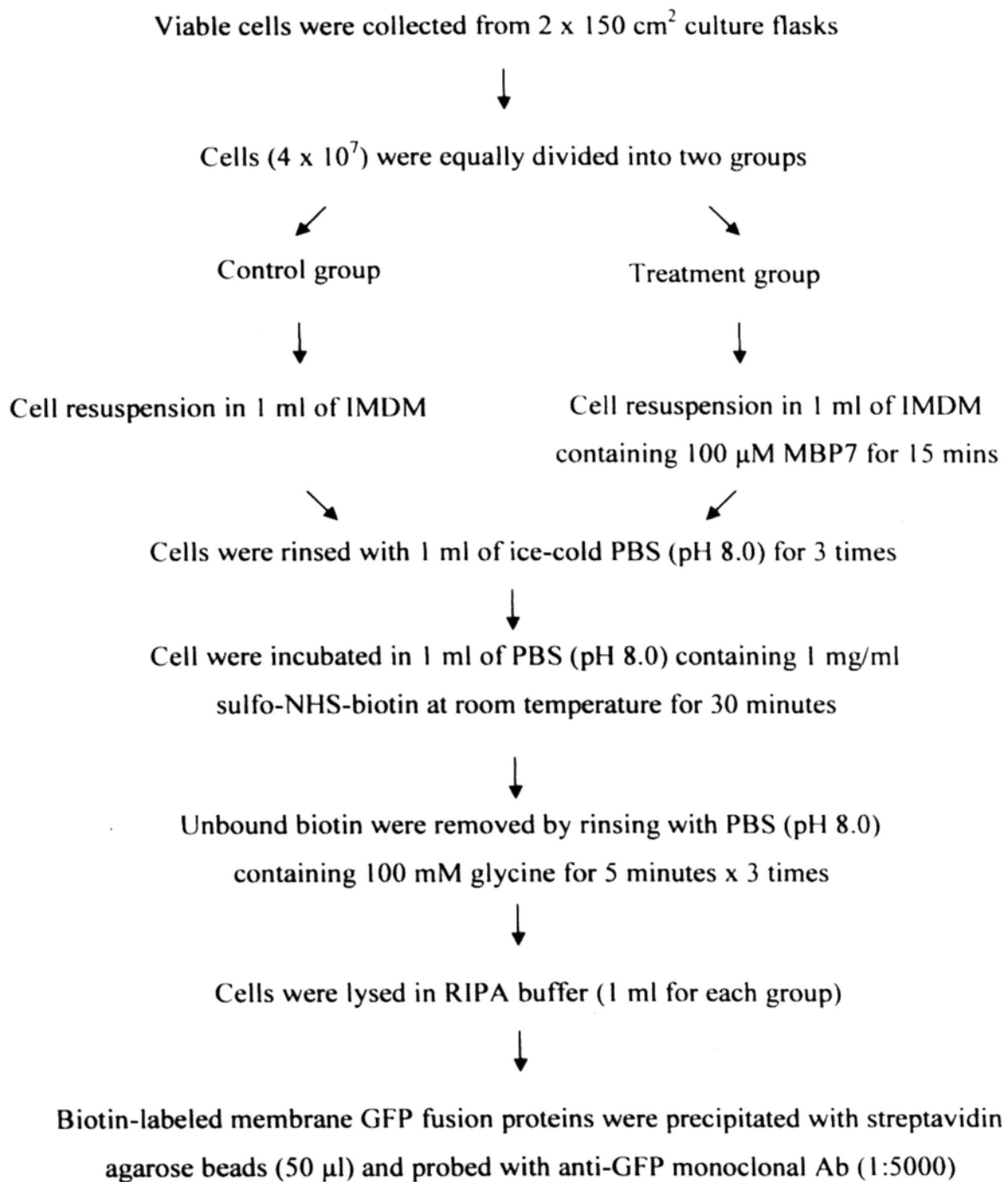


Figure 3.1 Biotinylation strategy 1 using sulfo-NHS-biotin.

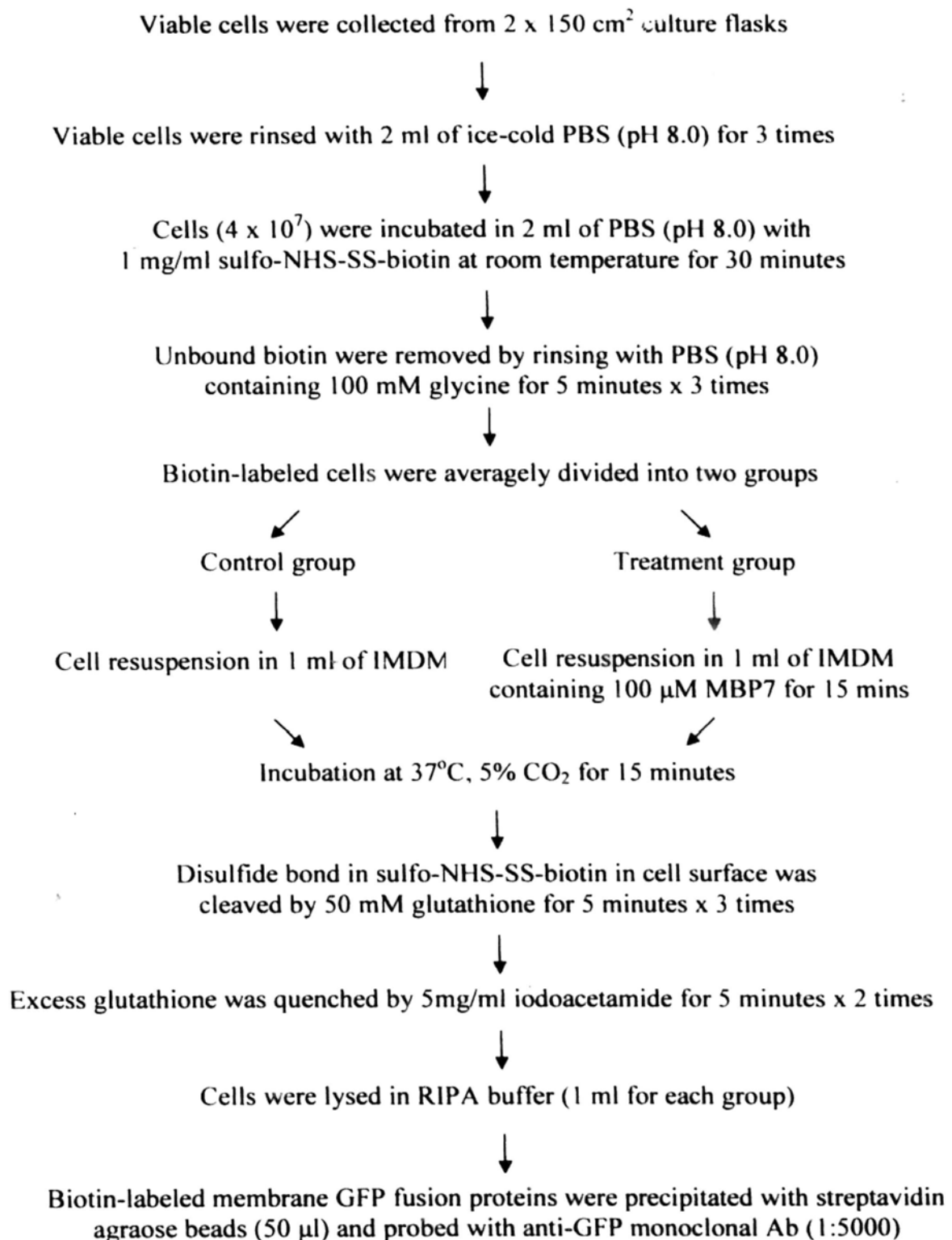


Figure 3.2 Biotinylation strategy 2 using sulfo-NHS-SS-biotin reagent.

3.2.2.3 Intracellular calcium ion concentration ($[Ca^{2+}]_i$) measurement

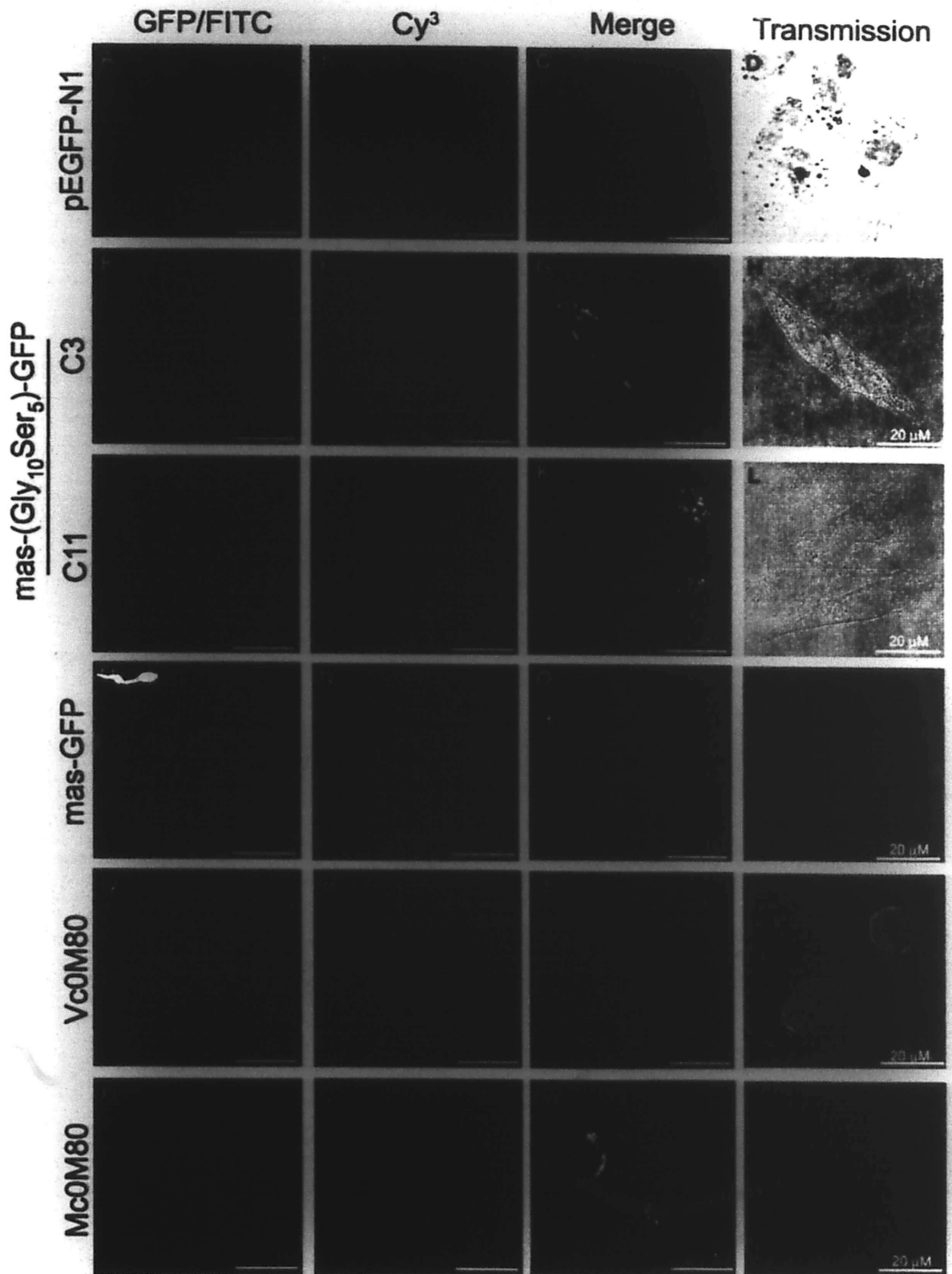
After growing on coverslips in a 6-well plate for 24 hours, cells (1×10^5) were loaded with $3\mu\text{M}$ Fura-2 AM* fluorescence dye and $1.6\mu\text{M}$ pluronic F-127 in bicarbonate-buffered Krebs-Henseleit (K-H) solution (117 mM NaCl, 24.8 mM NaHCO_3 , 4.7 mM KCl, 1.2 mM MgCl_2 , 1.2 mM KH_2PO_4 , 2.56 mM CaCl_2 and 11.1 mM glucose, pH 7.4) at 37°C , 5% CO_2 for 45 minutes. The coverslip was then assembled into a perfusion chamber containing 1 ml of K-H solution. Dye-loaded cells were observed with a 40x objective in an Olympus IX70 microscope equipped with a Photometrics CCD camera (Quantix A99G606). Fura-2 can be excited with dual wavelengths at 340 nm and 380 nm and monitored emission at 510 nm. $[Ca^{2+}]_i$ is positively correlated with the emission ratio at 510 nm, which is defined as emission intensity at 510 nm excited at 340 nm ($\text{Em}_{510_{340}}$) versus the emission intensity at 510 nm excited at 380 nm ($\text{Em}_{510_{380}}$). The emission ratio ($\frac{\text{Em}_{510_{340}}}{\text{Em}_{510_{380}}}$) is coded into a color scale bar to visually reflect $[Ca^{2+}]_i$ change. Stimulation by $30\mu\text{M}$ or $100\mu\text{M}$ MBP7 were carried out by injection of $3\mu\text{l}$ or $10\mu\text{l}$ of 10 mM MBP7 into the K-H solution, respectively. Data was analyzed by the Meta Fluor software (Molecular Devices Inc, CA, USA).

3.3 Results

3.3.1 *Phage binding assay*

To examine whether GFP direct tagging at mas C-terminus inhibited ligand binding, Mc0M80 expressing native mas and cells stably expressing two mas fusion variants were examined for phage binding activity. Cells expressing pEGFP-N1 and Vc0M80 expressing pFRSV were used as the vector control cell lines. Native mas and bound phages encoding mas ligand were detected with the anti-mas serum and an anti-M13 monoclonal antibody, respectively. Green fluorescence from GFP fused mas or FITC-labeled native mas was excited at 488 nm and detected by a 525±25 bandpass filter. Cy³-labeled phages were excited at 568 nm and red fluorescence was probed with a 590 nm longpass filter. In cells expressing the two different types of mas fusion variants, phages (red fluorescence) had strong and punctate binding to mas fusion proteins (Figure 3.3, Panels F, J & N). Furthermore, the bound and internalized phages in clone 11 of cells expressing mas-(Gly₁₀Ser₅)-GFP were much more than that in cells expressing mas-GFP. In cells expressing native mas, phages bound to the cell surface and internalized in large quantity and formed several clusters (Figure 3.3, Panel V). In comparison, the two vector control cell lines expressing pEGFP-N1 or pFRSV only showed a weak background but not the specific phage binding signals (Figure 3.3, Panel B & R).

Figure 3.3 Phage binding assay. Cells expressing pEGFP-N1, mas fusion proteins, Mc0M80 and Vc0M80 were examined in the experiment. Green fluorescence from FITC-labeled mas or mas fusion proteins were excited with 480 nm and detected with a 525±25 nm bandpass filter. Red fluorescence from Cy³-labeled phages were excited 568 nm and monitored with a 590 nm longpass filter. Native mas and mas fusion proteins were distributed clearly on the cell surface while GFP was localized in intracellular space. Phage expressing mas putative ligand specifically bound to cells expressing native mas or mas fusion proteins. Fluorescence images and transmission images were collected separately and merged together to produce overlay images. The yellow fluorescence represented co-localization of green and red fluorescence.



3.3.2 *Biotinylation assay*

To compare the translocation of different types of mas fusion proteins quantitatively, cells stably expressing mas-(Gly₁₀Ser₅)-GFP and mas-GFP were subjected to biotinylation assay. Cells expressing pEGFP-N1 were used as the vector control in the experiment. In strategy 1, cells were subjected to biotin incubation after MBP7 treatment in order to detect translocation of membrane mas fusion proteins. In strategy 2, cells were incubated with biotin before MBP7 treatment in order to label membrane mas fusion proteins being translocated into cytosol.

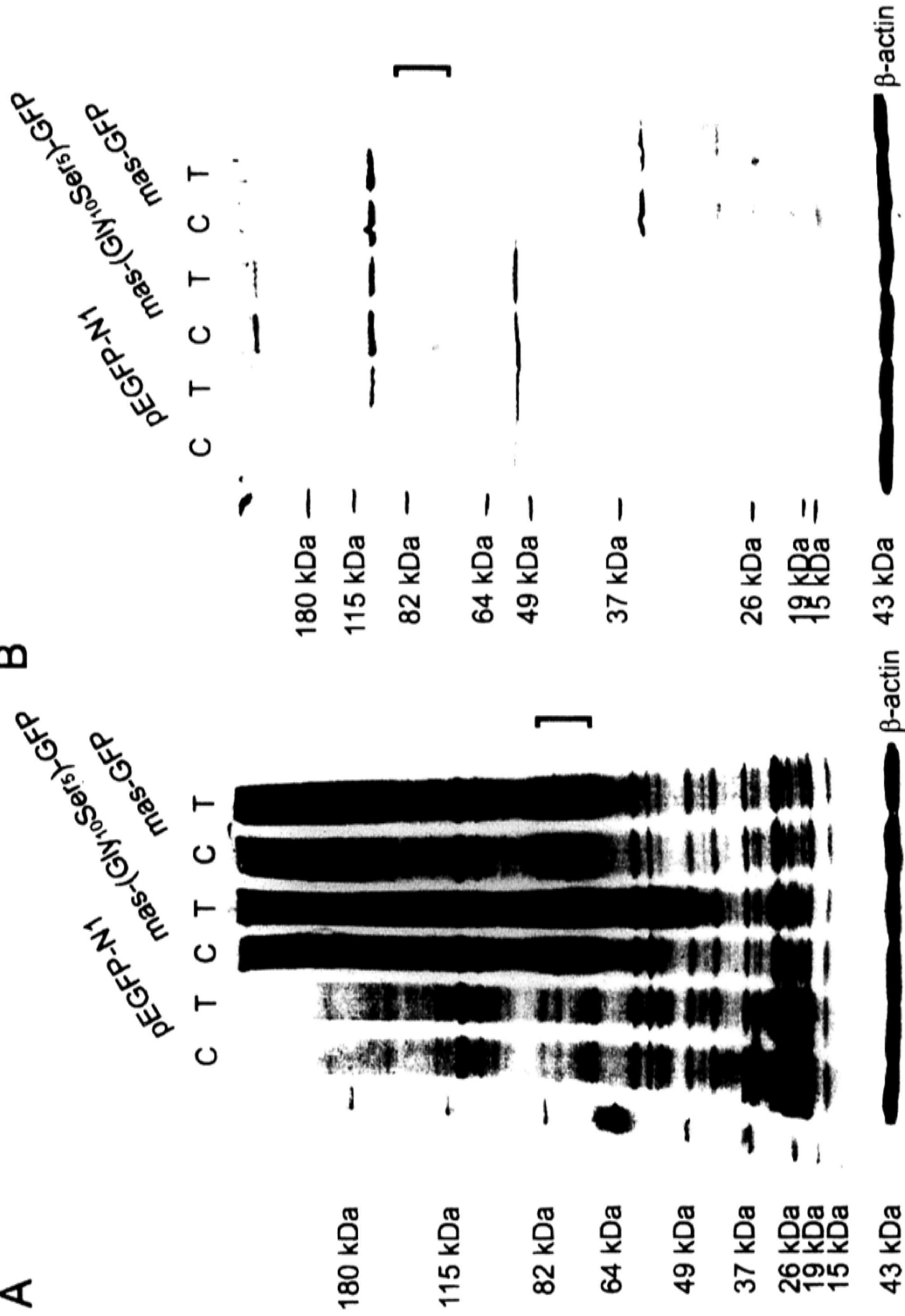
Specific bands for mas fusion proteins were detected between 64 kDa and 82 kDa with anti-GFP monoclonal antibody in cells expressing mas-(Gly₁₀Ser₅)-GFP or mas-GFP (Figure 3.4A & Figure 3.4B). The band intensity of each cell line in the basal condition or upon MBP7 treatment was quantified using the UN-SCAN-IT software and expressed as total pixels. Area between 64 kDa and 82 kDa in the control group of GFP-expressing cells was used as background control. The quantified band intensity was plotted against intensity of background control and showed a linear increase with the increase of background intensities (Figure 3.4C & Figure 3.4D). Hence, the background intensity between 64 kDa and 82 kDa in GFP-expressing cells (control group) was taken as basal, and band intensities in the corresponding area of other cell lines were normalized against the background intensity of the control group (Figure 3.4E & Figure 3.4F). The difference of band intensity between control (C) and treatment (T) group in cells expressing various mas fusion proteins indicated translocation difference of mas fusion proteins. Higher band intensity of mas fusion proteins was detected when cells were

treated with MBP7 before biotinylation (Figure 3.4A & 3.4E) indicating that MBP7 increased cell surface mas fusion proteins. In parallel, the band intensity of biotin-labeled cells treated with MBP7 showed less band intensity of mas fusion proteins than that of the control group (Figure 3.4B & 3.4F) indicating that MBP7 decreased internalization of surface mas fusion proteins. Alternatively, the intensity between 64 kDa and 82 kDa in the untreated cells of each cell line was expressed as 100% and the intensities of the MBP7-treatment cells were normalized against corresponding untreated cells (Figure 3.4G & 3.4H). The pattern was similar to that in Figure 3.4E and 3.4F. The results of the two strategies were in agreement with each other and proposed the possibility that MBP7 increased the membrane trafficking of mas fusion proteins by slowing down the constitutive internalization of them. In addition, less band intensity differences between control and MBP7 treatment groups were shown in cells expressing mas-GFP compared with cells expressing mas-(Gly₁₀Ser₅)-GFP indicating that mas-(Gly₁₀Ser₅)-GFP mas-GFP was more responsive to MBP7 than mas-GFP. Statistical analysis on normalized band intensity between control and MBP7-treatment group in each cell line summarized from two or three independent experiments were performed t-test and showed no difference.

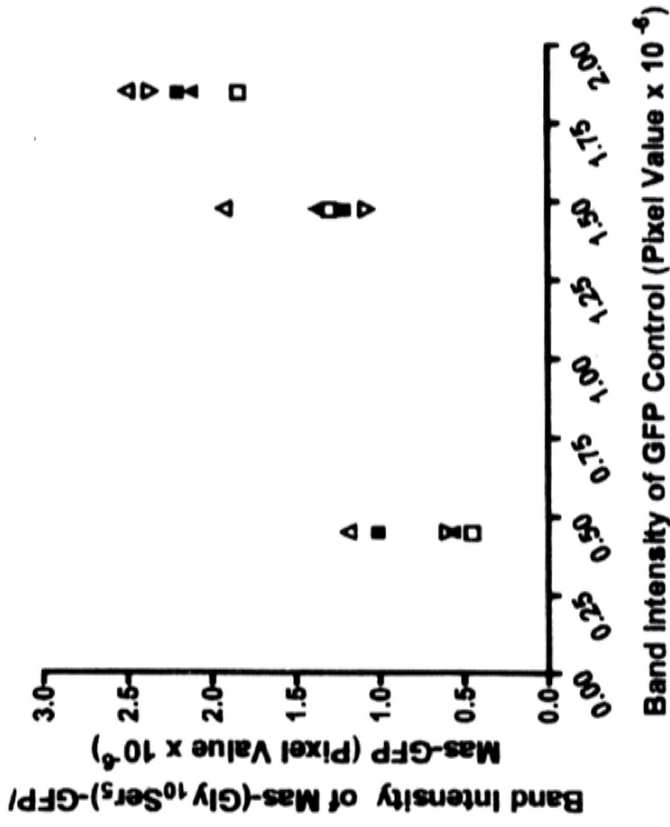
Figure 3.4 Biotinylation assay. (A & B) Western blot of biotinylated mas fusion proteins. Membrane mas-(Gly₁₀Ser₅)-GFP and mas-GFP were purified by cell surface biotinylation with sulfo-NHS-biotin (A) or sulfo-NHS-ss-biotin (B) followed with immobilized streptavidin precipitation and detected by anti-GFP monoclonal antibody. pEGFP-N1 was used as the control cell line and β -actin was used to indicate immunoprecipitation of equal amount of lysate from each sample. "C" and "T" represented control and treatment group, respectively. The difference of band intensity between control and MBP7-treatment group indicated difference of membrane mas fusion proteins amount (A) or internalized mas fusion proteins amount (B) before and after MBP7 treatment. (C & D) Spot graph showing quantitative band intensity of mas fusion proteins against band intensity of GFP in the basal condition. The immunoreactive bands in the protein blots were digitalized using a flat-bed scanner (EPSON GT-9500) with the UN-SCAN-IT™ software. Band intensity was displayed as pixel values and each pixel value ranged from 0 to 255, representing scale from white to black. Each symbol represented an individual cell line under certain treatment. Area between 64 kDa and 82 kDa in the control group of GFP-expressing cells was used as background control. (E & F) Band intensities of mas-GFP and mas-(Gly₁₀Ser₅)-GFP between 64 kDa and 82 kDa were normalized against background intensity of control group of GFP-expressing cells in the same location. (G & H) Band intensities of mas-GFP and mas-(Gly₁₀Ser₅)-GFP were normalized against individual untreated control and expressed as percentage. Data shown were mean \pm S.E.M from three to four independent experiments. The blots were representatives from three consistent experiments with similar results.

A

B



C



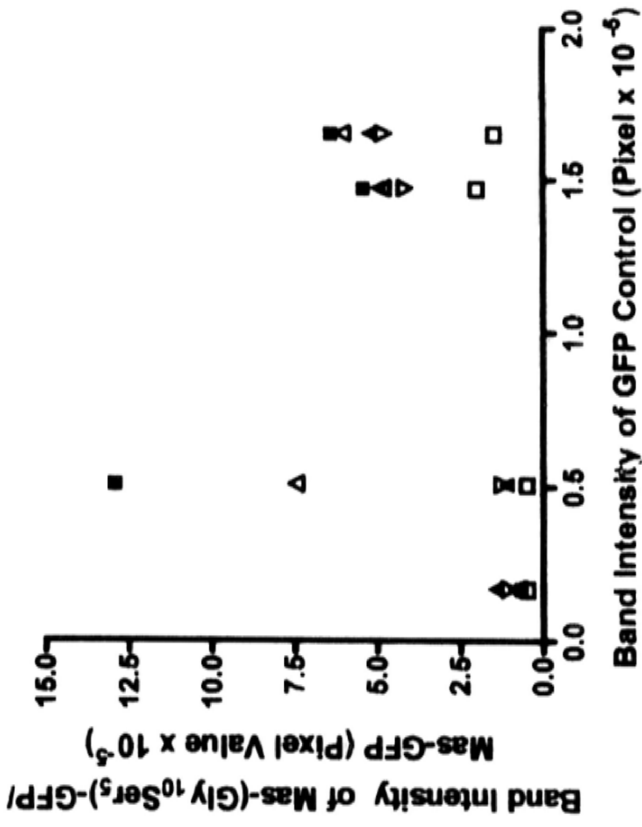
IP: sulfo-NHS-biotin & streptavidin beads

WB: anti-GFP mAb

■ Mas-(Gly₁₀Ser₅)-GFP control ▲ Mas-GFP control □ GFP MBP7

▲ Mas-(Gly₁₀Ser₅)-GFP MBP7 ▼ Mas-GFP MBP7

D

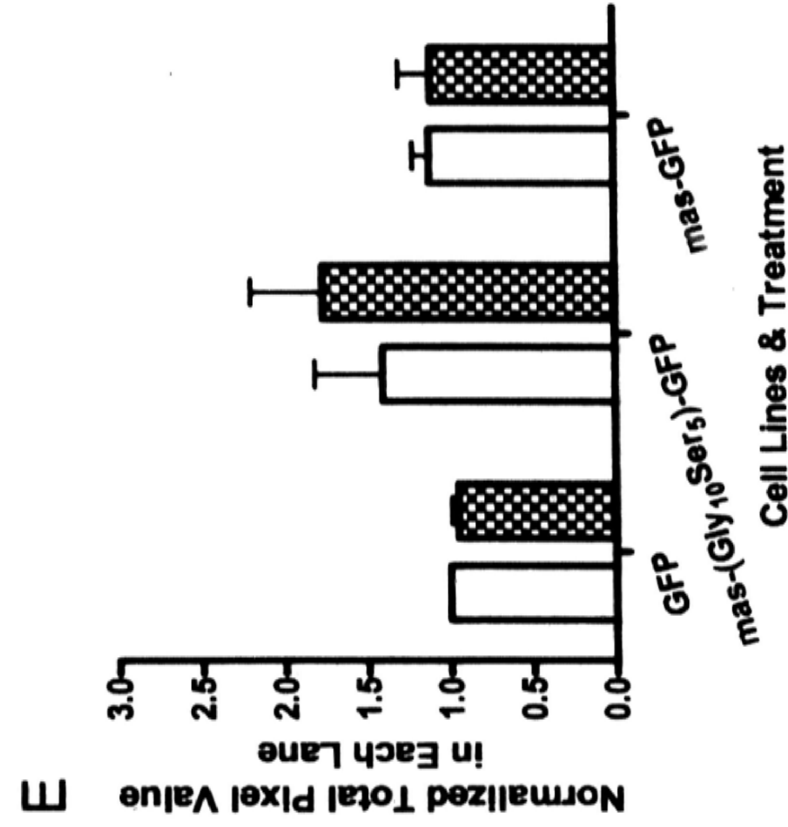


IP: sulfo-NHS-ss-biotin & streptavidin beads

WB: anti-GFP mAb

■ Mas-(Gly₁₀Ser₅)-GFP MBP7 ▲ Mas-GFP MBP7

▼ Mas-GFP MBP7

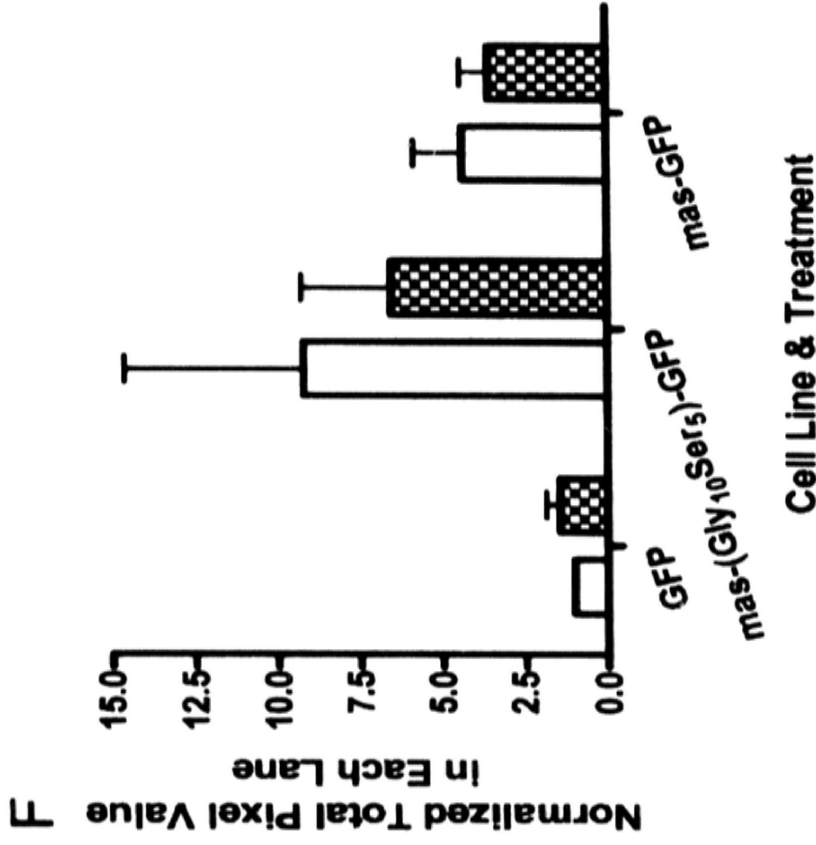


IP: sulfo-NHS-biotin & streptavidin beads

WB: anti-GFP mAb

□ Control

▨ 100 μ M MBP7



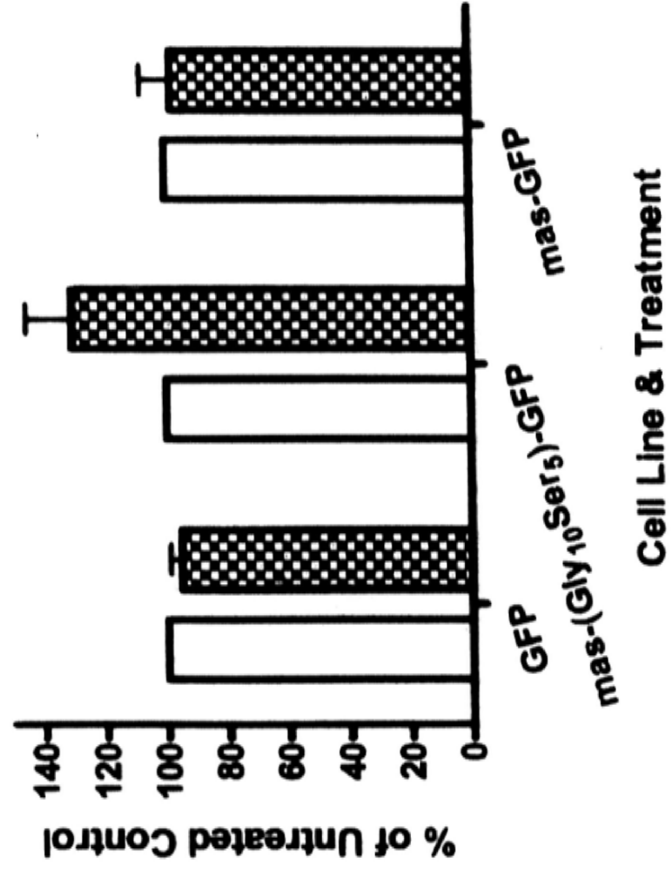
IP: sulfo-NHS-ss-biotin & streptavidin beads

WB: anti-GFP mAb

□ Control

▨ 100 μ M MBP7

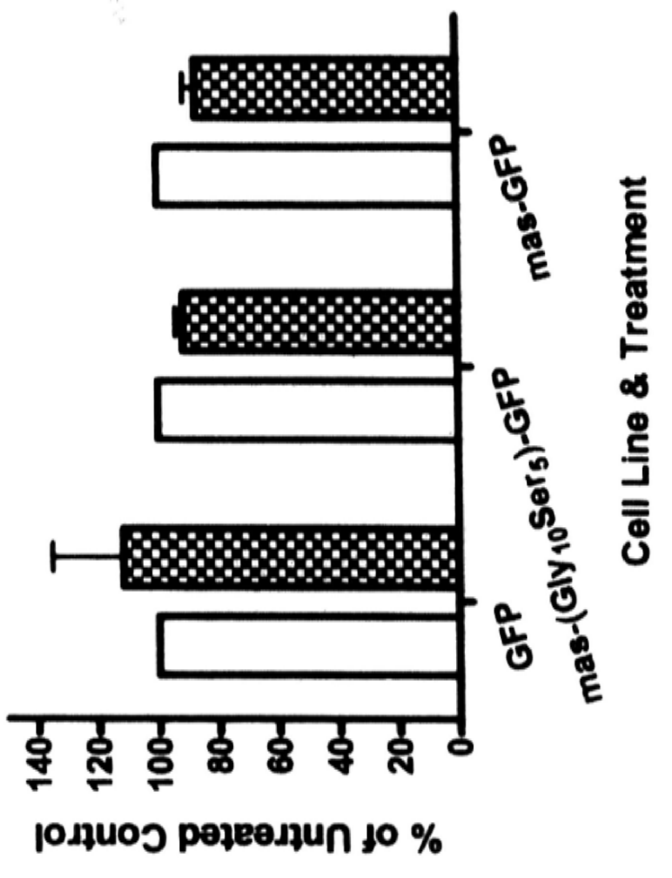
G



IP: sulfo-NHS-biotin & streptavidin beads
WB: anti-GFP mAb

□ Control
▨ 100 μM MBP7

H



IP: sulfo-NHS-ss-biotin & streptavidin beads
WB: anti-GFP mAb

□ Control
▨ 100 μM MBP7

3.3.3 Intracellular calcium ion concentration ($[Ca^{2+}]_i$) measurement

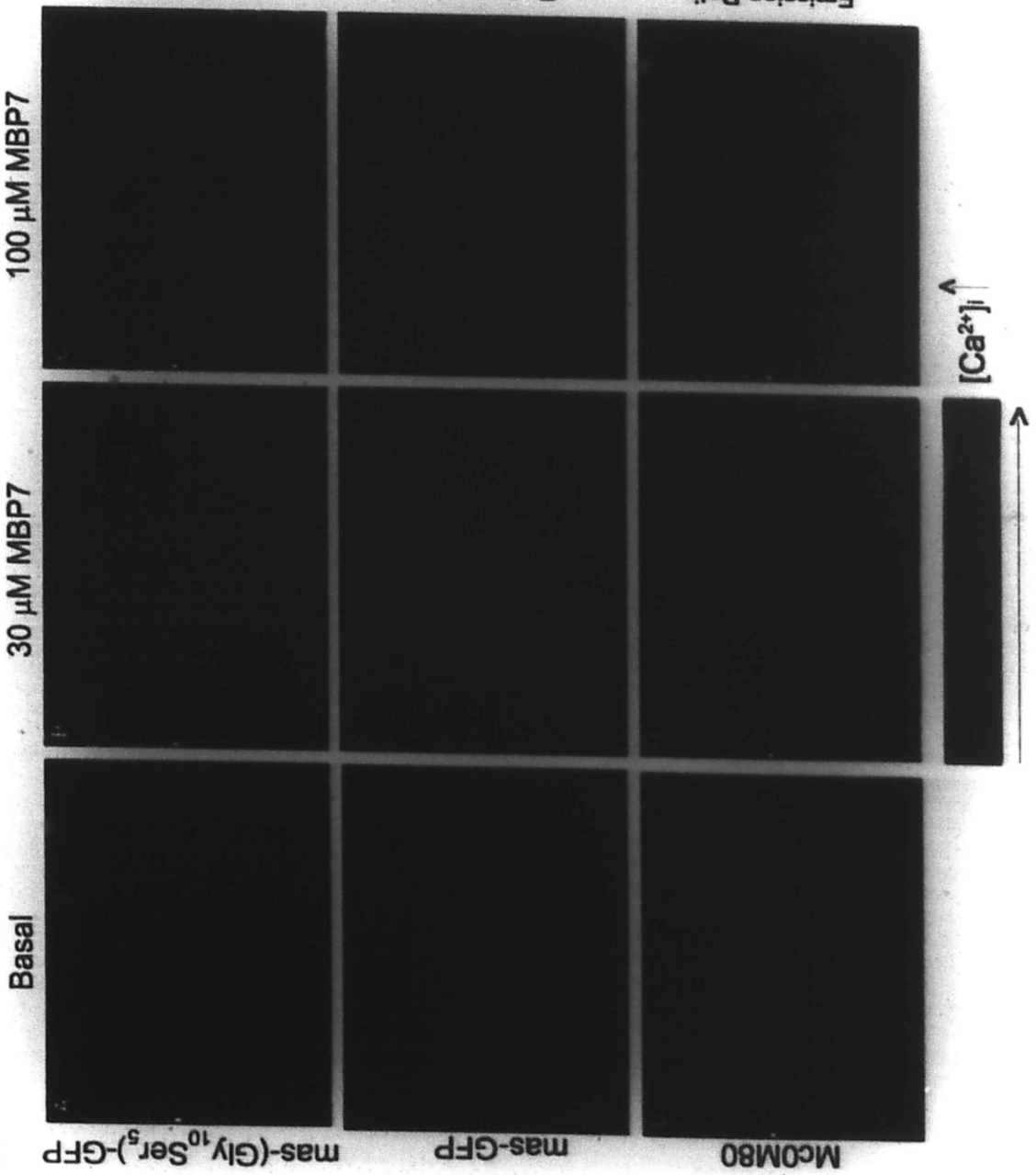
To investigate whether mas C-terminus affected downstream signaling after ligand binding, $[Ca^{2+}]_i$ were examined in the absence or presence of MBP7. Cells were preloaded with Fura-2, a fluorescence dye with high affinity to $[Ca^{2+}]_i$, for 45 minutes. The basal and MBP7-stimulated $[Ca^{2+}]_i$ were measured.

Fura-2 can be excited at 340 nm and 380 nm, and gives a maximal fluorescent emission at 510 nm. The rise of $[Ca^{2+}]_i$ can increase the emission at 510 nm ($Em_{510_{340}}$) upon excited at 340 nm while decrease the emission at 510 nm ($Em_{510_{380}}$) upon excitation at 380 nm. Therefore, $[Ca^{2+}]_i$ change can be indicated by the emission ratio at 510 nm excited at 340 nm and 380 nm, namely $\frac{Em_{510_{at\ 340}}}{Em_{510_{at\ 380}}}$. The emission ratio at 510 nm is then coded into a color scale bar to visually reflect the $[Ca^{2+}]_i$ change.

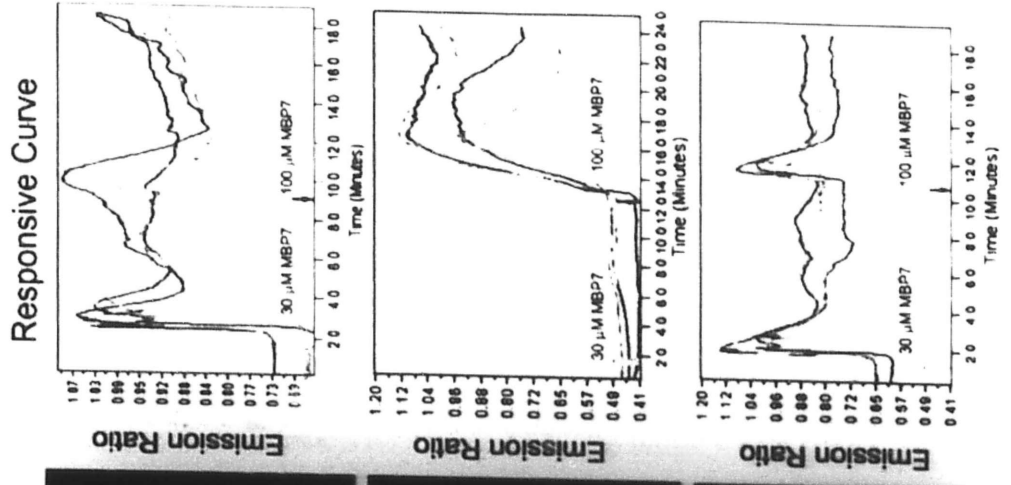
The basal $[Ca^{2+}]_i$ in Mc0M80 and in the cells expressing the two types of mas fusion proteins were low and represented in a blue pseudocolor. Upon stimulation with MBP7 (30 μ M and 100 μ M), $[Ca^{2+}]_i$ was increased rapidly and the rise of $[Ca^{2+}]_i$ was represented by a shift from blue to green pseudocolor. All the three cell lines showed increased $[Ca^{2+}]_i$ upon MBP7 stimulation (Figure 3.5A). However, differences were noted among the three cell lines when individual responsive curves were plotted from randomly selected responsive cells. Mc0M80 and cells expressing mas-(Gly₁₀Ser₅)-GFP responded to both 30 μ M and 100 μ M MBP7 stimulations. In contrast, cells expressing mas-GFP only responded to the higher concentration of MBP7 (Figure 3.5B).

Figure 3.5 Intracellular calcium ion concentration ($[Ca^{2+}]_i$) measurement for cells expressing mas fusion proteins or native mas. (A) Color photos indicating $[Ca^{2+}]_i$ change. Cells expressing mas fusion proteins and Mc0M80 expressing native mas were pre-loaded with Ca^{2+} -sensitive fluorescence dye Fura-2 AM*. The cells were excited at 340 nm and 380 nm, separately, and fluorescent emission was monitored at 510 nm. Increase of $[Ca^{2+}]_i$ was indicated by the increased emission ratio ($\frac{Em\ 510_{340}}{Em\ 510_{380}}$), which was coded into the color scale to visually reflect $[Ca^{2+}]_i$ change. (B) Individual responsive curves against time. Curves in various colors represented randomly selected responsive cells. The two stimulations from MBP7 were indicated at the X axis with an open (30 μ M) and a close (100 μ M) arrow, respectively. The Y axis showed the emission ratio ($\frac{Em\ 510_{340}}{Em\ 510_{380}}$) and the X axis recorded the experimental time. Data shown were representatives of at least three separate experiments with similar results.

A



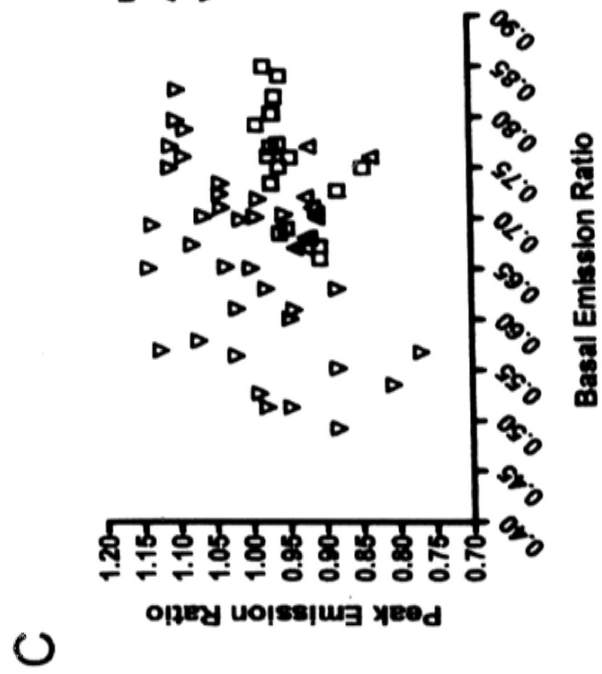
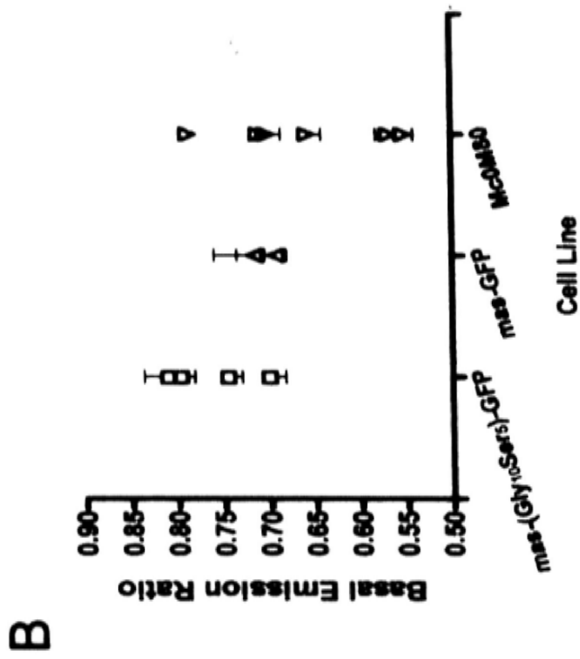
B



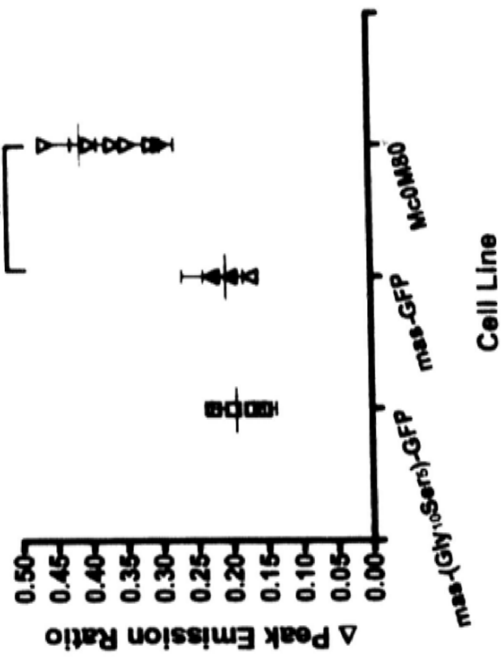
The change of emission ratio at 510 nm from the basal condition to the peak response or to the plateau response at five-minutes after peak response were quantitized from the responsive curves and represented as Δ Peak Emission Ratio and Δ Plateau Emission Ratio, respectively (Figure 3.6A). The duration from the time point of MBP7 stimulation to the time point of the peak emission was measured and expressed as Δ Peak Time (Figure 3.6A). For the cellular calcium reponse, only the first cellular reponse (30 μ M for Mc0M80 and mas-(Gly₁₀Ser₅)-GFP; 100 μ M for mas-GFP) were quantified. It was observed that the basal emission ratio was similar among Mc0M80 and the two cell lines expressing mas fusion variants (Figure 3.6B). Plotting the peak emission ratio of each individual cell against its corresponding basal emission ratio (Figure 3.6C), there showed no correlation between the basal emission raio and the peak emission ratio, indicating that the increase of emission ratio after MBP7 treatment was independent of the basal emission ratio.

Statistical analysis on the quantification data showed that Δ Peak Emission Ratio in Mc0M80 cells was significantly higher than that of cells expressing mas fusion proteins (Figure 3.6D). The Δ Plateau Emission Ratios in all the three cell lines were similar to each other (Figure 3.6E). However, Δ Peak Time in cells expressing mas-(Gly₁₀Ser₅)-GFP and Mc0M80 were similar to each other (Figure 3.6F). Both of them were remarkably shorter than that of cells expressing mas-GFP demonstrating that the response of native mas and mas-(Gly₁₀Ser₅)-GFP to ligand were faster than that of mas-GFP.

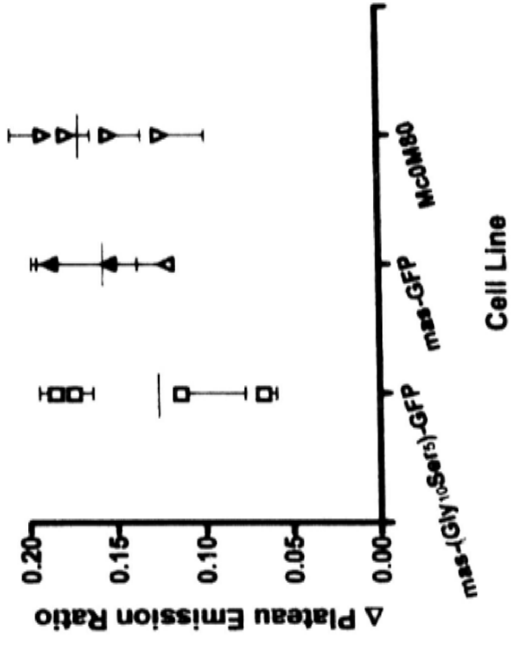
Figure 3.6 Quantification of calcium assay for cells expressing mas fusion proteins or native mas. (A) Quantification strategy of Δ Peak Emission Ratio, Δ Plateau Emission Ratio and Δ Peak Time. Δ Peak Emission Ratio was calculated as peak emission ratio subtracting basal emission ratio. Δ Plateau Emission Ratio was calculated as plateau emission ratio subtracting basal emission ratio. Δ Peak Time represented the time duration from the point of 30 μ M MBP7 addition to the point of highest emission ratio. (B) Basal emission ratio among Mc0M80 and cells expressing mas-(Gly₁₀Ser₅)-GFP or mas-GFP. (C) Peak emission ratio against basal emission ratio in Mc0M80 and cells expressing two types of mas fusion variants. (D) Quantification of Δ Peak Emission Ratio at 510 nm. (E) Quantification of Δ Plateau Emission Ratio at 510 nm. (F) Quantification of Δ Peak Time. The value of basal emission ratio, peak emission ratio, plateau emission ratio and Δ peak time were recorded from individual responsive curves. Each data point is mean \pm SD of five responsive cells from a counting field with 100 to 200 cells. Data shown were collected from three separate experiments with similar results. * indicated significant difference by One Way ANOVA analysis.



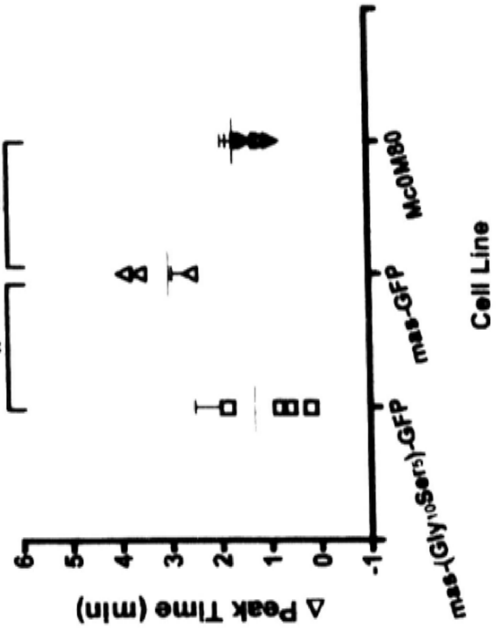
D



E



F



In parallel, fractions of cells responsive to either concentration of MBP7 were calculated as responsive cells versus all the cells in the sample fields. Similar to the difference in Δ Peak Emission Ratio, Mc0M80 cells had a notably higher percentage of responsive cells than both of the mas fusion proteins-expressing cells (Figure 3.7).

To examine how mas expression level affected cellular response to its ligand, $[Ca^{2+}]_i$ measurement was performed in cells expressing various levels of mas. They were two cell clones derived from Mc0, two from Mc7 and three from Mc35. Mc0M0, Mc7M0 and Mc35M0 were cell lines stably expressing native mas without MTX induction. Mc0M80, Mc7M80 and Mc35M80 were cell lines stably expressing native mas under 80 μ M MBP7 treatment while Mc35M4 was the mas-expression cell clone adjusted to medium containing 4 μ M MBP7. The experimental procedures were similar to that described for cells expressing mas fusion proteins. The basal $[Ca^{2+}]_i$ in all the mas-expressing clones were low as shown in a blue pseudocolor. After MBP7 stimulation, cell clones with relatively lower expression levels of mas, such as Mc7M0 and Mc35M0, showed nearly no increase of $[Ca^{2+}]_i$. However, Mc0M0, Mc0M80, Mc7M80, Mc35M4 and Mc35M80, with higher mas expression levels, there was a rapid increase of $[Ca^{2+}]_i$ as represented by the shift of pseudocolors and elevation of emission ratio in the responsive curves (Figure 3.8A & 3.8B).

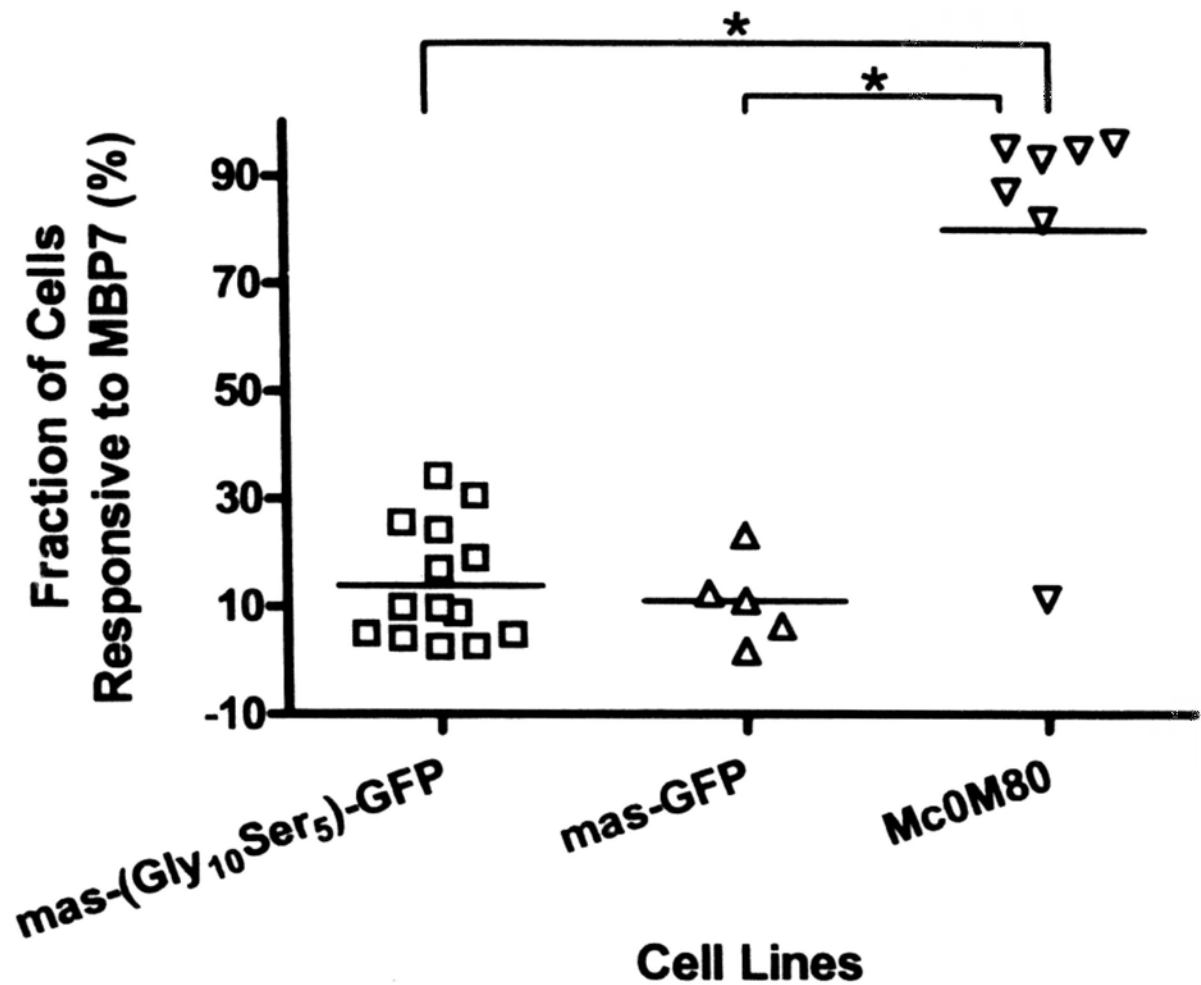
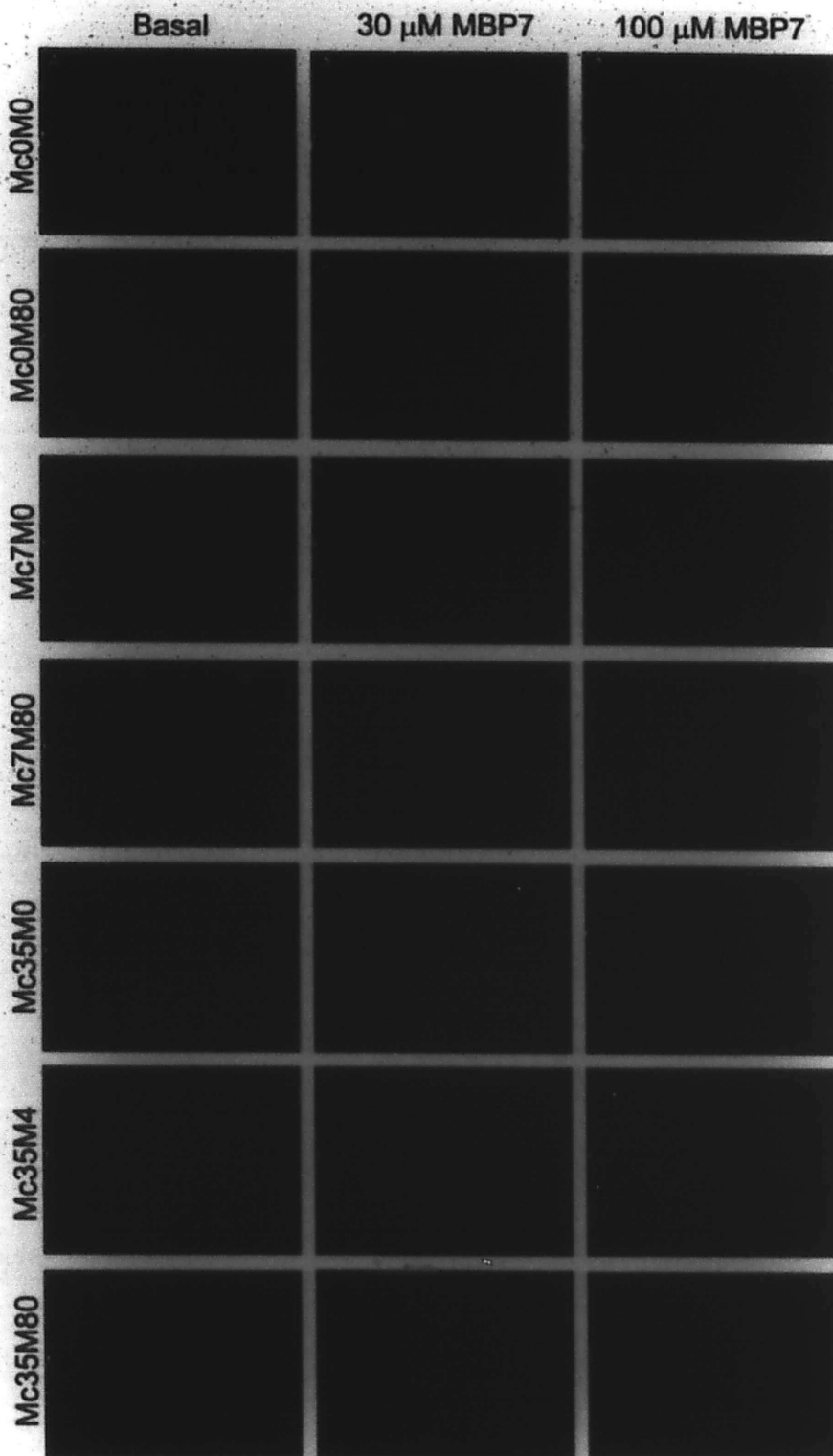


Figure 3.7 Responsive ratios in calcium ion concentration ($[Ca^{2+}]_i$) measurement in cells expressing mas fusion proteins or native mas. Cellular response to MBP7 were examined by $[Ca^{2+}]_i$ change before and after MBP7 treatment in cells expressing mas fusion proteins and native mas. The responsive rates were calculated as the percentage of responsive cells to either concentration of MBP7 versus all the cells in the sample field. Cell number in each sample field ranged from tens to about hundreds. Each symbol represented an individual sample in each assay. * represented statistical difference between the examined groups by one way ANOVA using SigmaStat program. Data were obtained from at least three separate experiments.

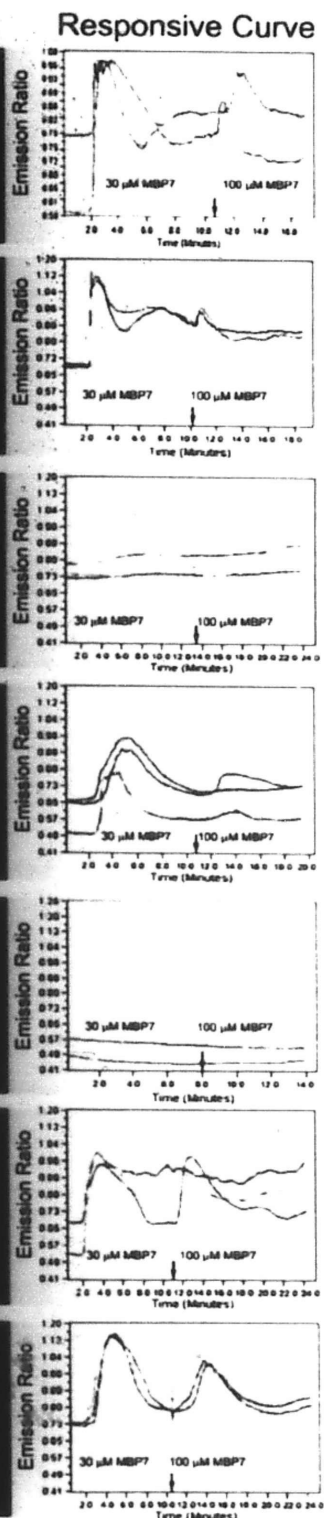
Figure 3.8 Intracellular calcium ion concentration ($[Ca^{2+}]_i$) measurement on cells with various mas expression levels. (A) Color photos representing $[Ca^{2+}]_i$ changes. There were two clones from Mc0 (Mc0M0 & Mc0M80), two from Mc7 (Mc7M0 & Mc7M80) and three from Mc35 (Mc35M0, Mc35M4 & Mc35M80). Clones with various native mas expression levels were pre-loaded with Ca^{2+} -sensitive fluorescence dye Fura-2 AM*. The cells were excited with 340 nm and 380 nm, separately, and fluorescent emission was monitored at 510 nm. Increase of $[Ca^{2+}]_i$ was indicated by the increased emission ratio ($\frac{Em_{510_{340}}}{Em_{510_{380}}}$), and visually represented in a color scale below. (B) Individual responsive curves against time. Curves in various colors represented randomly selected responsive cells. The two stimulations from MBP7 were indicated at the X axis with an open (30 μ M) and a closed (100 μ M) arrow, respectively. The Y axis and X axis were emission ratio ($\frac{Em_{510_{340}}}{Em_{510_{380}}}$) and experimental time, respectively. Data shown were representatives of at least three separate experiments with similar results.

A



$[Ca^{2+}] \uparrow$

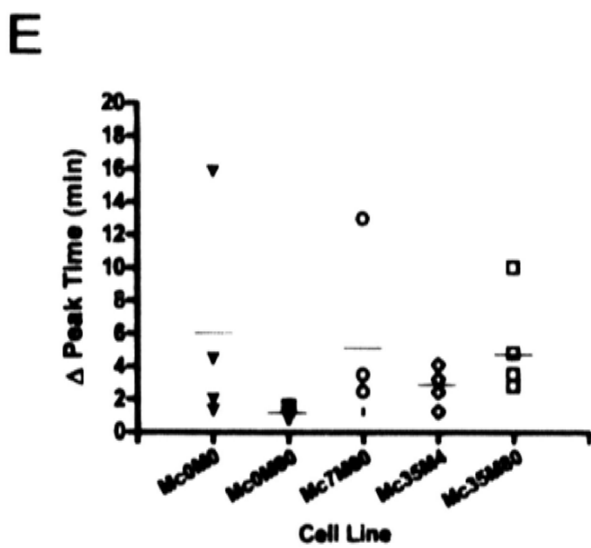
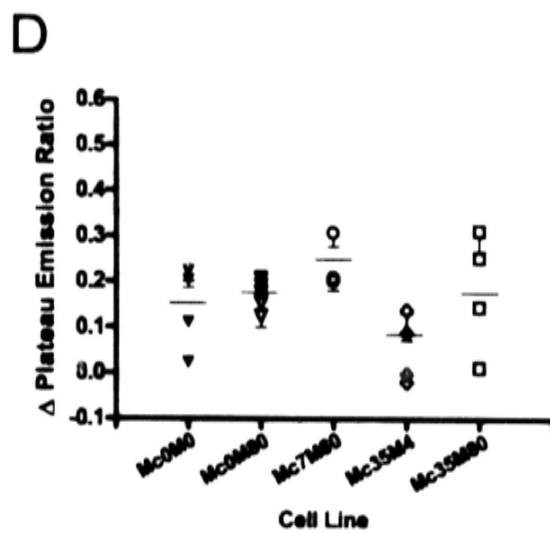
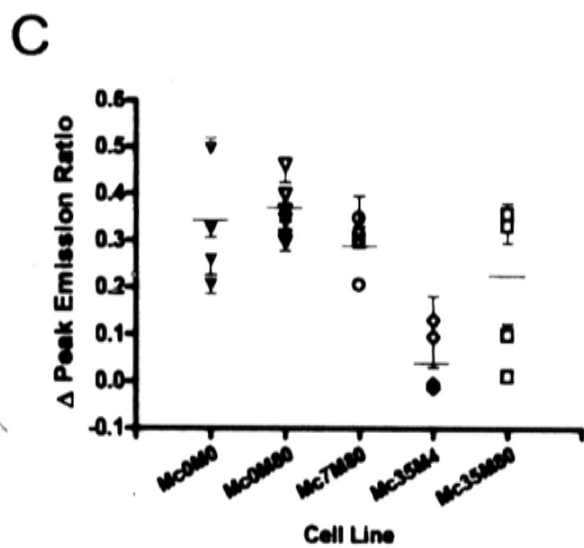
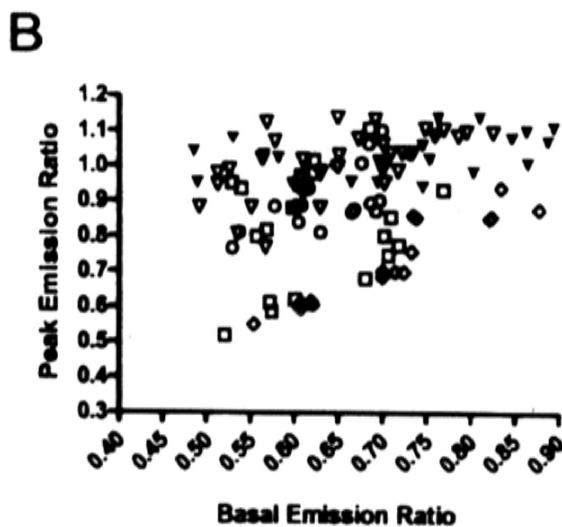
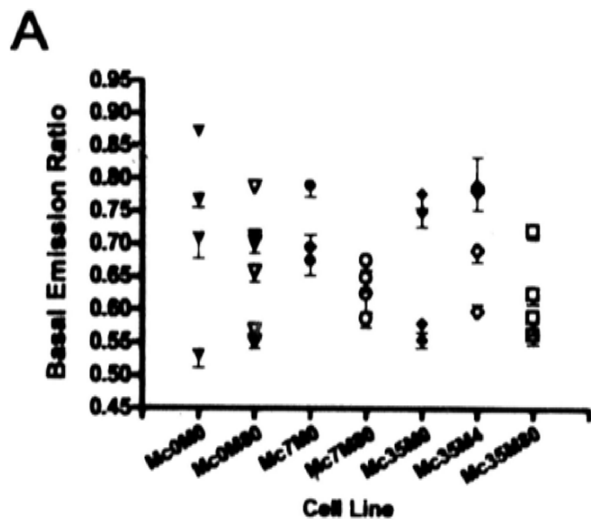
B



Quantification on Δ Peak Emission Ratio, Δ Plateau Emission Ratio and Δ Peak Time were performed in the same way as described above. There was no large difference among the basal emission ratio in various mas expressing clones (Figure 3.9A). The random distribution of peak emission ratio against basal emission ratio illustrated that the increase of peak emission ratios were not due to the elevated basal emission ratios (Figure 3.9B).

Subclones under 80 μ M MTX treatment (Mc0M80, Mc7M80 & Mc35M80) showed larger Δ Peak Emission Ratio than subclones without MTX treatment (Mc0M0, Mc7M0 & Mc35M0) within each individual mas clones (Figure 3.9C). However, statistical analysis indicated no significant difference. The Δ Plateau Emission Ratio and Δ Peak Time in all the mas clones were similar (Figure 3.9D & 3.9E).

Figure 3.9 Quantification of calcium assay for cells with various mas expression levels. (A) Basal emission ratio among various mas clones. (B) Peak emission ratio against basal emission ratio in mas clones with various mas expression levels. Mc0M0, Mc0M80, Mc7M0, Mc7M80, Mc35M0, Mc35M4 and Mc35M80 were represented as the symbol \blacktriangledown , ∇ , \circ , \diamond and \square , respectively. (C) Quantification of Δ Peak Emission Ratio at 510 nm. (D) Quantification of Δ Plateau Emission Ratio at 510 nm. (E) Quantification of Δ Peak Time. The value of basal emission ratio, peak emission ratio, plateau emission ratio and Δ peak time were retrieved from individual responsive curves. Each data point is mean \pm SD of five responsive cells from a counting field with about 100 to 200 cells. Data shown were collected from three separate experiments.



Apart from response in individual cells, responsive ratio of each cell line was calculated to compare the fraction of cells responsive to MBP7 in every sample field. The calculating method was similar to that for cells expressing mas fusion proteins. Mc0M0 and Mc0M80 cells which had highest expression level of mas showed highest responsive ratios. Mc7M80, Mc35M4 and Mc35M80 with medial levels of mas expression showed less responsive ratios than Mc0M80. The responsive ratios were nearly zero in the two clones with lowest expression level of mas, Mc7M0 and Mc35M0 and were statistically less than the responsive ratio of Mc0M80 (Figure 3.10).

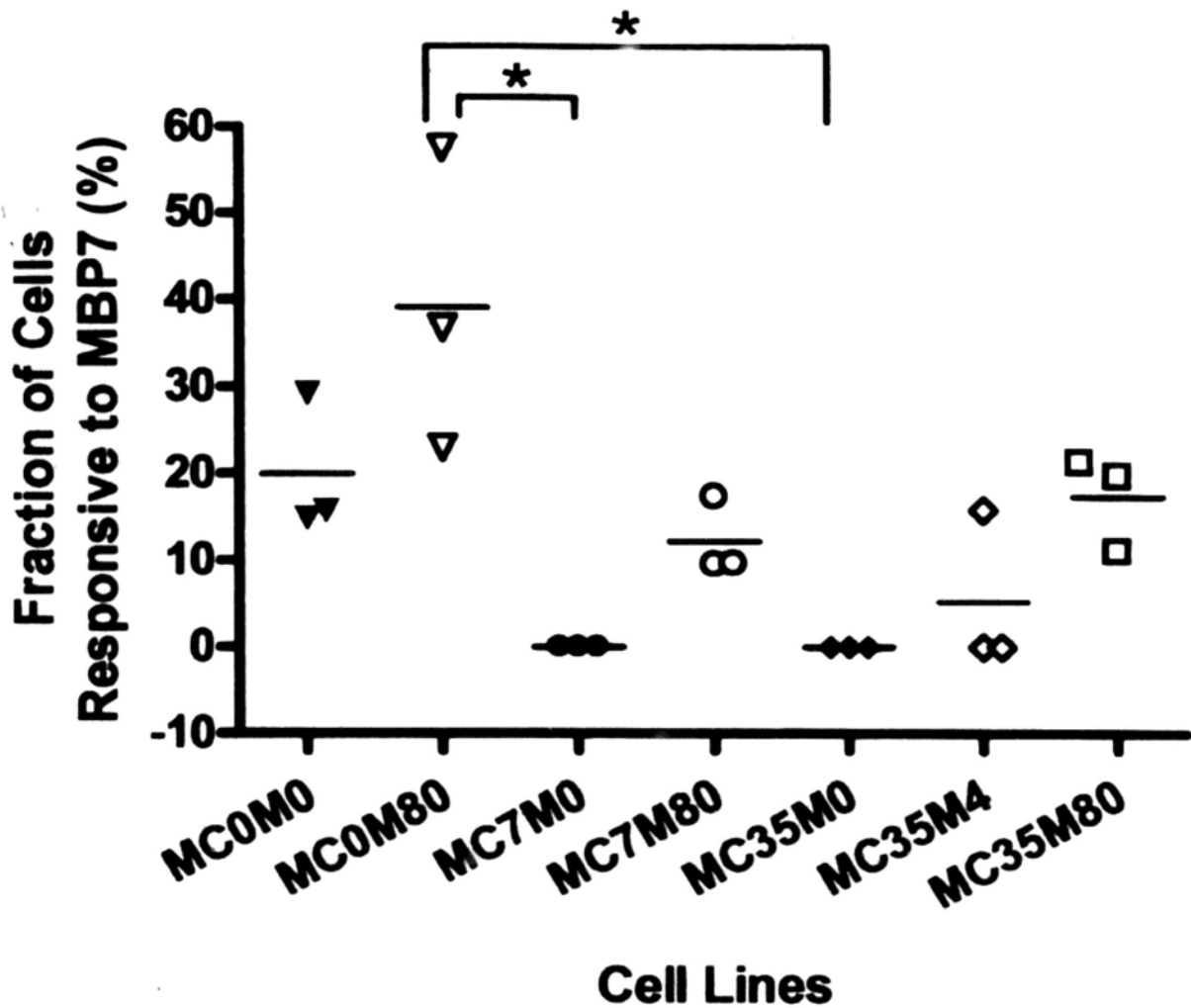


Figure 3.10 Fractions of cells responsive to MBP7. Two cell clones from Mc0 (Mc0M0 & Mc0M80), two from Mc7 (Mc7M0 & Mc7M80) and three from Mc35 (Mc35M0, Mc35M4 & Mc35M80) were examined for calcium mobilization upon MBP7 stimulation. The responsive ratios were calculated as the percentage of responsive cells under either concentration of MBP7 stimulation in the sample field containing tens to hundreds of cells. Each symbol represented an individual sample from each assay. * represented statistical difference between the examined group by one way ANOVA using SigmaStat program. Data were obtained from at least three separate experiments.

3.4 Discussion

3.4.1 *Phage binding assay*

Strong and punctuate binding of phages encoding mas ligand phage to cells expressing mas fusion proteins and Mc0M80 expressing native mas indicated that mas fusion proteins folded properly and functioned similarly to native mas.

In the cell line expressing mas-(Gly₁₀Ser₅)-GFP, phage ligand signals was more significant in the cytoplasm implying that more ligands were internalized than in the cells expressing mas-GFP. The different extent of phage ligand internalization might result from the different status of mas C terminus in the fusion variants. In mas-GFP, mas C-terminus was located closer to GFP and more susceptible to its tagging effect. After the insertion of a flexible peptide linker between mas and GFP, mas was separated further from GFP and less affected by the steric hindrance. In general, the difference in phage binding assay between mas-(Gly₁₀Ser₅)-GFP and mas-GFP proved that the peptide linker was effective to alleviate the tagging effect of GFP on mas.

Mc0M80 showed strongest red signals among all the cell lines. It had highest membrane expression level of native mas that enabled more phages expressing mas putative ligand to bind with.

3.4.2 *Biotinylation assay*

Biotin is a natural and small vitamin (244 Da). The covalent modification of proteins with biotin mainly relies on the *N*-hydroxysuccinimide (NHS) ester bond which efficiently binds primary amine groups (-NH₂) via stable amide bond in alkaline buffer (pH 7 ~ 9). The sulfo residue is cell membrane impermeable which ensures only membrane proteins to be labeled by the biotin reagents. In addition, biotin has high affinity to avidin and streptavidin. Therefore, proteins labeled with biotin can be isolated using immobilized avidin or streptavidin and be further examined by Western Blot, ELISA and so on (Daniels & Amara, 1998; Huh & Wenthold, 1999).

In this project, membrane biotinylation assay was used to quantify the amount of translocated cell surface mas fusion proteins (strategy 1) or intracellular mas fusion proteins (strategy 2). The differences of bands intensities between control and treatment group reflected different extent of mas trafficking in the absence or presence of MBP7 stimulation. In strategy 1, the bands intensities after MBP7 treatment were stronger than the non-treated ones indicating that MBP7 triggered more mas fusion proteins to be transported to the cell surface. In strategy 2, the bands intensities upon MBP7 stimulation were less than the non-treated ones indicating that fewer mas fusion proteins were internalized after MBP7 challenge. The results implied that mas was constitutively circulated between cell surface and intracellular pools, and MBP7 treatment slowed down the inward movement of mas. Indeed, the constitutive trafficking of GPCR between cell surface and intracellular pool have been reported in β 2 adrenergic receptor, M3

muscarinic receptor, melanocortin-4 receptor and CB₁ cannabinoid receptor and so on (McDonald et al., 2007; Mohammad et al., 2007; Scarselli & Donaldson, 2009).

The different band intensities in the absence or presence of MBP7 treatment in cell line expressing mas-(Gly₁₀Ser₅)-GFP were more significant than that of cells expressing mas-GFP. Such differences might originate from the different status of mas C terminus in the two constructs. As mentioned before, the C terminus of mas in mas-GFP was under GFP tagging effect. Therefore, the binding competencies and translocation efficiency in response to MBP7 were affected. The results of biotinylation assay illustrated that the peptide linker in mas-(Gly₁₀Ser₅)-GFP effectively recovered mas translocation upon MBP7 activation.

3.4.3 Calcium ion concentration ($[Ca^{2+}]_i$) measurement

Decreased ligand binding and translocation of mas-GFP compared with that of mas-(Gly₁₀Ser₅)-GFP indicated that mas C-terminus was responsible for downstream activations. In order to find out GFP tagging effect on mas downstream signaling, $[Ca^{2+}]_i$ measurement was carried out in cells stably expressing mas.

Calcium is a key effector in the secondary signaling pathway in various cells ranging from bacteria to specialized neurons (Figure 3.9). A series of events following ligand-receptor interactions mediate the elevation of $[Ca^{2+}]_i$ concentrations from ~100 nM to ~1 μM within seconds to minutes. Various bio-processes are triggered by the increase of $[Ca^{2+}]_i$, for instance, release of synaptic transmitters, hormone secretion, muscle

contraction, cell migration, apoptosis and so on. Therefore, measurement of $[Ca^{2+}]_i$ change was important to understand the mechanisms of many physiological or pathological activities (Berridge, 1997).

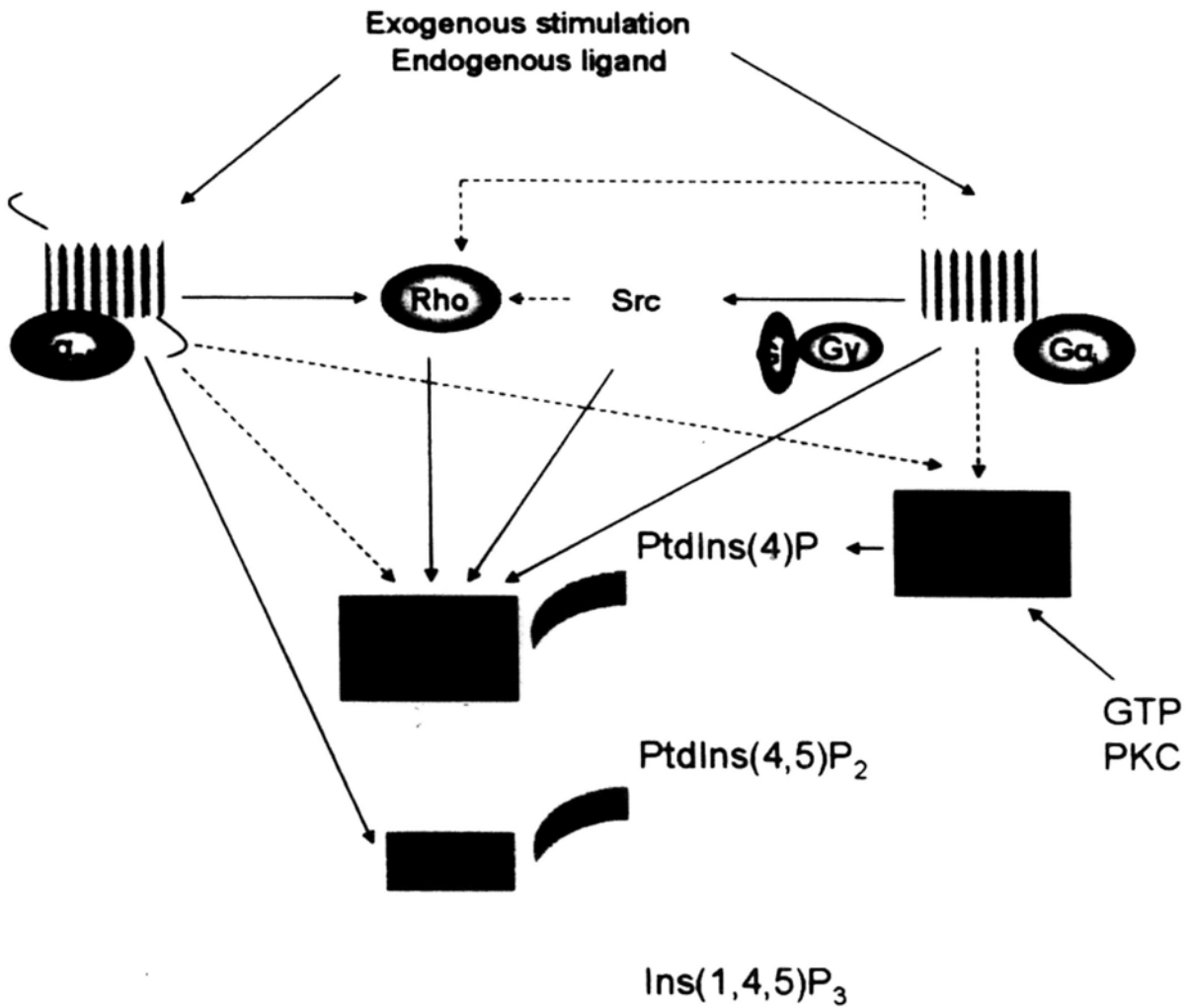


Figure 3.11 GPCR-activated increase of $[Ca^{2+}]_i$. $G_{q/11}$ -coupled GPCR upon ligand binding triggers activation of phospholipase $C\beta$ isoform ($PLC\beta$) and catalyzes PIP_2 into IP_3 . Accumulated IP_3 subsequently increase of $[Ca^{2+}]_i$. Agonist-stimulated G_i -coupled GPCR, GTP and PKC act on $PtdIns$ 4-kinase and subsequent $PtdIns$ 5-kinase which results in the accumulation of IP_3 and elevation of $[Ca^{2+}]_i$. The close lines and dotted lines represent known and unknown effect. [modified from the picture in (Werry et al., 2003)]

In figure 3.5, some cells in the three cell lines shifted from blue to green color indicating an increase of $[Ca^{2+}]_i$ levels upon MBP7 stimulation. However, the individual responsive curves from randomly selected responsive cells were different. In Mc0M80 and cells expressing mas-(Gly₁₀Ser₅)-GFP, the curves showed quick increase of $[Ca^{2+}]_i$ triggered by 30 μ M MBP7. The two cells lines also responded to the second stimulation of 100 μ M MBP7 within a short period of time. As known, GPCR undergoes desensitization and resensitization processes after exogenous stimulations. Desensitization is realized, e.g., by receptor internalization. The desensitized GPCR won't respond to stimulations until they are resensitized. From the curve patterns, it was obvious that both native mas and mas-(Gly₁₀Ser₅)-GFP had short desensitizing time so that they can respond to both stimulations from MBP7. However, the curves in cell line expressing mas-GFP only showed a delayed elevation of $[Ca^{2+}]_i$ in response to higher concentration of MBP7 indicating that the threshold of mas-GFP activation was relatively higher. The quantified Δ Peak Emission Ratios were similar in cells expressing mas-(Gly₁₀Ser₅)-GFP and mas-GFP. Both of them are smaller than the Δ Peak Emission Ratio in Mc0M80 indicating larger increase of $[Ca^{2+}]_i$ in cells expressing native mas than in cells expressing mas fusion proteins. On the other hand, the Δ Peak Time in cells expressing mas-GFP was significantly longer than that of cells expressing mas-(Gly₁₀Ser₅)-GFP and Mc0M80 implying that mas-GFP was possibly less responsive to MBP7 and needed more time to be stimulated. The difference also demonstrated that GFP tagging might inhibit downstream signaling of mas while a peptide linker partially revived mas receptor activity.

When comparing the fractions of cells responsive to MBP7, Mc0M80 mas was the most responsive one among the three cell lines. Thus, it was assumed that the expression level of mas might affect the responsive ratios to ligand. To prove the assumption, cell lines with various mas expression levels were subjected to $[Ca^{2+}]_i$ measurement.

As expected, Mc0M0 and Mc0M80 with highest expression levels of mas showed highest fractions of responsive cells. Cell lines such as Mc7M80, Mc35M4 and Mc35M80 with medial levels of mas expression had less responsive cells than Mc0M0 and Mc0M80. Consistently, nearly no response to MBP7 in $[Ca^{2+}]_i$ measurement was observed in Mc7M0 and Mc35M0 which had lowest expression levels of mas. Furthermore, quantification data showed larger Δ Peak Emission Ratio in Mc0M80, Mc7M80 and Mc35M80 than that in Mc0M0, Mc7M0 and Mc35M0, respectively, indicating that higher mas expression levels made larger increase of $[Ca^{2+}]_i$. Therefore it was concluded that mas expression levels might play an essential role in cellular response to ligand.

Chapter 4

Cellular Glucose Uptake in mas-expressing cells

4.1 General introduction

4.1.1 *Glucose Transporter (GLUT) type and tissue distribution*

Glucose is an indispensable energy source for cell growth and proliferation. Mammalian cells rely on glucose transporter in the cell membrane to transport glucose through the hydrophobic lipid bilayer into the cytoplasm. Up till now, 13 types of glucose transporters (GLUTs) have been identified (Joost & Thorens, 2001).

The similarities between GLUT1 and other members of the GLUT family are over 28%. They share several common features in the sequences. First, all of them have 12 membrane-spanning helices which enable them to integrate in the cell membrane. Secondly, there are seven conserved glycine residues within the transmembrane helices. Lastly, two conserved tryptophan residues as well as two tyrosine residues are localized in the intracellular part of GLUT sequences (Joost & Thorens, 2001).

4.1.2 *Classification of GLUTs*

Based on the sequence similarity, GLUT family can be divided into three main sub-families:

- ◆ **Class I:** GLUT1 to GLUT4 characterizing with the appearance of a glutamine residue in helix 5 and STSIF-motif in extracellular loop 7 (Joost & Thorens, 2001).
- ◆ **Class II:** GLUT5, GLUT7, GLUT9 and GLUT11 in charge of fructose-related transportation. Tryptophan deficiency was noted following the conserved GPXXXP motif in helix 10 (Joost & Thorens, 2001).

◆ **Class III:** GLUT6, GLUT8, GLUT10, GLUT12 and HMIT1 (myoinositol transporter 1) symbolized as having a glycosylation site in extracellular loop 9 (Joost & Thorens, 2001).

4.1.3 *Function of GLUTs*

Different GLUTs express preferably in different cell types and have various functions in regulation of cellular glucose uptake. For instance, GLUT4 expresses abundantly in muscle and insulin-responsive tissues while GLUT3 mainly exists in brain. The tissue distributions and functions of GLUTs were summarized in Table 4.1 & Table 4.2.

4.1.4 *Purpose of study*

The homology between MBP7 and GLUT sequence (GLUT7 and monosaccharide transporter 1) implied that mas might potentially interact with GLUT. On the other hand, several reports have demonstrated GPCRs-modified glucose uptake (Hagi et al., 2000; Winzell & Ahren, 2007). Therefore, experiments were performed to find out whether mas expression might regulate cellular glucose uptake and how C-terminal GFP tagging affected the coupling of mas to GLUT.

Table 4.1 Chromosomal localization and distribution of GLUT

| Protein | Alias | Gene Name | Chromosome Localization | Accession No. | | Expression |
|---------|--------|-----------|-------------------------|---------------|----------------------|------------------------------------|
| | | | | cDNA | Gene ensemble | |
| GLUT1 | | SLC2A1 | 1p35-31.3(47.7MB) | K03195 | AC023331 | Erythrocyte Brain (vascular) |
| GLUT2 | | SLC2A2 | 3q26.2-27(186.9MB) | J03810 | AC068853 | Liver Islets |
| GLUT3 | | SLC2A3 | 12p13.3(8.1MB) | J04069 | AC007536 | Brain (neuronal) |
| GLUT4 | | SLC2A4 | 17p13(8.4) | M20747 | AC003688 | Muscle Heart Fat |
| GLUT5 | | SLC2A5 | 1p36.2(8.2MB) | J05461 | AC041046 | Intestine Testis Kidney |
| GLUT6 | GLUT9 | SLC2A6 | 9q34(136.5MB) | Y17803 | AC002355 | Spleen Leukocytes Brain |
| GLUT7 | | SLC2A7 | 1p36.2(8.2MB) | | AC356306 | Intestine |
| GLUT8 | GLUTX1 | SLC2A8 | 9(129.9MB) | Y17801 | AL445222 | Testis Blastocyst Brain |
| GLUT9 | GLUTX | SLC2A9 | 4p15.3-16(10.2MB) | AF210317 | AC005674 | Liver Kidney |
| GLUT10 | | SLC2A10 | 20q12-13.1(47.3MB) | AF321240 | AC031055 | Liver Pancreas |
| GLUT11 | GLUT10 | SLC2A11 | 22q11.2(20.8MB) | AJ271290 | AP000350 | Heart Muscle |
| GLUT12 | GLUT8 | SLC2A12 | 6q23.2(145.5MB) | | AL449363, AL35699 | Heart Prostate |

modified from (Joost & Thorens, 2001; Joost et al., 2002)

Table 4.2 Tissue distribution and function of GLUT

| Designation | Major sites of expression | Function |
|---|---|---|
| A. Sodium-dependent glucose transporters | | |
| SGLT1 | Small intestine, Kidney | Active uptake of dietary glucose from lumen of the small intestine and reabsorption of filtered glucose in the proximal tubule of the kidney |
| B. Facilitative glucose transporters | | |
| GLUT1 | Placenta, Brain, Kidney, Colon | Basal uptake of glucose of cells and transportation of glucose across blood-tissue barriers |
| GLUT2 | Liver, Pancreatic β -cell, Small Intestine, Kidney | Uptake and release of glucose by hepatocytes β -cell glucose transporter; Release of absorbed glucose across the basolateral surface of absorptive epithelial cells of small intestine and kidney |
| GLUT3 | Brain, Placenta & Kidney | Basal uptake of glucose by all cells |
| GLUT4 | Skeletal & Cardiac Muscle, Adipose tissue | Insulin-stimulated glucose uptake |
| GLUT5 | Small Intestine (jejunum) | Absorption of sugars from the lumen of the small intestine |
| GLUT7 | Small Intestine, Colon, Testis, Prostate | Transportation of glucose and fructose; an intermediate between class II GLUTs and class I member GLUT2 |

modified from (Joost & Thorens, 2001; Joost et al., 2002)

4.2 Materials and Methods

4.2.1 Materials

4.2.1.1 Chemicals

Iscove's modified DMEM medium, F12-Nutrient Mixture (Ham), fetal bovine serum, penicillin/streptomycin, TRIzolTM reagent, Lipofactamine 2000, all DNA primers, dNTP, 1kb Plus DNA marker and agarose (electrophoresis grade) were from Invitrogen (Carlsbad, CA, USA). Gel extraction kit was from GE Healthcare (Piscataway, NJ, USA). Plasmid midi kit was from iNtRON Biotechnology (Seongnam-Si, Gyeonggi-do, Korea). pGEM[®]-T Easy Vector System was from Promega (Madison, WI, USA). G418 was from Merck Biosciences (Whitehouse Station, NJ, USA). Nitroblue tetrazolium chloride (NBT) and 5-bromo-4-chloro-3-indolylyl-phosphate-4-toluidine salt (BCPIP) were from Roche (Roche Diagnostics Corporation, IN, USA). Nitrocellulose transfer membrane was from Whatman (Hahnstrabe 3, Dassel, Germany). 2-deoxy-D-[1-³H]-glucose and OptiPhase HiSafe 2 liquid scintillation cocktail were from Perkin Elmer (Waltham, MA, USA). 2-deoxy-D-glucose and phloretin and all other chemicals and reagents were of molecular grade and from Sigma-Aldrich (St. Louis, MO, USA).

4.2.1.2 Enzyme

SuperScriptTM II reverse transcriptase, T4 DNA ligase and trypsin were from Invitrogen Corporation (Carlsbad, CA, USA). PFU ultra high fidelity DNA polymerase was from Stratagene (Cedar Creek, TX, USA). Taq DNA polymerase was from Genesis (UK). All the restriction enzymes were from New England Biolabs (Beverly, MA, USA).

4.2.2 Methods

4.2.2.1 Examination of glucose transporter (GLUT) and insulin receptor (IR) in CHO cells

4.2.2.1.1 Isolation of RNA

CHO cells ($\sim 1 \times 10^6$) were seeded in 100 mm culture plate and grown for 3 to 4 days. After reaching 80% confluence, medium was removed and cells were washed once with PBS. TRIzol reagent (2 ml) was added to detach and lyse cells. The lysate was passed through a pipette for several times and transferred to 1.5-ml eppendorf tubes. Chloroform (0.2 ml for per ml of lysate) was added and mixed completely by shaking the tubes vigorously for 15 seconds. The mixture was then incubated at room temperature for 2 to 3 minutes and centrifuged at 12000 g for 15 minutes at 4°C. The aqueous phase in each tube was transferred to a new eppendorf tube and mixed with 0.5 ml of isopropanol. The mixture was incubated at room temperature for 10 minutes and centrifuged at 12000 g for another 10 minutes at 4°C. The supernatant was removed and RNA pellet was washed once with 75% ethanol (1 ml) by shaking the tubes up and down. RNA was spin down by centrifugation at 7500g for 5 minutes at 4°C. The dried RNA pellet was dissolved in 30 μ l to 50 μ l of DEPC H₂O depending on the size of the pellet. The RNA concentration was measured at 260 nm. The measuring procedure was similar to that described in section **2.2.2.1.12** except that one absorbance unit at OD_{260 nm} represents 40 μ g/ml RNA.

4.2.2.1.2 Preparation of cDNA

The reverse transcription was performed in the Applied Biosystems Elmer Gene Amp 9700 PCR machine. Oligo dT (1 μ l, 0.5 μ g/ μ l), extracted RNA (5 μ g) and 10 mM dNTPs (1 μ l) were mixed with DEPC H₂O up to 13 μ l in volume. The mixture was incubated at 65°C for 5 minutes to denature the 2nd structure of RNA. Then 5x first strand buffer (4 μ l) and 0.1 M DTT (2 μ l) were added to the above mixture and incubated at 42°C for 2 minutes. After that, superscript reverse transcriptase (1 μ l, 200 U/ μ l) was added to the tube and incubated at 42°C for 50 minutes to process reverse transcription. Finally the reaction was stopped by incubating at 70°C for 15 minutes to inactivate the enzyme. The composition of 5x first strand buffer was 25 mM Tris-HCl (pH 8.3, at 25°C), 375 mM KCl and 15 mM MgCl₂.

4.2.2.1.3 Designation of primers

Individual primers for GLUT and IR were designed to screen out GLUT isoform(s) and IR endogenously expressed in CHO cells. The sequences of primers were derived from highly conserved regions in the sequence of GLUTs and IR from mouse, rat and human (Table 4.3).

Table 4.3 Information of GLUT and IR primers for screening

| Gene | Primer | primer sequence | Putative size |
|-------------|---------------|------------------------|----------------------|
| GLUT1 | GLUT1-F1092 | AGTGCAGGGAGGAGAG | 262 bp |
| | GLUT1-R1093 | AACCAGCCATTTATATCT | |
| GLUT2 | GLUT2-F1094 | GGCATTCTTATTAGTCAGAT | 854 bp |
| | GLUT2-R1095 | CCTTTGGTTTCTGGA ACT | |
| GLUT3 | GLUT3-F1096 | GCTGGGCATCGTTGT | 697 bp |
| | GLUT3-R1097 | GCCCTGGCTGAAGAG | |
| GLUT4 | GLUT4-F1098 | AGGAGCTGGTGTGGTC | 332 bp |
| | GLUT4-R1099 | TCCGCAACATACTGGA | |
| GLUT5 | GLUT5-F1100 | ATCCGGAAGGAGGATG | 603 bp |
| | GLUT5-R1101 | AGATGTAGATGGTGGTGAG | |
| GLUT6 | GLUT6-F1102 | AGCTTCATGCCCAACTC | 772 bp |
| | GLUT6-R1103 | ACACAGCAGCCTGTGA | |
| GLUT7 | GLUT7-F1104 | TCCTGATGGGAGTCAG | 916 bp |
| | GLUT4-R1105 | TTGGTGAGCCAGTGC | |
| IR | IR3455-F1454 | ACGCCAAGAAGTTTGT | 468 bp |
| | IR3923-R1455 | GGAGCCTTGTTCTCCT | |

4.2.2.1.4 Amplification of GLUTs and IR fragments by RT-PCR

The fragments of GLUT1 to GLUT7 and IR were amplified with CHO cDNA and specific primers by RT-PCR. The PCR reaction system was composed of 10x PCR buffer (2.5 μ l), 25 mM MgCl₂ (1.5 μ l), 10 mM dNTP (0.5 μ l), cDNA (2 μ l), 10 mM forward primer (1 μ l), 10 mM reverse primer (1 μ l) and deionized water (16 μ l) making up to a volume of 24.5 μ l. The PCR reaction was performed with hot start program in Applied Biosystems Elmer Gene Amp 9700 PCR machine. After denaturing at 94°C for 3 minutes, 0.5 μ l of Taq DNA polymerase (5 U/ μ l) was added to the reaction system and heated up for two more minutes. After that, PCR reaction was running for 30 cycles with a denature temperature of 94°C for 30 seconds, an annealing temperature of 51°C (for GLUT1, GLUT6 and GLUT7), 53°C (for GLUT2 to GLUT5) or 50°C (for IR) for 30 seconds and an extension temperature of 72°C for 30 to 60 seconds depending on the length of the fragment to be amplified. An extending incubation at 72°C for 7 minutes was added at the end of the amplification cycles. The detailed PCR condition for each individual GLUT and IR amplification was listed in **Table 4.4**. The 10x PCR buffer contained 1 M Tris-HCl (pH 8.3) and 5 M KCl.

Table 4.4 PCR condition for GLUT and IR screening

| Gene | Denature | Annealing | Extension | PCR Cycles |
|-------------|-----------------|------------------|------------------|-------------------|
| GLUT1 | 94°C, 30s | 51°C, 30s | 72°C, 30s | 30 |
| GLUT2 | 94°C, 30s | 53°C, 30s | 72°C, 1 min | 30 |
| GLUT3 | 94°C, 30s | 53°C, 30s | 72°C, 1 min | 30 |
| GLUT4 | 94°C, 30s | 53°C, 30s | 72°C, 30s | 30 |
| GLUT5 | 94°C, 30s | 53°C, 30s | 72°C, 1 min | 30 |
| GLUT7 | 94°C, 30s | 51°C, 30s | 72°C, 1 min | 30 |
| IR | 94°C, 30s | 50°C, 30s | 72°C, 30s | 30 |

4.2.2.1.5 Subcloning to pGEM[®]-T Easy vector

Amplification of putative GLUT fragment from RT-PCR amplification was separated by agarose gel electrophoresis and was purified by gel extraction. Rapid ligation buffer (2x, 5 μ l), T4 ligase (1 μ l), pGEM[®]-T Easy vector (1 μ l) and certain amount of purified PCR product were mixed in a ratio of 1:1, 1:3 and 1:5 (vector: insert, w/w) and incubated at 16°C over night. The 2x rapid ligation buffer was composed of 60 mM Tris-HCl (pH 7.8), 20 mM MgCl₂, 20 mM DTT, 2 mM ATP and 10% polyethylene glycol (MW 8000, ACS Grade). The ligation products were transformed into DH5 α competent cells and spread in LB agar plates containing 100 μ g/ml Ampicillin. After overnight growing at 37°C, 5 positive clones were picked. pGEM[®]-T Easy Vectors contain T7 and SP6 RNA Polymerase promoters which are outside of the two ends of the multiple cloning site (MCS) holding an α -peptide coding region for the enzyme β -galactosidase. Insertion of exogenous DNA inactivates the α -peptide resulting white color in positive colonies. Each positive clone was grown in 2 ml of LB medium containing 100 μ g/ml Ampicillin at 37°C over night. Plasmids were extracted in mini-preparation scale. The detailed processes were similar to those being described in section [2.2.2.1.4](#) to [2.2.2.1.11](#).

4.2.2.1.6 Sequencing of PCR products

The concentrations of purified vector DNAs containing PCR products were measured and then sent for custom sequencing by a sequencing company (Macrogen) as described in section [2.2.2.1.12](#) and [2.2.2.1.13](#).

4.2.2.2 2-DOG uptake assay

Cells (2×10^5) were seeded in 24-well plate and cultured at 37°C, 5% CO₂ for 24 hours. Complete medium was replaced with serum-free medium for a four hour-starvation before the experiment. In the assay, cells were rinsed three times with PBS (1ml per well) and once with ice-cold KRP buffer (0.5 ml per well) (130 mM NaCl, 5 mM KCl, 1.3 mM CaCl₂-2H₂O, 1.3 mM MgSO₄-7H₂O and 10 mM Na₂HPO₄, pH 7.4). Then cells were incubated with the KRP buffer (0.5 ml per well) at 37°C for 30 minutes. After that, hot/cold mixture (0.2 ml per well) containing 0.35 mM 2-deoxy-D-glucose and 3.5 μCi/ml 2-deoxy-D-[1-³H]-glucose was added. Cells were incubated at 37°C for 10 minutes for glucose uptake. The uptake process was stopped by removing excess 2-deoxy-D-glucose and 2-deoxy-D-[1-³H]-glucose. Cells were then rinsed three times with ice-cold stop solution (1 ml per well) containing 0.3 mM of phloretin in PBS. SDS lysis buffer (0.1%, 500 μl per well) was added to the cell and incubated at room temperature for 30 minutes. Cell lysate (400 μl) was transferred to scintillation vial and mixed with 4 ml of scintillation fluid by vigorously shaking. The radioactivity was measured using a Beckman LS 6500 multipurpose scintillation counter (Fullerton, CA, USA). The [1-³H]-labelled 2-DOG uptake amount was indicated by the CPM values (pmol). The rest of the lysate (100 μl) was used to measure protein concentration by BCA assay as described in section 2.2.2.2.6.

4.2.2.3 Transient transfection of pcDNA 3.1+ RhoA variants or pCX2-GLUT1 myc

The RhoA plasmid variants were generously bestowed by Prof. Wong Yung-Hou from Hong Kong University of Science and Technology. They were commercially available at UMR cDNA Resource Center at University of Missouri-Rolla (Rolla, MO, USA). N-terminal 3x-hemagglutinin tagged wild type human RhoA was cloned into pcDNA3.1+ (Invitrogen) at Kpn I (5') and Xho I (3') and named as RhoA-WT. T19N and G14V mutations were introduced into the RhoA-WT sequence separately to produce dominant negative and dominant positive variants and were named as RhoA-TN and RhoA-GV, respectively. The size of RhoA-WT, RhoA-TN and RhoA-GV were 680 bp, 690 bp and 680 bp, respectively (Figure 4.1).

pCX2-GLUT1 myc mammalian plasmid was a generous gift from Prof. Yousuke Ebina of The University of Tokushima. A myc tag was inserted in frame with rat GLUT1 sequence in the first ectodomain (Figure 4.2). The full length GLUT1-myc was cloned into pCX2 vector at dual EcoR I cutting sites. The insert size of rat GLUT1 myc was 1521 bp.

For transient transfection, Mc0M80 and (or) Vc0M80 cells (5×10^6) were seeded in 100 mm plate and grown at 37°C, 5% CO₂ for 24 hours. Each type of RhoA plasmid variants or pCX2-GLUT1 myc (2.4 µg) and lipofectamine (6 µl) were incubated separately in 150 µl of serum free DMEM for 5 minutes and then mixed at room temperature for another 15 minutes. The mixture together with 1.2 ml of serum free DMEM were added to the

Mc0M80 or Vc0M80 cells after removal of the IMDM complete medium. After 5 hours of incubation at 37°C, 5% CO₂, medium was changed back to IMDM complete medium.

4.2.2.4 2-DOG uptake assay in RhoA variants or pCX2-Glut1 myc transfectants

After the transient transfection for 24 hours, cells were seeded and grown in a 24-well plate with a cell number of 2×10^5 per well for another 24 hours. The working procedure for 2-DOG uptake assay in transfected Mc0M80 or Vc0M80 cells was the same as that described in section 4.2.2.3. The cellular glucose uptake in the basal condition and under different treatments were measured and compared.

Figure 4.1 Vector map of pcDNA 3.1+ RhoA plasmid variants. The full length of mammalian expression vector pcDNA 3.1+ (3.0 kb) was digested out in Kpn I and Xho I cutting sites. The full length of human RhoA sequence was ligated into the vector at the Kpn I and Xho I cutting sites. The open reading frame of human RhoA was cloned downstream of CMV promoter. The expression vector encoded ampicillin resistant gene for selection in bacterial hosts. A 3x-hemagglutinin tag was added to the N-terminus of the RhoA sequence. Besides the wild type RhoA (RhoA-WT), two mutations of T19N and G14V were produced by Quickchange mutagenesis kit (Stratagene). RhoA-TN and RhoA-GV represented the dominant negative and dominant positive phenotypes of RhoA, respectively.

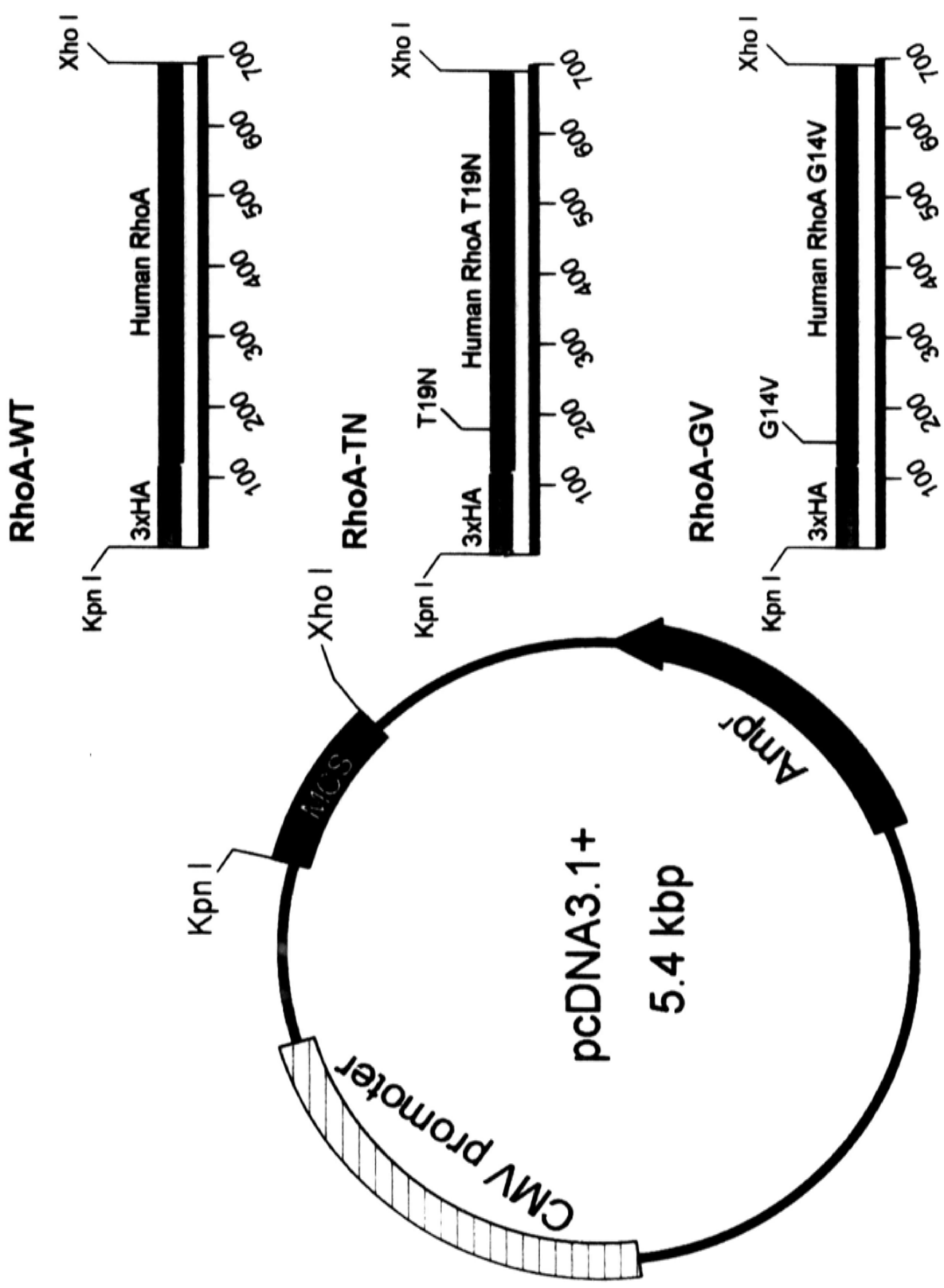
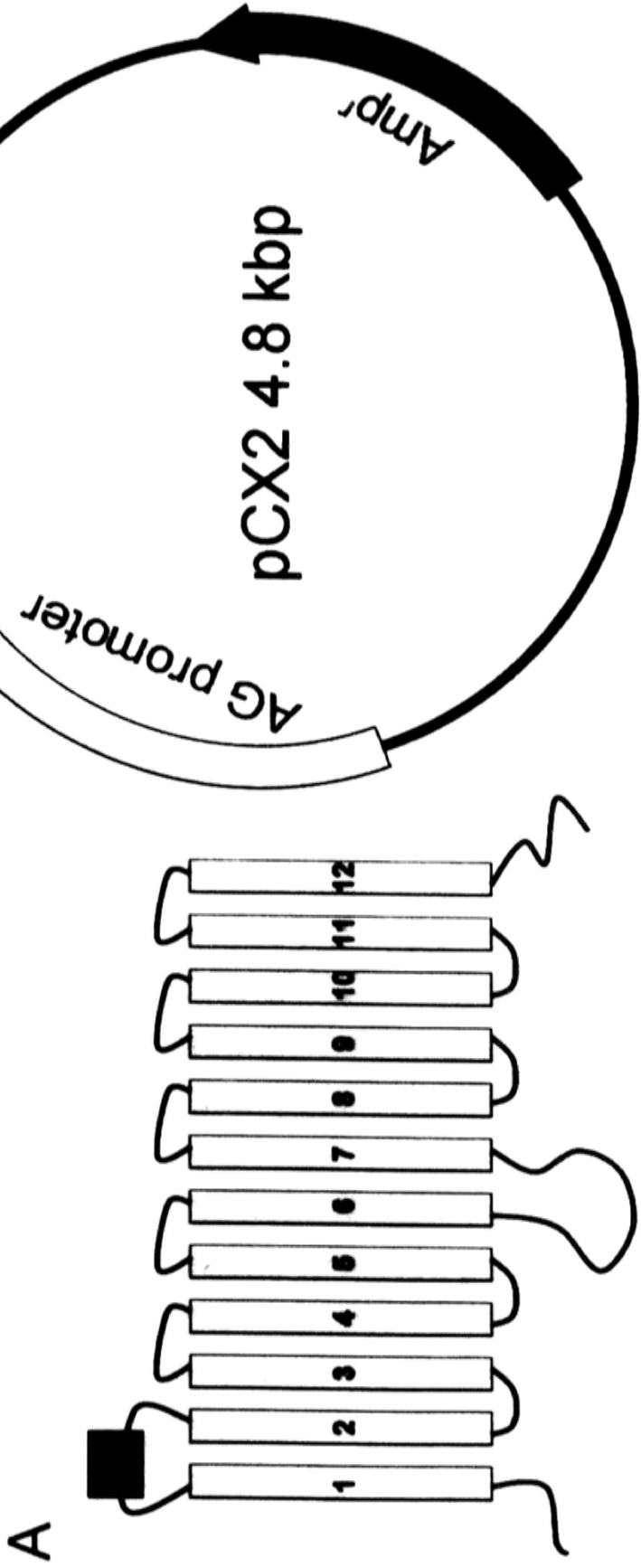


Figure 4.2 Structure and vector map of pCX 2-GLUT1 myc. (A) structure of GLUT1-myc. GLUT1 contains 12 transmembrane segments linked by extracellular and intracellular loops. Myc sequence was inserted into the first ectodomain loop of rat GLUT1 sequence in frame. (B) Vector map of pCX 2-GLUT1 myc. The full length of mammalian expression vector pCX2 (4.8 kb) was digested out in dual *EcoR* I cutting sites. The full length of rat GLUT1-myc sequence was ligated into the vector at the dual *EcoR* I cutting sites. The open reading frame of GLUT1-myc was cloned downstream of AG promoter. The expression vector encoded ampicillin resistant gene for selection in bacterial hosts.



4.2.2.5 Statistical analysis

All the data were represented as the mean±S.E.M from two or three independent experiments each performed in triplicate. Statistical difference between two groups was detected by t-test. Statistical analysis among three or more groups was conducted by One-Way ANOVA or Two-Way ANOVA regarding the number of impact factors in the experiment.

4.3 Results

4.3.1 Screening of GLUT type in CHO cells

To examine GLUT expression in CHO cells, RNA from CHO cells was extracted and performed RT-PCR using sub-type specific primers. The validity of primers was confirmed by RT-PCR in the positive controls from different rat tissues (Figure 4.3). Surprisingly, only GLUT4 fragment was successfully detected and amplified (Figure 4.4). The gel-extracted PCR fragment of putative GLUT4 was subcloned into pGEM[®]-T Easy vector for sequence confirmation. Totally five positive clones were selected and mini-prepared for sequencing. The sequencing results were aligned with rat GLUT4 (Figure 4.5) and GLUT1 (Figure 4.6) sequence using ClustalW software and showed 89% and 70% similarity to them, respectively. These results suggested CHO cell expressing a GLUT4 homologue.

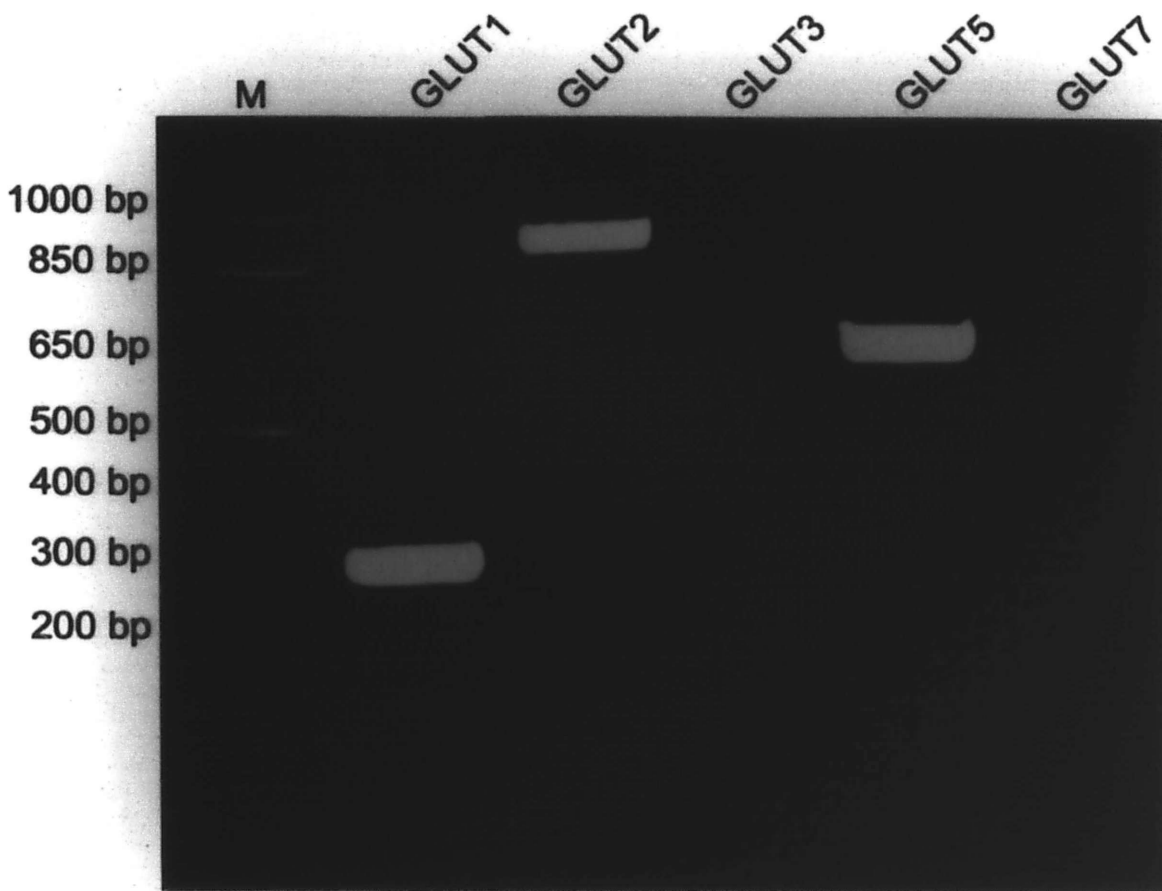


Figure 4.3 Positive control of GLUT fragment amplification. The validity of GLUT primers was confirmed by RT-PCR using rat tissues with differential GLUT expression. GLUT1 and GLUT3 were amplified from rat brain RNA while GLUT5 and GLUT7 were amplified from rat intestine RNA. RNA of rat liver was used to amplify GLUT2. The PCR products were performed electrophoresis in 1% agarose gel. Lanes from left to right represented PCR amplification of GLUT1 to GLUT7, respectively. The DNA marker was Invitrogen 1kb Plus DNA ladder.



Figure 4.4 GLUT screening in non-transfected CHO-K1 cell. Various GLUT fragments were amplified by RT-PCR using native CHO RNA. The PCR products were performed electrophoresis in 1% agarose gel. Lanes from left to right represented PCR amplification of GLUT1 to GLUT7, respectively. The loading amount was confirmed with GAPDH. Specific band was visualized by UV exposure in MultiImage™ Light Cabinet. The DNA marker was Invitrogen 1kb Plus DNA ladder.

C3_ -----AGGAGCTGGTGTGGTCAACA 20
 C13_ -----AGGAGCTGGTGTGGTCAACA 20
 C5_ -----AGGAGCTGGTGTGGTCAACA 20
 C4_ -----AGGAGCTGGTGTGGTCAACA 20
 C14_ -----AGGAGCTGGTGTGGTCAACA 20
 D28561.1|RAT GLUT4 TGGGGTGGAAACAGCCAGCCTACGCCACCATAGGAGCTGGTGTGGTCAATA 1000

***** *

C3_ CTGTCTTCACATTGGTCTCGGTGTTCTTAGTAGAACGGGCTGGGCGACGG 70
 C13_ CTGTCTTCACATTGGTCTCGGTGTTCTTAGTAGAACGGGCTGGGCGACGG 70
 C5_ CTGTCTTCACATTGGTCTCGGTGTTCTTAGTAGAACGGGCTGGGCGACGG 70
 C4_ CTGTCTTCACATTGGTCTCGGTGTTCTTAGTAGAACGGGCTGGGCGACGG 70
 C14_ CTGTCTTCACATTGGTCTCGGTGTTCTTAGTAGAACGGGCTGGGCGACGG 70
 D28561.1|RAT GLUT4 CCGTCTTCACGTTGGTCTCGGTGCTCTTAGTAGAGCGAGCTGGGCGACGG 1050

* ***** * ***** *

C3_ ACACTCCATCTCTTGGGCCTGGCAGGCATGTGTGGCTGTGCCATCTTGAT 120
 C13_ ACACTCCATCTCTTGGGCCTGGCAGGCATGTGTGGCTGTGCCATCTTGAT 120
 C5_ ACACTCCATCTCTTGGGCCTGGCAGGCATGTGTGGCTGTGCCATCTTGAT 120
 C4_ ACACTCCATCTCTTGGGCCTGGCAGGCATGTGTGGCTGTGCCATCTTGAT 120
 C14_ ACACTCCATCTCTTGGGCCTGGCAGGCATGTGTGGCTGTGCCATCTTGAT 120
 D28561.1|RAT GLUT4 ACACTCCATCTCTTGGGCCTGGCAGGCATGTGTGGCTGTGCCATCTTGAT 1100

***** ***** *****

C3_ GACTGTGGCTCTGCTTCTGCTGGAACGGGTTCCAGCCATGAGCTATGTCT 170
 C13_ GACTGTGGCTCTGCTTCTGCTGGAACGGGTTCCAGCCATGAGCTATGTCT 170
 C5_ GACTGTGGCTCTGCTTCTGCTGGAACGGGTTCCAGCCATGAGCTATGTCT 170
 C4_ GACTGTGGCTCTGCTTCTGCTGGAACGGGTTCCAGCCATGAGCTATGTCT 170
 C14_ GACTGTGGCTCTGCTTCTGCTGGAACGGGTTCCAGCCATGAGCTATGTCT 170
 D28561.1|RAT GLUT4 GACGGTGGCTCTGCTGCTGCTGGAGCGGGTTCCATCCATGAGTTATGTGT 1150

*** ***** ***** ***** *

C3_ CCATTGTGGCCATATTTGGCTTTGTG-CCTTCTTTGAGATTGGCCCTGGC 219
 C13_ CCATTGTGGCCATATTTGGCTTTGTGGCCTTCTTTGAGATTGGCCCTGGC 220
 C5_ CCATTGTGGCCATATTTGGCTTTGTGGCCTTCTTTGAGATTGGCCCTGGC 220
 C4_ CCATTGTGGCCATATTTGGCTTTGTGGCCTTCTTTGAGATTGGCCCTGGC 220
 C14_ CCATTGTGGCCATATTTGGCTTTGTGGCCTTCTTTGAGATTGGCCCTGGC 220
 D28561.1|RAT GLUT4 CCATCGTGGCCATATTTGGCTTTGTGGCCTTCTTTGAGATTGGTCTTGGC 1200

**** ***** ***** *****

```

C3_          CCCATCCCCTGGTTCATTGTGGCCGAGCTCTTCAGCCAAGGACCCCGCCC 269
C13_        CCCATCCCCTGGTTCATTGTGGCCGAGCTCTTCAGCCAAGGACCCCGCCC 270
C5_         CCCATCCCCTGGTTCATTGTGGCCGAGCTCTTCAGCCAAGGACCCCGCCC 270
C4_         CCCATCCCCTGGTTCATTGTGGCCGAGCTCTTCAGCCAAGGACCCCGCCC 270
C14_        CCCATCCCCTGGTTCATTGTGGCCGAGCTCTTCAGCCAAGGACCCCGCCC 270
D28561.1|RAT GLUT4 CCCATCCCCTGGTTCATTGTGGCCGAGCTCTTCAGCCAGGGCCCCCGCCC 1250
*****
C3_          AGCAGCCATGGCTGTAGCTGGTTTCTGCCAACTGGACGTGTAAC TTCATC 319
C13_        AGCAGCCATGGCTGTAGCTGGTTTCT-CCA ACTGGACGTGTAAC TTCATC 319
C5_         AGCAGCCATGGCTGTAGCTGGTTTCT-CCA ACTGGACGTGTAAC TTCATC 319
C4_         AGCAGCCATGGCTGTAGCTGGTTTCT-CCA ACTGGACGTGTAAC TTCATC 319
C14_        AGCAGCCATGGCTGTAGCTGGTTTCT-CCA ACTGGACGTGTAAC TTCATC 319
D28561.1|RAT GLUT4 AGCAGCCATGGCTGTAGCTGGTTTCT-CCA ACTGGACCTGTAAC TTCATC 1299
*****
C3_          GTTGGCATGGGTTTCCAGAATGTTGCGGAAATC--GAATTCCCGCGGCCG 367
C13_        GTTGGCATGGGTTTCCAGTATGTTGCGGAAATC--GAATTCCCGCGGCCG 367
C5_         GTTGGCATGGGTTTCCAGTATGTTGCGGAAATC--GAATTCCCGCGGCCG 367
C4_         GTTGGCATGGGTTTCCAGTATGTTGCGGAAATC--GAATTCCCGCGGCCN 367
C14_        GTTGGCATGGGTTTCCAGTATGTTGCGGAAATC--GAATTCCCGCGGCNN 367
D28561.1|RAT GLUT4 GTTGGCATGGGTTTCCAGTATGTTGCGGATGCTATGGGTCCCTACGTCTT 1349
*****
C3_          CCATNCGNC----- 376
C13_        CCA----- 370
C5_         CCAGGCGC----- 375
C4_         CC----- 369
C14_        GCC----- 370
D28561.1|RAT GLUT4 CCTTCTATTTGCCGTCCTCCTGCTTGGCTTCTTCATCTTCACCTTCCTAA 1399
*

```

Figure 4.5 Multiple alignments of PCR products with Rat GLUT4. PCR amplified putative GLUT4 fragment was purified by gel extraction and subcloned into pGEM®-T Easy Vector. Totally five positive clones (clone 3, 4, 5, 13, 14) were picked and mini-prepared for sequencing. The sequencing results were aligned with rat GLUT4. * represented the homologous nucleotide.


```

C13_          GCCCCATCCCCTGGTTCATTGTGGCCGAGCTCTTCAGCCAAGGACCCCGC 268
C3_           GCCCCATCCCCTGGTTCATTGTGGCCGAGCTCTTCAGCCAAGGACCCCGC 267
C5_           GCCCCATCCCCTGGTTCATTGTGGCCGAGCTCTTCAGCCAAGGACCCCGC 268
C4_           GCCCCATCCCCTGGTTCATTGTGGCCGAGCTCTTCAGCCAAGGACCCCGC 268
C14_          GCCCCATCCCCTGGTTCATTGTGGCCGAGCTCTTCAGCCAAGGACCCCGC 268
BC061873.1|Rat GLUT1  GTCCTATTCCATGGTTCATTGTGGCCGAGCTGTTTCAGCCAGGGGGCCCGA 1200
                * * * * *
                * * * * *

C13_          CCAGCAGCCATGGCTGTAGCTGGTTTCT-CCAAGTGGACGTGTAAGTCA 317
C3_           CCAGCAGCCATGGCTGTAGCTGGTTTCTGCCAAGTGGACGTGTAAGTCA 317
C5_           CCAGCAGCCATGGCTGTAGCTGGTTTCT-CCAAGTGGACGTGTAAGTCA 317
C4_           CCAGCAGCCATGGCTGTAGCTGGTTTCT-CCAAGTGGACGTGTAAGTCA 317
C14_          CCAGCAGCCATGGCTGTAGCTGGTTTCT-CCAAGTGGACGTGTAAGTCA 317
BC061873.1|Rat GLUT1  CCTGCTGCTGTTGCTGTGGCTGGCTTCT-CTAAGTGGACCTCAAAGTCA 1249
                ** * * * * *
                * * * * *

C13_          TCGTTGGCATGGGTTTCCAGTATGTTGCGGAAAT-CGAATTCCC GCGGCC 366
C3_           TCGTTGGCATGGGTTTCCAGTATGTTGCGGAAAT-CGAATTCCC GCGGCC 366
C5_           TCGTTGGCATGGGTTTCCAGTATGTTGCGGAAAT-CGAATTCCC GCGGCC 366
C4_           TCGTTGGCATGGGTTTCCAGTATGTTGCGGAAAT-CGAATTCCC GCGGCC 366
C14_          TCGTTGGCATGGGTTTCCAGTATGTTGCGGAAAT-CGAATTCCC GCGGCN 366
BC061873.1|Rat GLUT1  TCGTGGGCATGTGCTTCCAATATGTGGAGCAACTGTGTGGCCCTACGTC 1299
                ***** * ***** * * * * * * * * * *
                * * * * *

C13_          GCCA----- 370
C3_           GCCATNCGNC----- 376
C5_           GCCAGGCGC----- 375
C4_           NCC----- 369
C14_          NGCC----- 370
BC061873.1|Rat GLUT1  TTCATCATCTTCACGGTGCT 1329
                *

```

Figure 4.6 Multiple alignments of PCR products with Rat GLUT1. PCR amplified putative GLUT4 fragment was purified by gel extraction and subcloned into pGEM®-T Easy Vector for transformation and sequencing. The sequencing results were aligned with rat GLUT1. * represented the homologous nucleotide.

4.3.2 Examination of IR in CHO cells

IR expression in CHO cell was examined by RT-PCR with IR specific primers. Primer validity was confirmed by successful amplification of IR fragment in the positive control using hamster liver cDNA. The PCR product was separated in 1% agarose gel electrophoresis and the quality of cDNA was ensured by β -actin amplification. Interestingly, insulin receptor amplification was not detected in CHO cells (Figure 4.7).

4.3.3 Standardization of working condition for 2-DOG uptake assay

To optimize the cell number and uptake time for 2-DOG uptake assay, various number of cells (5×10^5 , 2×10^5 and 1×10^5 per well) were seeded in 24-well plate and treated for 5 minutes, 10 minutes and 15 minutes respectively. The 2-DOG uptake level (pmol) increased linearly with both cell number and uptake time (Figure 4.8). Cell number of 2×10^5 and uptake time of 10 minutes were located in the middle of the linear region and considered as standard working condition for 2-DOG uptake assay. Normalization of the uptake level (pmol) with protein amount (μg) showed similar values indicating a constant uptake rate with the same cell type in different trials (Figure 4.9).

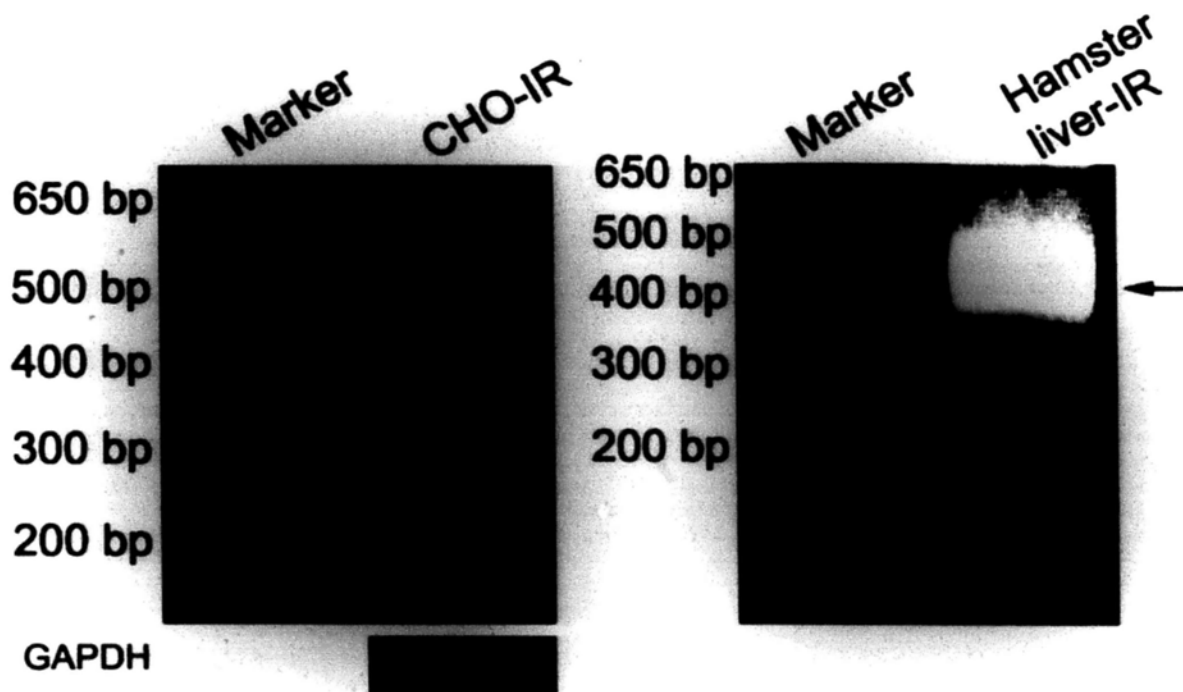


Figure 4.7 Insulin receptor (IR) screening in CHO cell. IR fragment was amplified by RT-PCR using hamster liver and CHO RNA. Validity of IR primers was confirmed by PCR amplification of IR fragment from hamster liver cDNA as the positive control. PCR products were performed electrophoresis in 1% agarose gel. Loading amount was controlled by GAPDH. The DNA marker was Invitrogen 1kb Plus DNA ladder.

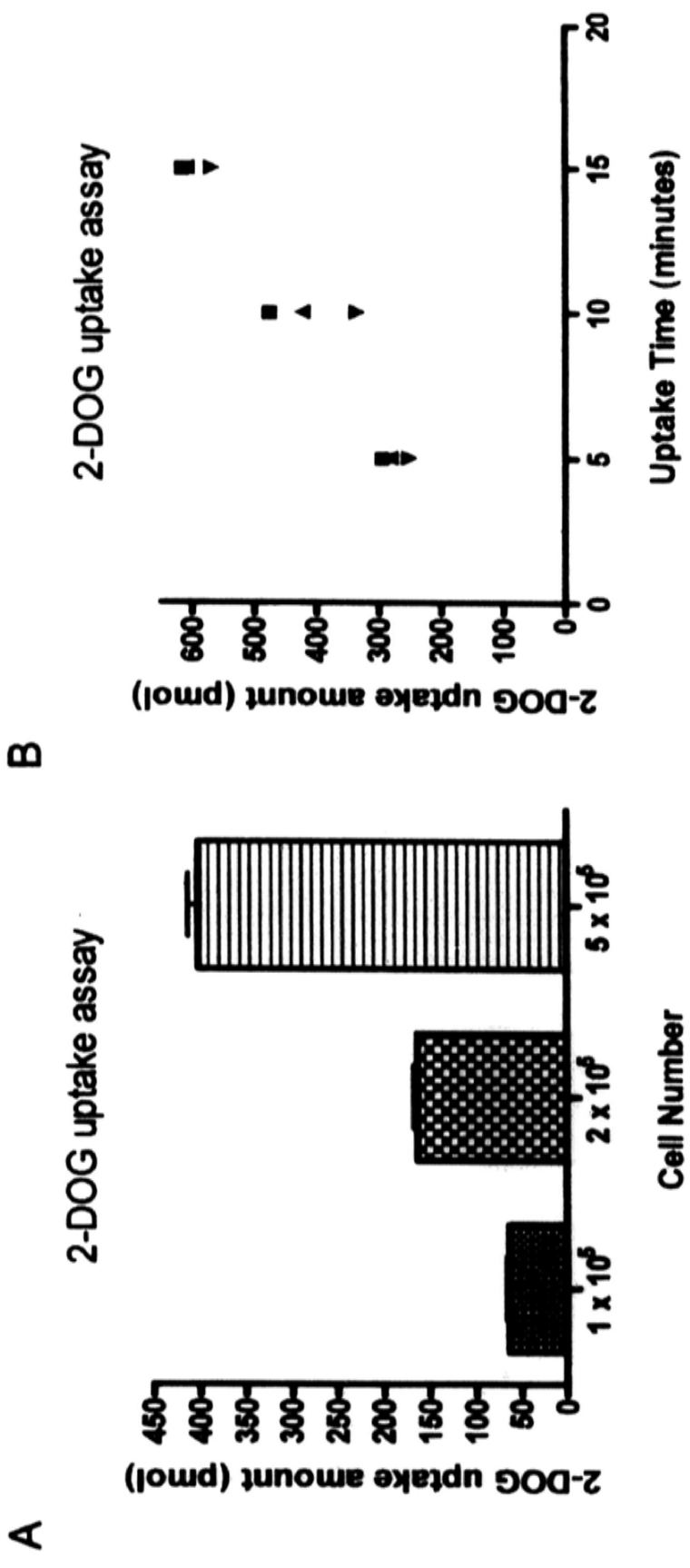


Figure 4.8 Standardization of working conditions for 2-DOG uptake assay. To standardize working conditions for 2-DOG uptake assay, uptake levels (pmol) with three different cell numbers of Mc0M80 (1×10^5 , 2×10^5 and 5×10^5) and uptake time durations (5 minutes, 10 minutes and 15 minutes) were examined. The 2-DOG uptake amount was plotted against cell number (A) and uptake time (B). Data shown was mean \pm S.E.M of triplicates in a single experiment.

2-DOG uptake assay

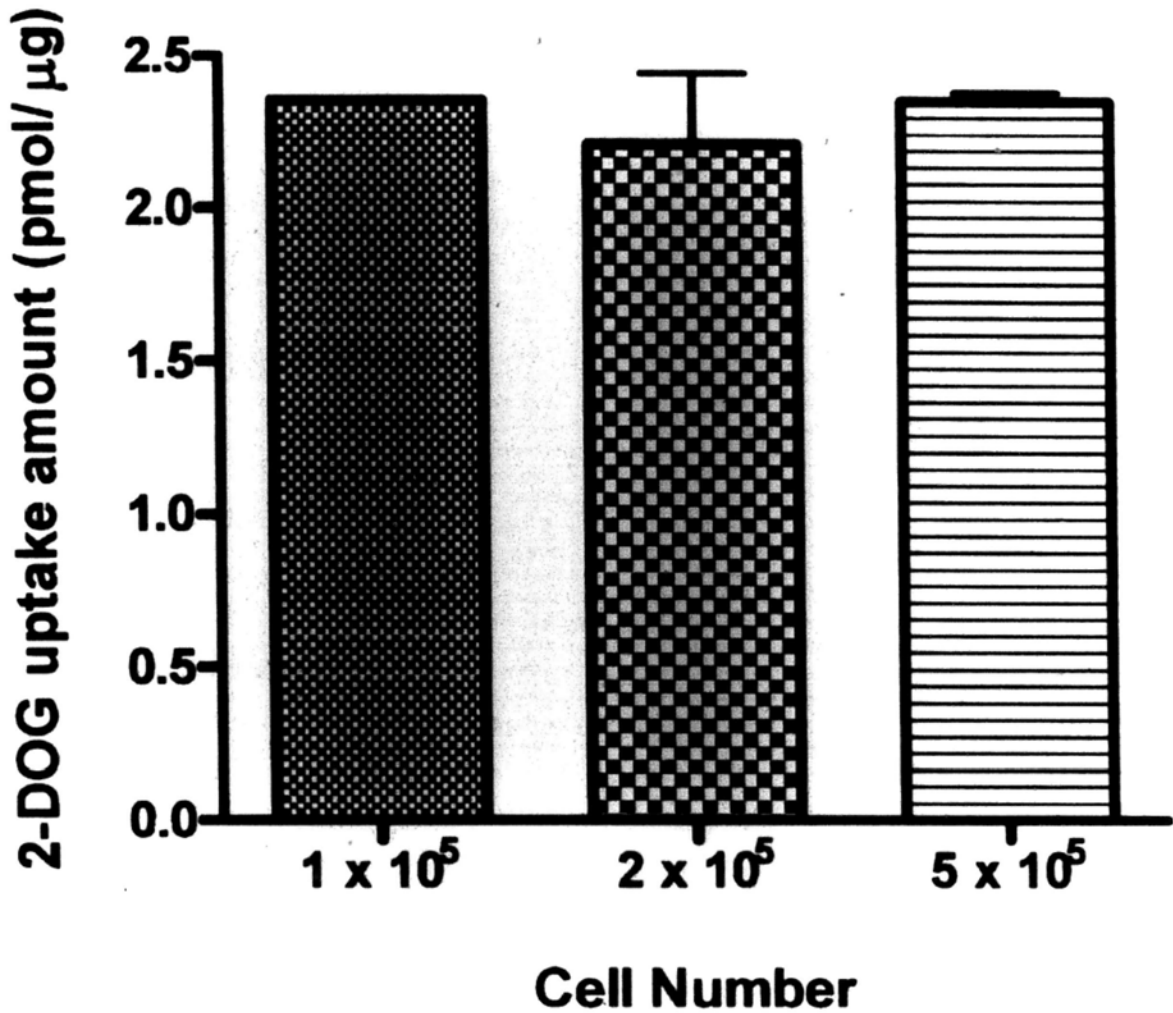


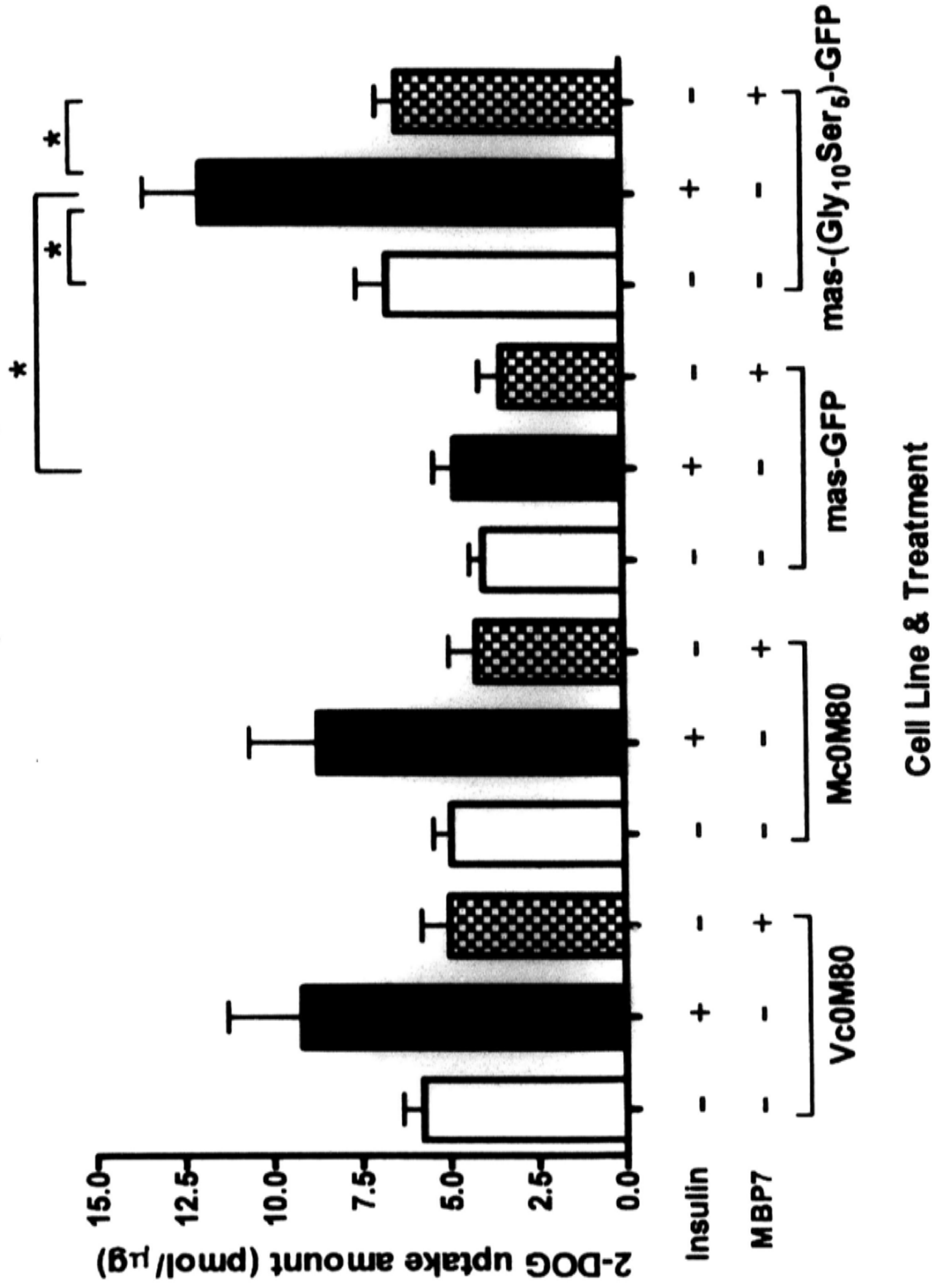
Figure 4.9 Normalization of 2-DOG uptake with protein amount. The 2-DOG uptake levels (pmol) of various cell numbers of Mc0M80 (1×10^5 , 2×10^5 , 5×10^5) were normalized with protein amount (μg) and were displayed as "pmol/ μg ". The uptake level was plotted against protein amount. Data shown was mean \pm S.E.M of triplicates in a single experiment.

4.3.4 Glucose uptake in Vc0M80, Mc0M80 and CHO cells expressing mas fusion variants

2-DOG uptake assay was performed to compare glucose uptake level in Vc0M80, Mc0M80 and CHO cells expressing mas fusion variants. Briefly, cells (2×10^5 per well) in a 24-well plate were starved for 4 hours and then washed thoroughly with KRP buffer. After incubation with KRP buffer for additional 30 minutes, cellular glucose uptake was estimated by measuring the uptake amount of ^3H -2-DOG in a time duration of 10 minutes. The change of glucose uptake triggered by insulin or MBP7 was detected by co-incubation of ^3H -2-DOG with 100 nM insulin or 30 μM MBP7 (Figure 4.10). Group differences in different cell lines under various treatments were analyzed by Two Way ANOVA. All of the cell lines uptake glucose similarly in the basal condition and responded to insulin stimulation as indicated by elevation of glucose uptake. The insulin's positive effect on glucose uptake was especially significant in cell expressing mas-(Gly₁₀Ser₅)-GFP compared with its basal and MBP7-triggered glucose uptake levels. In addition, insulin stimulated glucose uptake in cells expressing mas-(Gly₁₀Ser₅)-GFP was significantly higher than that in cells expressing mas-GFP ($P < 0.05$). MBP7 hardly induce any change in glucose uptake among all the cell lines.

Figure 4.10 2-DOG uptake in Vc0M80, Mc0M80 and CHO cells expressing mas fusion variants. 2-DOG uptake assay was performed in Vc0M80, Mc0M80 and CHO cells expressing mas fusion variants. The open, close and dotted columns represented 2-DOG uptake in the basal condition and under 100 nM insulin or 30 μ M MBP7 stimulation, respectively. Data shown were mean \pm S.E.M collected from two independent experiments each performed in triplicate. * indicated statistical difference ($P<0.05$) in the examined groups by Two Way ANOVA analysis using SigmaStat 3.0 program.

2-DOG uptake assay



4.3.5 Evaluation of mas effect on glucose uptake

To determine whether mas expression level brought a difference in cellular glucose uptake, Vc0M80 and CHO cells with various expression levels of mas were subjected to 2-DOG uptake assay (Figure 4.11). Cell clones expressing various levels of mas were Mc0M80, Mc7M80 and Mc35M80. Apart from basal condition, cellular glucose uptake in response to 100 nM insulin or 30 μ M MBP7 was also measured. The uptake level (pmol) was normalized against protein amount (μ g) and displayed as "pmol/ μ g". All of the cell lines uptake glucose similarly in the basal condition and showed an increase of glucose uptake in response to insulin. In comparison, MBP7 seemed to induce little change in cellular glucose uptake. No statistical difference was found by Two Way ANOVA analysis using SigmaStat 3.0 program.

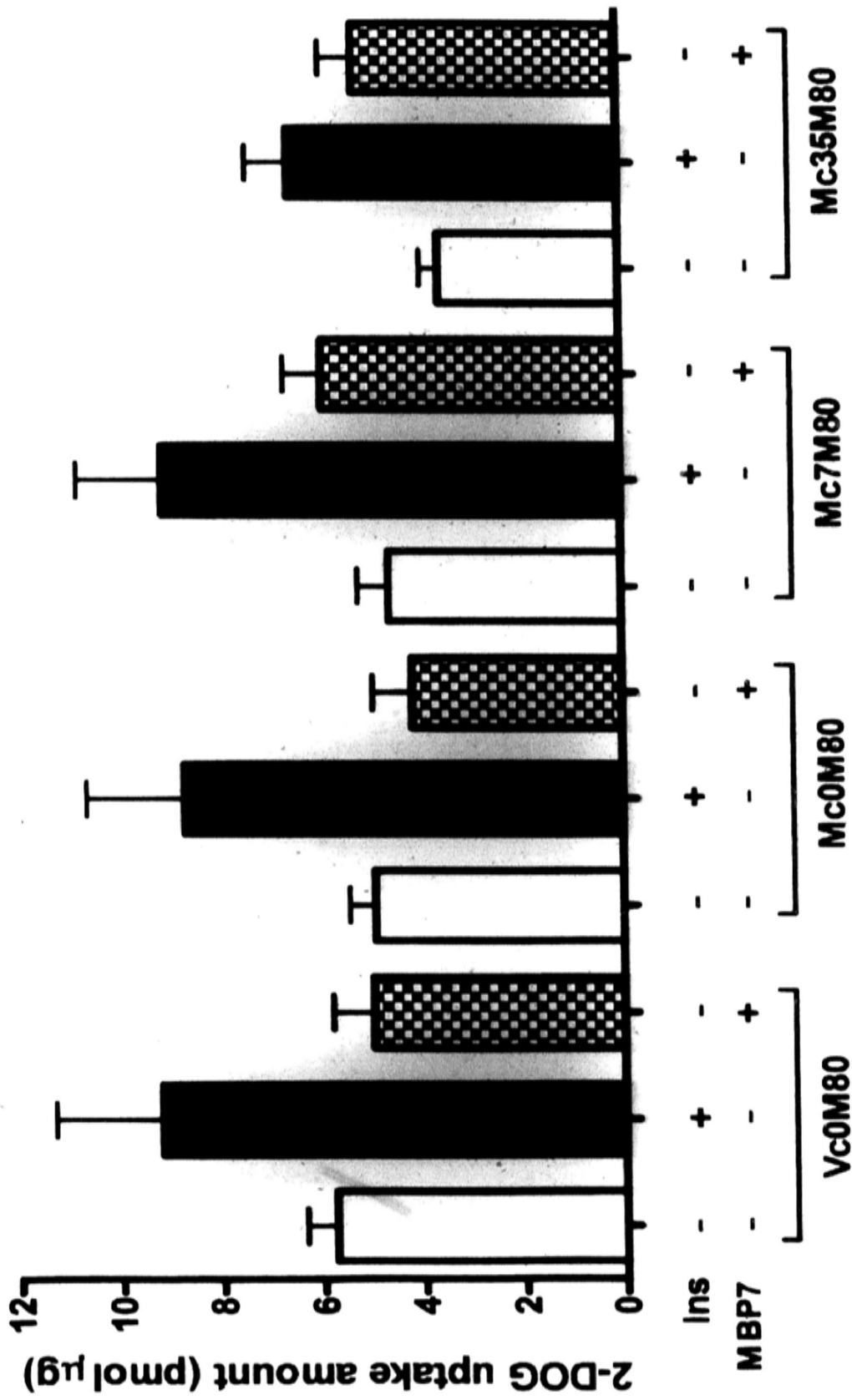
4.3.6 RhoA effect on mas regulated glucose uptake

To examine whether RhoA limits cellular response to mas activation, 2-DOG uptake assay was performed in Mc0M80 cells transiently expressing RhoA plasmid variants. Glucose uptake of Mc0M80 transfected with each single RhoA plasmid in the absence or presence of 30 μ M MBP7 was measured (Figure 4.12). The glucose uptake (pmol) was normalized against protein amount (μ g). The basal glucose uptake in RhoA-WT and RhoA-TN transfected Mc0M80 cells were slightly higher while RhoA-GV transfected Mc0M80 showed less glucose uptake compared with non-transfected Mc0M80. However, statistically there was no significant difference in basal glucose uptake amongst those cell lines. On the other hand, MPB7 up-regulated glucose uptake in RhoA-WT or RhoA-GV

transfected Mc0M80 cells while down-regulated glucose uptake in RhoA-TN transfected Mc0M80. Similarly no group difference was detected in different RhoA transfected Mc0M80 under various treatments by Two Way ANOVA.

Figure 4.11 Glucose uptake in cells of various mas expression levels. Vc0M80 and CHO cells with various mas expression levels were subjected to 2-DOG uptake assay. Cell clones which expressed various levels of mas were Mc0M80, Mc7M80 and Mc35M80. The open, close and dotted columns represented 2-DOG uptake in the basal condition and under 100 nM insulin or 30 μ M MBP7 stimulation, respectively. The uptake level (pmol) was normalized against protein amount (μ g) and represented as pmol/ μ g. Statistical difference among different cell lines under various treatments was analyzed by Two Way ANOVA using SigmaStat 3.0 program. Data shown was mean \pm S.E.M of three independent experiments each performed in triplicate.

2-DOG uptake assay



Cell Line & Treatment

2-DOG uptake assay

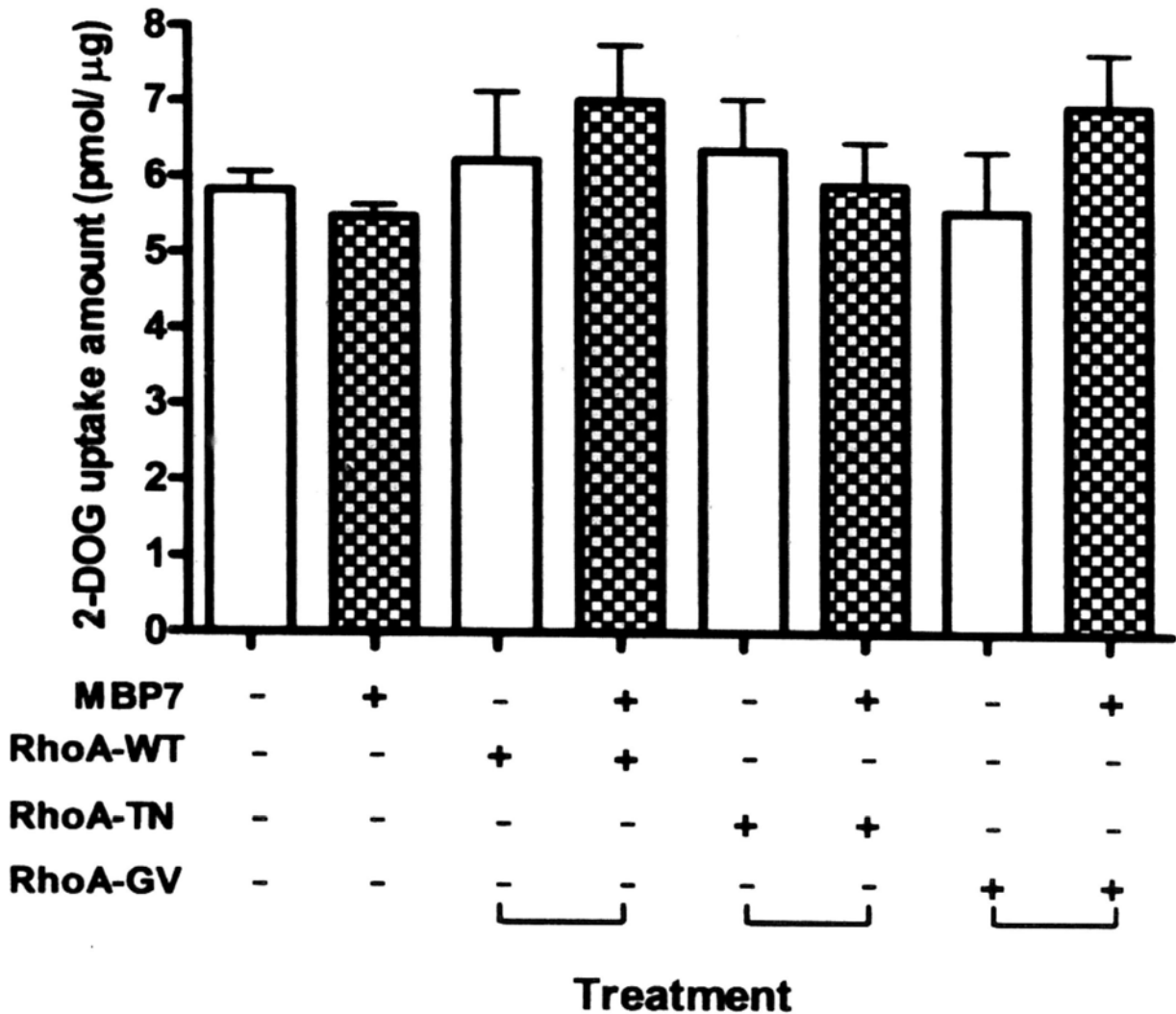


Figure 4.12 RhoA effect on glucose uptake in Mc0M80 cells. 2-DOG uptake assay was performed in Mc0M80 cells transiently expressing RhoA variants. RhoA-WT, RhoA-TN and RhoA-GV represented wild type, dominant negative and dominant active RhoA plasmid, respectively. The open and dotted columns represented 2-DOG uptake in the basal condition and under 30 μ M MBP7 stimulation. Statistical difference among different RhoA constructs-transfected Mc0M80 under various treatments was analyzed by Two Way ANOVA using SigmaStat 3.0 program. Data shown was mean \pm S.E.M of two independent experiments each performed in triplicates.

4.3.7 Pathways involved in glucose uptake of Mc0M80 cells

To identify which signaling pathway mediated cellular glucose uptake in Mc0M80 cells, inhibitors of various protein kinases were added 24 hours before the 2-DOG uptake assay.

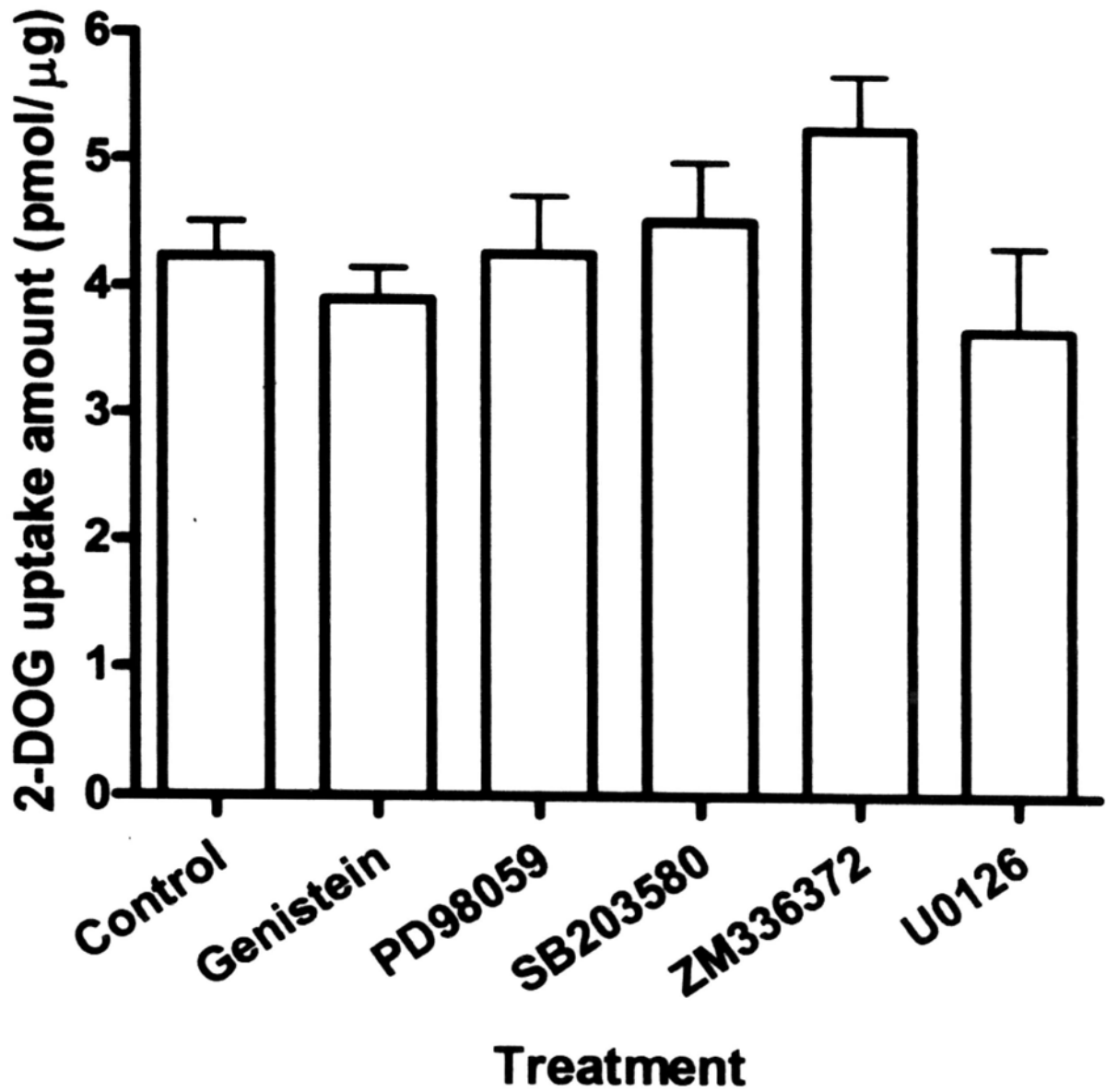
Genistein is a highly selective inhibitor of epidermal growth factor receptor (EGFR). PD98059, SB203580, ZM 336372 and U0126 are series of inhibitors in mitogen activated protein kinase (MAPK) signaling pathway and they inhibit MAPKK/MEK, p38, C-Raf and MAPK/MEK1/MEK2, respectively.

The working concentration for Genistein, PD98059, SB203580, ZM336372 and U0126 were individually optimized to 10 μ M, 20 μ M, 10 μ M, 10 μ M and 10 μ M, respectively (Linassier et al., 1990; Arai et al., 1993; Vlahos et al., 1994; Alessi et al., 1995; Cuenda et al., 1995; Dudley et al., 1995; Saklatvala et al., 1996; Favata et al., 1998; Record et al., 1998; Hall-Jackson et al., 1999a; Hall-Jackson et al., 1999b; Itoh et al., 1999; Narumiya, 1999; Slack et al., 1999; Davies et al., 2000; Narumiya et al., 2000; Sward et al., 2000; Dang et al., 2003). All these inhibitors were incubated with Mc0M80 cells for 24 hours in the IMDM complete medium before starting the experiment.

It was found that Genistein and U0126 decreased while SB203580 and ZM336372 increased basal glucose uptake of Mc0M80 cells. There was not much change in basal glucose uptake of PD98059 treatment group (Figure 4.13). However, no statistical differences was detected among various kinase inhibitor-treated groups by Kruskal-Wallis One Way ANOVA on Ranks using SigmaStat 3.0 program.

Figure 4.13 Effect of protein kinase inhibitors on glucose uptake in Mc0M80 cells. 2-DOG uptake under treatment of various protein kinase inhibitors was examined and represented in different colored open columns. The working concentrations for Genistein, PD98059, SB203580, ZM336372, U0126, were 10 μ M, 20 μ M, 10 μ M, 10 μ M and 10 μ M, respectively. Statistical difference of basal glucose uptake among various kinase inhibitor treatment groups were evaluated by Kruskal-Wallis One Way ANOVA on Ranks using SigmaStat 3.0 program. Data shown was mean \pm S.E.M of two independent experiments each performed in triplicate.

2-DOG uptake assay

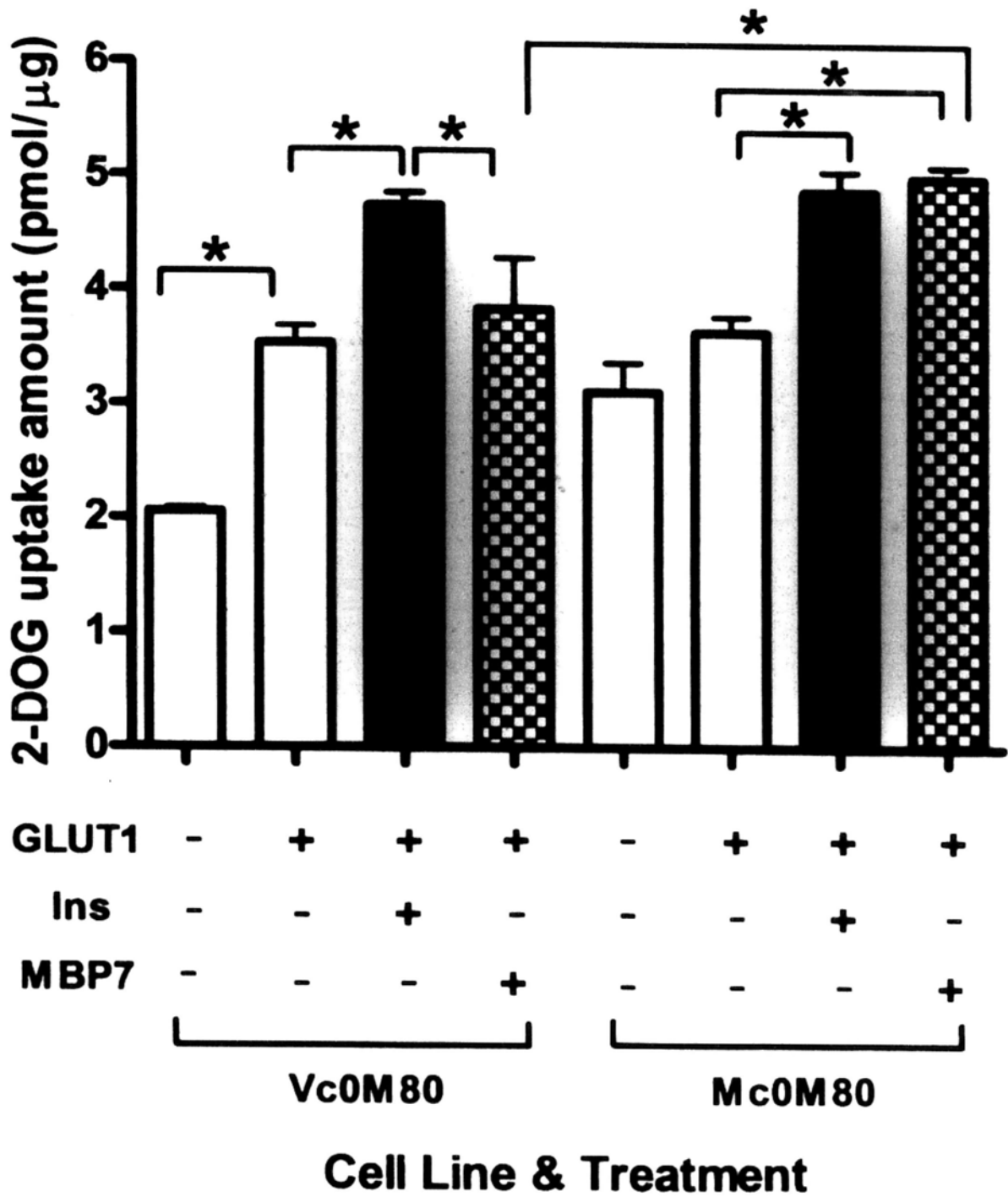


4.3.8 Effect of mas on GLUT1-mediated glucose uptake

It was reported that mas-binding concensus motif 1 (RQALRRLLRRGL) showed more than 80% similarity with peptide sequence of human intestinal facilitative GLUT7 (Accession # NP_997303.1) (Bikkavilli et al., 2006). The peptide sequences of human facilitative GLUT1 and GLUT7 were aligned and more than 40% similarity was found (Figure 4.14). To test whether mas exerted any effect on GLUT1-mediated glucose uptake, Vc0M80 and Mc0M80 cells were subjected to 2-DOG uptake assay at 24 hours after transient transfection with rat GLUT1-myc (Figure 4.15). The glucose uptake of transfected Vc0M80 and Mc0M80 in the basal condition and under 100 nM insulin or 30 μ M MBP7 stimulation were measured and compared. Transient expression of GLUT1 enhanced basal 2-DOG uptake in both cell lines compared with the non-transfected cells and the additive effect was especially apparent in transfected Vc0M80 cells ($P < 0.05$) as indicated by One Way ANOVA. The group differences in transfected Vc0M80 and Mc0M80 under various treatments were analyzed by Two Way ANOVA. Insulin significantly increased GLUT1-mediated 2-DOG uptake in both Vc0M80 and Mc0M80 ($P < 0.05$). MBP7 was surprisingly found to specifically and significantly elevate glucose uptake in Mc0M80 cells to an extent similar to insulin ($P > 0.05$). Glucose uptake of MBP7-treated transfected Mc0M80 was significantly higher than that of transfected Vc0M80 treated with MBP7 ($P < 0.05$). All the statistical analyses were performed using SigmaStat 3.0 program.

Figure 4.15 GLUT1-mediated glucose uptake. Vc0M80 and Mc0M80 cells transiently transfected with rat GLUT1-myc were subjected to 2-DOG uptake assay. The open, close and dotted columns represented 2-DOG uptake in the basal condition and under 100 nM insulin or 30 μ M MBP7 stimulation, respectively. Statistical difference in basal glucose uptake between non-transfected and transfected cells was analyzed by One Way ANOVA. Group difference among different transfected cell lines under various treatments was detected by Two Way ANOVA. Statistical significance was represented as *. Data shown was mean \pm S.E.M of three independent experiments each performed in triplicate.

2-DOG uptake assay



4.4 Discussion

4.4.1 *Screening of GLUT and IR in CHO cells*

The expressions of particular GLUT(s) or IR were examined by RT-PCR which was a quick and sensitive approach. The cell type tested in this experiment was CHO cell because all the stable cell lines were constructed from it. However, no sequence information on CHO GLUT and IR was found in the NCBI nucleotide database. So the primers for GLUT and IR screening were designed from the most highly conserved regions in GLUT and IR sequences of rat, mouse and human.

Because GLUT1 and GLUT4 are from the same class of GLUT family and have high homology with each other in the DNA sequence, the sequencing result was aligned with both of them. The amplified sequence was found to show 89% and 70% similarity with rat GLUT4 and GLUT1, respectively. Therefore, it was concluded that GLUT4 rather than GLUT1 was more likely to be expressed in CHO cells.

IR was surprisingly failed to be detected in CHO cells using RT-PCR. However, various cell lines constructed from CHO cells such as Vc0M80 and several clones which expressed mas showed increased 2-DOG uptake level in response to insulin. Insulin signaling was a complicated network which involved many effectors (Chang et al., 2004; Jiang & Zhang, 2005; Laviola et al., 2006; Musi & Goodyear, 2006; Noguchi & Kasuga, 2006; White, 2006; Ferre, 2007; Gonzalez-Sanchez & Serrano-Rios, 2007; Karlsson & Zierath, 2007; Zaid et al., 2008). On the other hand, some G protein-coupled receptors

were reported to be involved in insulin signaling previously (Roettger et al., 1995; Winzell & Ahren, 2007). So IR deficiency in Mc0M80 cells was not contradictory with cellular response to insulin in the 2-DOG uptake assay.

4.4.2 *Standardization of 2-DOG uptake assay*

Glucose analogs 2-deoxy-D-glucose (2-DOG) and radiolabelled 2-DOG can be transported across cell membrane competitively and then accumulated in the intracellular space due to inability to be metabolized. The cellular glucose uptake competency in 2-DOG uptake assay is reflected by radioactive value from ^3H -2-DOG in the total cell lysate after normalized against protein amount (Tanti et al., 2001). The uptake time for 2-DOG uptake ranges from seconds to minutes or even one hour depending on different cell types (D'Amore et al., 1986; Gaitan et al., 1997; Bosch et al., 2003; Yoo et al., 2005). Thus optimizing working condition of 2-DOG uptake assay in CHO cell established stable cell lines was important. In this experiment, 2×10^5 of cell number and 10 minutes of uptake time were found to be in the middle of linear region of the uptake curve and considered as standards for 2-DOG uptake assay.

4.4.3 *Glucose uptake in the absence or presence of mas*

The homology between the motif 1 of mas binding peptide and human facilitative GLUT7 sequence proposed the possible interaction between GLUT and mas. So cell clones expressing mas were subjected to 2-DOG uptake assay and compared with Vc0M80 in glucose uptake level to determine whether mas made a difference in cellular

glucose uptake. Because insulin was reported to induce GLUT4 membrane trafficking and increase cellular glucose uptake, 100 nM insulin was used as a positive control in the 2-DOG uptake assay.

To our surprise, cells expressing mas-(Gly₁₀Ser₅)-GFP showed an extremely huge increase of glucose uptake to insulin stimulation. In addition, 2-DOG uptake of cell expressing mas-(Gly₁₀Ser₅)-GFP were always higher than that of cell expressing mas-GFP in any condition. Actually the difference in phage ligand binding and membrane mas fusion proteins translocation between cells expressing mas-(Gly₁₀Ser₅)-GFP and mas-GFP implied that the glucose uptake level of the two cell lines might be different as well. The result indicated that mas-(Gly₁₀Ser₅)-GFP was better to interact with downstream signaling molecule.

It was of interest to know whether mas could facilitate cellular glucose uptake. To confirm the assumption, cell clones with various mas expression levels were subjected to 2-DOG uptake assay and compared with Vc0M80. Statistical analysis on the data collected from two independent experiments each performed in triplicate showed no significant difference among Mc0M80, Mc7M80, Mc35M80 and Vc0M80. It was thus concluded that mas expression was unlikely to induce change in cellular glucose uptake.

4.4.4 *RhoA effect on mas-MBP7 regulated glucose uptake*

Rho family contains three classes of small GTP-binding proteins which are Rac, Rho and others such as TC10, TTF and CDC42Hs. Several phenomena linked mas to Rho family. For instance, mas-transformed NIH3T3 cells formed foci in the same pattern with that induced by Rho and Rac. Cytoskeleton in mas-expressing cells was similar to that in cells expressing Rac (Zohn et al., 1998). It was of interest to find out whether the lack of response to mas activation was due to the inavailability of Rho proteins in mas-transfected cells. 2-DOG uptake assay was performed in Mc0M80 cells transiently transfected with RhoA plasmid variants.

Surprisingly, RhoA wild type (RhoA-WT) and dominant negative RhoA (RhoA-TN) showed similar effect on Mc0M80 and slightly increased basal glucose uptake. On the contrary, a minor decrease of glucose uptake was observed in dominant positive RhoA (RhoA-GV) transfected Mc0M80 cells. Because RhoA was only functional in RhoA-WT and RhoA-GV but not RhoA-TN, inagreement in cellular glucose uptake in the presence of RhoA-WT and RhoA-GV indicated that RhoA was not likely to be involved in basal glucose uptake in Mc0M80 cells. In addition, consistent with the lack of any stimulatory effect of MBP7 in cells expressing various GFP fusion constructs, there was also lack of response to MBP7 in Mc0M80 cells upon transfection with various RhoA proteins.

4.4.5 *Kinase inhibitors effect on mas-MBP7 mediated glucose uptake*

Mas was previously proposed to activate Gαq and subsequent PLCβ. Therefore, via which downstream signaling pathway(s) mas mediating cellular glucose uptake was

studied. Several kinase inhibitors in different signaling pathways were selected for 2-DOG uptake assay in Mc0M80 cells. All of these inhibitors were soluble in DMSO or PBS and membrane permeable that enabled cells to be pre-treated in culture medium for 24 hours.

All the kinase inhibitors exerted no statistically significant effect on basal glucose uptake of Mc0M80 cells showing that the basal glucose uptake in Mc0M80 cells was not regulated by the examined signaling pathways.

4.4.6 *Mas effect on GLUT1-mediated glucose uptake*

Apart from GLUT4, GLUT1 was reported to respond to insulin and increased glucose uptake although not to an extent as high as GLUT4 did (Bell et al., 1990). As expected, the response patterns of GLUT1-transfected Vc0M80 and Mc0M80 cells to insulin were similar to that of non-transfected cells which expressed endogenous GLUT4. However, it was unexpected that MBP7 triggered a similar increase of glucose uptake as insulin only in GLUT1-transfected Mc0M80, but not in Vc0M80 cells. Contrast between GLUT4- and GLUT1-mediated glucose uptake in Mc0M80 cells under MBP7 treatment indicated that downstream signaling of MBP7-activated mas was possibly coupled with GLUT1 rather than GLUT4.

Chapter 5

General Discussion

Mas, as a proto-oncogene, has been studied for more than twenty years (Young et al., 1986; Rabin et al., 1987; Janssen et al., 1988; van 't Veer et al., 1988; Hanley et al., 1990; Metzger et al., 1995; Kumar et al., 1996; Riesewijk et al., 1996; Alenina et al., 2002; Canals et al., 2006). Up till now endogenous ligand for mas has not been fully confirmed yet.

Mas was once reported to encode an angiotensin receptor and induce angiotensin responsiveness in mas-expressing cells (Jackson et al., 1988; Dean & Boynton, 1990; Von Bohlen und Halbach et al., 2000; Walther et al., 2000; Canals et al., 2006). However, other studies indicated that angiotensin inhibitor displayed no growth inhibition in cells expressing mas (Barak et al., 1997; Kostenis et al., 2005). The viewpoint of mas as an angiotensin receptor was thus challenged. Recent research demonstrated that angiotensin-(1-7) specifically bound to and activated mas-expressing cells and was proposed to be a new candidate for endogenous ligand of mas (Santos et al., 2003; Hellner et al., 2005; Tallant et al., 2005).

In our lab, no stimulatory effect was detected in Mc0M80 cells over-expressing mas upon angotensin-(1-7) (10 mM) treatment in PI turnover assay. In comparison, MBP7 (10 μ M) and ATP (100 μ M) showed significantly additive or synergistic effect specifically on Mc0M80 cells (Bikkavilli et al., 2006). Therefore, MBP7 was used as a surrogate ligand for mas in the functional assays in this project.

Based on the GPCR structure, ligand generally binds to the exogenous pocket formed by N terminal extracellular loops and the transmembrane segments, activating downstream signaling via intracellular loops at C-terminus. Receptor-ligand interaction usually triggers receptor translocation as observed in mas protein. Although MBP7 specifically bound to mas-GFP, it poorly induced its translocation. Different responses to MBP7 between native mas and mas-GFP indicated that GFP tagging at the C terminus might partially suppress mas interaction with downstream effectors. Actually GFP tagging effect had been reported in other GPCRs (Barak et al., 1997; Xiao et al., 1997)

It was noted that a member of mas-related protein family which was eighteen amino acid longer than mas at C-terminus had no inhibition effect from GFP tagging (Milasta et al., 2006). Therefore, it was hypothesized that tagging the short C-terminal tail of mas with GFP blocked its interaction with downstream signaling molecules. Here in this project, to find out whether C terminus of mas was critical for its downstream signaling after ligand binding, two different mas fusion constructs were produced which were mas-GFP and mas-(Gly₁₀Ser₅)-GFP. The peptide linker between mas and GFP was derived from the linker that was commonly used in the single chain antibody. The peptide linker was characterized with good stability and little spatial hindrance.

Both immunoprecipitation blots and confocal images indicated that mas-GFP and mas-(Gly₁₀Ser₅)-GFP had similar molecular weights and distribution patterns. However, mas-(Gly₁₀Ser₅)-GFP showed more efficient ligand binding and higher translocation capability than mas-GFP. In addition, MBP7 triggered elevation of intracellular free

calcium in cells expressing mas-(Gly₁₀Ser₅)-GFP and native mas, and gave an sustained reponse that lasted longer than that of mas-GFP. The data from the functional assays illustrated that mas C-terminus was very important for its interaction with ligand and downstream signaling while the peptide linker alleviated mas from the blockage by GFP without altering its biological activity.

Mas was once characterized as constitutively activating $G\alpha_{q/11}$ signaling pathway (Canals et al., 2006). In the functional assays, although the basal levels of inositol phosphate or free calcium were similar among all the cell lines, accumulation of intracellular inositol phosphate or free calcium mobilization was only detected after MBP7 stimulation in cells expressing mas. These phenomena indicated that only MBP7-activated mas transmitted signals via $G\alpha_q$ to subsequent phospholipase C and finally invoked calcium mobilization.

Although MBP7 was an artificially synthesized peptide, MBP7-like sequence motif could be found in several classes of endogenous proteins such as some membrane receptors, GPCRs, enzyme and regulatory proteins (Bikkavilli et al., 2006). The homology between MBP7 and glucose transporter 7 as well as putative monosaccharide transporter 1 aroused interests in the potential regulation of mas on glucose uptake.

GLUT 7 was mainly expressed in the urogenital and digestive system responsible for transportation of glucose and fructose while GLUT4 was preferably expressed in muscle and fat tissues in charge of insulin-stimulated glucose uptake (Joost & Thorens, 2001; Joost et al., 2002). GLUT1 is expressed ubiquitously and is required for basal glucose

uptake. GLUT4 is characterized with quick translocation to cell membrane in response to insulin. Actually, although GLUT1 preferably distributes in the cell surface, still a huge amount is reserved in the intracellular space and ready to move to membrane after insulin stimulation (Yang & Holman, 1993; Ishii et al., 1995).

It was found in one previous literature that CHO cell endogenously expressed GLUT1 and insulin receptor ((Ishii et al., 1995). Review of the literature provided no additional information on GLUT type in CHO cell except the statement. So the point of view was challenged and requested further examination.

The homology between PCR amplification of putative GLUT4 in CHO cells and rat GLUT4 was 89% compared to the similarity of 70% with rat GLUT1 indicating that GLUT4 was more likely to be endogenously expressed in CHO cell. Mc0M80 was established from CHO cells and endogenously expressed GLUT4. The phenomenon that MBP7 could increase GLUT1-mediated rather than GLUT4-mediated glucose uptake indicated that activated mas was likely to couple with GLUT1 but not GLUT4 in the downstream signaling.

Rapid growth rate of cancer cell requires more glucose for the correspondingly higher metabolizing rate (Ganapathy et al., 2009). So up-regulation and aberrant induction of GLUT might be a sign for transformation of normal cell to cancer. For instance, GLUT1 expression was considered as a bad prognosticator for pancreas cancer because it was involved in the early stage of pancreas carcinogenesis and triggered higher glucose

uptake in poorly differentiated and highly proliferative pancreatic cancer cells (Pizzi et al., 2009). Targeting GLUT might be developed as a new adjuvant approach for cancer. In vitro studies on some GLUT inhibitors and analogues demonstrated that partial inhibition on glucose transport sensitized cells to death receptor stimuli and facilitated apoptosis (Wood et al., 2008).

Higher basal glucose uptake level in Mc0M80 and cells expressing mas fusion variants proposed the potential of mas in facilitating cellular glucose uptake. However, insignificant statistical difference among cell clones expressing various levels of mas and Vc0M80 disproved the assumption and indicated that mas might not affect GLUT4-mediated glucose uptake significantly.

In this project, evaluation of glucose uptake level in the absence or presence of MBP7 in cells pretreated with different kinase inhibitors helped to screen out potential signaling pathways for mas in regulating glucose uptake. p38 and RhoA signaling pathways were reported to be activated by mas in the formation of cytoskeleton and other physiological processes previously (Zohn et al., 1998). Apart from them, mas activation on EGFR as well as PI3K was proposed for the first time. Actually mas activation on Gαq and subsequent PLCβ had been well defined before. In our lab, mas-MBP7 interaction was shown to trigger elevation of intracellular calcium which consequently activated protein kinase C (PKC). PKC and PI3K contributed together to GLUT4 membrane trafficking and increased glucose uptake. In this regard, mas-MBP7 interaction possibly affected PI3K signaling. Abnormal expression of EGFR is closely related with cancers, for

example, lung carcinoma (Tang et al., 2008). Therefore, research on mas-EGFR interaction is worth to be further studied.

Unlike GLUT4, MBP7 significantly increased GLUT1-mediated glucose uptake. Tumor cells was known to facilitate glucose uptake mainly from the induction of GLUT1 as well as SGLUT1 (Ganapathy et al., 2009). GLUT1 translocation could be partially stimulated by GPCR-ligand interaction via $G\alpha$ signaling ((Hagi et al., 2000). Mas activation on $G\alpha_{q/11}$ had been demonstrated previously in the up-regulation of angiotensin II type 1 receptor (Canals et al., 2006). So it was probable that MBP7-activated mas downstream signaling affected GLUT1 membrane trafficking through $G\alpha_q$. The altered glucose uptake after MBP7 stimulation in Mc0M80 cells might be resulted from the re-distribution of GLUT1 and GLUT4 upon downstream signaling of activated mas and could be confirmed by immunocytochemistry.

Different outcomes between mas-(Gly₁₀Ser₅)-GFP and mas-GFP in calcium mobilization and glucose uptake illustrated the importance of mas C-terminus for receptor activity. To identify the particular amino acid(s) or any motifs that determines downstream signaling of mas in detail, point mutation and C-terminus truncation could be applied in the future.

Taken together, the project demonstrated that C-terminus was very important for mas downstream signaling in the functional assays using different mas fusion proteins. In addition, studies on the potential regulation on glucose uptake by mas suggested that mas might selectively regulate GLUT1 via an unidentified pathway yet.

Reference

Alenina N, Baranova T, Smirnow E, Bader M, Lippoldt A, Patkin E, Walther T. (2002). "Cell type-specific expression of the Mas proto-oncogene in testis." *J Histochem Cytochem* 50:691-696.

Alessi DR, Cuenda A, Cohen P, Dudley DT, Saltiel AR. (1995). "PD 098059 is a specific inhibitor of the activation of mitogen-activated protein kinase kinase in vitro and in vivo." *The Journal of biological chemistry* 270:27489-27494.

Andrawis NS, Dzau VJ, Pratt RE. (1992). "Autocrine stimulation of mas oncogene leads to altered growth control." *Cell biology international reports* 16:547-556.

Arai M, Sasaki Y, Nozawa R. (1993). "Inhibition by the protein kinase inhibitor HA1077 of the activation of NADPH oxidase in human neutrophils." *Biochemical pharmacology* 46:1487-1490.

Baldwin JM. (1993). "The probable arrangement of the helices in G protein-coupled receptors." *The EMBO journal* 12:1693-1703.

Barak LS, Ferguson SS, Zhang J, Martenson C, Meyer T, Caron MG. (1997). "Internal trafficking and surface mobility of a functionally intact beta2-adrenergic receptor-green fluorescent protein conjugate." *Molecular pharmacology* 51:177-184.

Bell GI, Kayano T, Buse JB, Burant CF, Takeda J, Lin D, Fukumoto H, Seino S. (1990). "Molecular biology of mammalian glucose transporters." *Diabetes care* 13:198-208.

Berridge MJ. (1997). "The AM and FM of calcium signalling." *Nature* 386:759-760.

Bikkavilli RK, Tsang SY, Tang WM, Sun JX, Ngai SM, Lee SS, Ko WH, Wise H, Cheung WT. (2006). "Identification and characterization of surrogate peptide ligand for orphan G protein-coupled receptor mas using phage-displayed peptide library." *Biochemical pharmacology* 71:319-337.

Bosch RR, Bazuine M, Wake MM, Span PN, Olthaar AJ, Schurmann A, Maassen JA, Hermus AR, Willems PH, Sweep CG. (2003). "Inhibition of protein kinase C β 1 increases glucose uptake in 3T3-L1 adipocytes through elevated expression of glucose transporter 1 at the plasma membrane." *Molecular endocrinology (Baltimore, Md)* 17:1230-1239.

Bunnemann B, Fuxe K, Metzger R, Mullins J, Jackson TR, Hanley MR, Ganten D. (1990). "Autoradiographic localization of mas proto-oncogene mRNA in adult rat brain using in situ hybridization." *Neuroscience letters* 114:147-153.

Cabrera-Vera TM, Vanhauwe J, Thomas TO, Medkova M, Preininger A, Mazzoni MR, Hamm HE. (2003). "Insights into G protein structure, function, and regulation." *Endocrine reviews* 24:765-781.

Canals M, Jenkins L, Kellett E, Milligan G. (2006). "Up-regulation of the angiotensin II type I receptor by the MAS proto-oncogene is due to constitutive activation of Gq/G11 by MAS." *The Journal of biological chemistry* 281:16757-16767.

Chalmers DT, Behan DP. (2002). "The use of constitutively active GPCRs in drug discovery and functional genomics." *Nature reviews* 1:599-608.

Chang L, Chiang SH, Saltiel AR. (2004). "Insulin signaling and the regulation of glucose transport." *Molecular medicine (Cambridge, Mass)* 10:65-71.

Coleman DE, Berghuis AM, Lee E, Linder ME, Gilman AG, Sprang SR. (1994). "Structures of active conformations of Gi alpha 1 and the mechanism of GTP hydrolysis." *Science (New York, NY)* 265:1405-1412.

Cuenda A, Rouse J, Doza YN, Meier R, Cohen P, Gallagher TF, Young PR, Lee JC. (1995). "SB 203580 is a specific inhibitor of a MAP kinase homologue which is stimulated by cellular stresses and interleukin-1." *FEBS letters* 364:229-233.

D'Amore T, Duronio V, Cheung MO, Lo TC. (1986). "Isolation and characterization of hexose transport mutants in L6 rat myoblasts." *Journal of cellular physiology* 126:29-36.

Dang ZC, Audinot V, Papapoulos SE, Boutin JA, Lowik CW. (2003). "Peroxisome proliferator-activated receptor gamma (PPARgamma) as a molecular target for the soy phytoestrogen genistein." *The Journal of biological chemistry* 278:962-967.

Daniels GM, Amara SG. (1998). "Selective labeling of neurotransmitter transporters at the cell surface." *Methods in enzymology* 296:307-318.

Davies SP, Reddy H, Caivano M, Cohen P. (2000). "Specificity and mechanism of action of some commonly used protein kinase inhibitors." *The Biochemical journal* 351:95-105.

Dean NM, Boynton AL. (1990). "Angiotensin II causes phosphatidylinositol turnover and increases 1,2-diacylglycerol mass but is not mitogenic in rat liver T51B cells." *The Biochemical journal* 269:347-352.

Dohlman HG, Bouvier M, Benovic JL, Caron MG, Lefkowitz RJ. (1987). "The multiple membrane spanning topography of the beta 2-adrenergic receptor. Localization of the sites of binding, glycosylation, and regulatory phosphorylation by limited proteolysis." *The Journal of biological chemistry* 262:14282-14288.

Dong X, Han S, Zylka MJ, Simon MI, Anderson DJ. (2001). "A diverse family of GPCRs expressed in specific subsets of nociceptive sensory neurons." *Cell* 106:619-632.

Downes GB, Gautam N. (1999). "The G protein subunit gene families." *Genomics* 62:544-552.

Drmotá T, Gould GW, Milligan G. (1998). "Real time visualization of agonist-mediated redistribution and internalization of a green fluorescent protein-tagged form of the thyrotropin-releasing hormone receptor." *The Journal of biological chemistry* 273:24000-24008.

Dudley DT, Pang L, Decker SJ, Bridges AJ, Saltiel AR. (1995). "A synthetic inhibitor of the mitogen-activated protein kinase cascade." *Proceedings of the National Academy of Sciences of the United States of America* 92:7686-7689.

Favata MF, Horiuchi KY, Manos EJ, Daulerio AJ, Stradley DA, Feeser WS, Van Dyk DE, Pitts WJ, Earl RA, Hobbs F, Copeland RA, Magolda RL, Scherle PA, Trzaskos JM. (1998). "Identification of a novel inhibitor of mitogen-activated protein kinase kinase." *The Journal of biological chemistry* 273:18623-18632.

Ferre P. (2007). "[Insulin signaling and insulin resistance]." *Therapie* 62:277-284.

Fredriksson R, Lagerstrom MC, Lundin LG, Schioth HB. (2003). "The G-protein-coupled receptors in the human genome form five main families. Phylogenetic analysis, paralogon groups, and fingerprints." *Molecular pharmacology* 63:1256-1272.

Gaitan S, Escribano S, Sancho P, Cuenllas E, Tejero C. (1997). "Glucose metabolism in bone marrow cells and granulocytes of adult mice after X-ray (5 Gy) irradiation: relationship to cell functionality." *British journal of haematology* 96:559-565.

Ganapathy V, Thangaraju M, Prasad PD. (2009). "Nutrient transporters in cancer: Relevance to Warburg hypothesis and beyond." *Pharmacology & therapeutics* 121:29-40.

Gonzalez-Sanchez JL, Serrano-Rios M. (2007). "Molecular basis of insulin action." *Drug news & perspectives* 20:527-531.

Hagi A, Hayashi H, Kishi K, Wang L, Ebina Y. (2000). "Activation of G-protein coupled fMLP or PAF receptor directly triggers glucose transporter type I (GLUT1) translocation in Chinese hamster ovary (CHO) cells stably expressing fMLP or PAF receptor." *J Med Invest* 47:19-28.

Hall-Jackson CA, Evers PA, Cohen P, Goedert M, Boyle FT, Hewitt N, Plant H, Hedge P. (1999a). "Paradoxical activation of Raf by a novel Raf inhibitor." *Chemistry & biology* 6:559-568.

Hall-Jackson CA, Goedert M, Hedge P, Cohen P. (1999b). "Effect of SB 203580 on the activity of c-Raf in vitro and in vivo." *Oncogene* 18:2047-2054.

Hamm HE. (1998). "The many faces of G protein signaling." *The Journal of biological chemistry* 273:669-672.

Han SK, Dong X, Hwang JI, Zylka MJ, Anderson DJ, Simon MI. (2002). "Orphan G protein-coupled receptors MrgA1 and MrgC11 are distinctively activated by RF-amide-related peptides through the Galpha q/11 pathway." *Proceedings of the National Academy of Sciences of the United States of America* 99:14740-14745.

Hanley MR, Cheung WT, Hawkins P, Poyner D, Benton HP, Blair L, Jackson TR, Goedert M. (1990). "The mas oncogene as a neural peptide receptor: expression, regulation and mechanism of action." *Ciba Foundation symposium* 150:23-38; discussion 38-46.

Hellner K, Walther T, Schubert M, Albrecht D. (2005). "Angiotensin-(1-7) enhances LTP in the hippocampus through the G-protein-coupled receptor Mas." *Molecular and cellular neurosciences* 29:427-435.

Huh KH, Wenthold RJ. (1999). "Turnover analysis of glutamate receptors identifies a rapidly degraded pool of the N-methyl-D-aspartate receptor subunit, NR1, in cultured cerebellar granule cells." *The Journal of biological chemistry* 274:151-157.

Ishii K, Hayashi H, Todaka M, Kamohara S, Kanai F, Jinnouchi H, Wang L, Ebina Y. (1995). "Possible domains responsible for intracellular targeting and insulin-dependent translocation of glucose transporter type 4." *The Biochemical journal* 309 (Pt 3):813-823.

Itoh K, Yoshioka K, Akedo H, Uehata M, Ishizaki T, Narumiya S. (1999). "An essential part for Rho-associated kinase in the transcellular invasion of tumor cells." *Nature medicine* 5:221-225.

Jackson TR, Blair LA, Marshall J, Goedert M, Hanley MR. (1988). "The mas oncogene encodes an angiotensin receptor." *Nature* 335:437-440.

Janssen JW, Steenvoorden AC, Schmidtberger M, Bartram CR. (1988). "Activation of the mas oncogene during transfection of monoblastic cell line DNA." *Leukemia* 2:318-320.

Jiang G, Zhang BB. (2005). "Modulation of insulin signalling by insulin sensitizers." *Biochemical Society transactions* 33:358-361.

Joost HG, Bell GI, Best JD, Birnbaum MJ, Charron MJ, Chen YT, Doege H, James DE, Lodish HF, Moley KH, Moley JF, Mueckler M, Rogers S, Schurmann A, Seino S, Thorens B. (2002). "Nomenclature of the GLUT/SLC2A family of sugar/polyol transport facilitators." *Am J Physiol Endocrinol Metab* 282:E974-976.

Joost HG, Thorens B. (2001). "The extended GLUT-family of sugar/polyol transport facilitators: nomenclature, sequence characteristics, and potential function of its novel members (review)." *Molecular membrane biology* 18:247-256.

Kallal L, Benovic JL. (2000). "Using green fluorescent proteins to study G-protein-coupled receptor localization and trafficking." *Trends in pharmacological sciences* 21:175-180.

Karlsson HK, Zierath JR. (2007). "Insulin signaling and glucose transport in insulin resistant human skeletal muscle." *Cell biochemistry and biophysics* 48:103-113.

Kostenis E, Milligan G, Christopoulos A, Sanchez-Ferrer CF, Heringer-Walther S, Sexton PM, Gembardt F, Kellett E, Martini L, Vanderheyden P, Schultheiss HP, Walther T. (2005). "G-protein-coupled receptor Mas is a physiological antagonist of the angiotensin II type I receptor." *Circulation* 111:1806-1813.

Kumar M, Grammas P, Giacomelli F, Wiener J. (1996). "Selective expression of c-mas proto-oncogene in rat cerebral endothelial cells." *Neuroreport* 8:93-96.

Lambright DG, Noel JP, Hamm HE, Sigler PB. (1994). "Structural determinants for activation of the alpha-subunit of a heterotrimeric G protein." *Nature* 369:621-628.

Lander ES, Linton LM, Birren B, Nusbaum C, Zody MC, Baldwin J, Devon K, Dewar K, Doyle M, FitzHugh W, Funke R, Gage D, Harris K, Heaford A, Howland J, Kann L, Lehoczky J, LeVine R, McEwan P, McKernan K, Meldrim J, Mesirov JP, Miranda C, Morris W, Naylor J, Raymond C, Rosetti M, Santos R, Sheridan A, Sougnez C, Stange-Thomann N, Stojanovic N, Subramanian A, Wyman D, Rogers J, Sulston J, Ainscough R,

Beck S, Bentley D, Burton J, Clee C, Carter N, Coulson A, Deadman R, Deloukas P, Dunham A, Dunham I, Durbin R, French L, Grafham D, Gregory S, Hubbard T, Humphray S, Hunt A, Jones M, Lloyd C, McMurray A, Matthews L, Mercer S, Milne S, Mullikin JC, Mungall A, Plumb R, Ross M, Shownkeen R, Sims S, Waterston RH, Wilson RK, Hillier LW, McPherson JD, Marra MA, Mardis ER, Fulton LA, Chinwalla AT, Pepin KH, Gish WR, Chissoe SL, Wendl MC, Delehaunty KD, Miner TL, Delehaunty A, Kramer JB, Cook LL, Fulton RS, Johnson DL, Minx PJ, Clifton SW, Hawkins T, Branscomb E, Predki P, Richardson P, Wenning S, Slezak T, Doggett N, Cheng JF, Olsen A, Lucas S, Elkin C, Uberbacher E, Frazier M, Gibbs RA, Muzny DM, Scherer SE, Bouck JB, Sodergren EJ, Worley KC, Rives CM, Gorrell JH, Metzker ML, Naylor SL, Kucherlapati RS, Nelson DL, Weinstock GM, Sakaki Y, Fujiyama A, Hattori M, Yada T, Toyoda A, Itoh T, Kawagoe C, Watanabe H, Totoki Y, Taylor T, Weissenbach J, Heilig R, Saurin W, Artiguenave F, Brottier P, Bruls T, Pelletier E, Robert C, Wincker P, Smith DR, Doucette-Stamm L, Rubenfield M, Weinstock K, Lee HM, Dubois J, Rosenthal A, Platzer M, Nyakatura G, Taudien S, Rump A, Yang H, Yu J, Wang J, Huang G, Gu J, Hood L, Rowen L, Madan A, Qin S, Davis RW, Federspiel NA, Abola AP, Proctor MJ, Myers RM, Schmutz J, Dickson M, Grimwood J, Cox DR, Olson MV, Kaul R, Raymond C, Shimizu N, Kawasaki K, Minoshima S, Evans GA, Athanasiou M, Schultz R, Roe BA, Chen F, Pan H, Ramser J, Lehrach H, Reinhardt R, McCombie WR, de la Bastide M, Dedhia N, Blocker H, Hornischer K, Nordsiek G, Agarwala R, Aravind L, Bailey JA, Bateman A, Batzoglu S, Birney E, Bork P, Brown DG, Burge CB, Cerutti L, Chen HC, Church D, Clamp M, Copley RR, Doerks T, Eddy SR, Eichler EE, Furey TS, Galagan J, Gilbert JG, Harmon C, Hayashizaki Y, Haussler D,

Hermjakob H, Hokamp K, Jang W, Johnson LS, Jones TA, Kasif S, Kasprzyk A, Kennedy S, Kent WJ, Kitts P, Koonin EV, Korf I, Kulp D, Lancet D, Lowe TM, McLysaght A, Mikkelsen T, Moran JV, Mulder N, Pollara VJ, Ponting CP, Schuler G, Schultz J, Slater G, Smit AF, Stupka E, Szustakowski J, Thierry-Mieg D, Thierry-Mieg J, Wagner L, Wallis J, Wheeler R, Williams A, Wolf YI, Wolfe KH, Yang SP, Yeh RF, Collins F, Guyer MS, Peterson J, Felsenfeld A, Wetterstrand KA, Patrinos A, Morgan MJ, de Jong P, Catanese JJ, Osoegawa K, Shizuya H, Choi S, Chen YJ. (2001). "Initial sequencing and analysis of the human genome." *Nature* 409:860-921.

Laviola L, Perrini S, Cignarelli A, Giorgino F. (2006). "Insulin signalling in human adipose tissue." *Archives of physiology and biochemistry* 112:82-88.

Lefkowitz RJ, Pitcher J, Krueger K, Daaka Y. (1998). "Mechanisms of beta-adrenergic receptor desensitization and resensitization." *Advances in pharmacology* (San Diego, Calif 42:416-420.

Linassier C, Pierre M, Le Pecq JB, Pierre J. (1990). "Mechanisms of action in NIH-3T3 cells of genistein, an inhibitor of EGF receptor tyrosine kinase activity." *Biochemical pharmacology* 39:187-193.

Malbon CC. (2005). "G proteins in development." *Nat Rev Mol Cell Biol* 6:689-701.

Marrari Y, Crouthamel M, Irannejad R, Wedegaertner PB. (2007). "Assembly and trafficking of heterotrimeric G proteins." *Biochemistry* 46:7665-7677.

McDonald NA, Henstridge CM, Connolly CN, Irving AJ. (2007). "An essential role for constitutive endocytosis, but not activity, in the axonal targeting of the CB1 cannabinoid receptor." *Molecular pharmacology* 71:976-984.

Metzger R, Bader M, Ludwig T, Berberich C, Bunnemann B, Ganten D. (1995). "Expression of the mouse and rat mas proto-oncogene in the brain and peripheral tissues." *FEBS letters* 357:27-32.

Milasta S, Pediani J, Appelbe S, Trim S, Wyatt M, Cox P, Fidock M, Milligan G. (2006). "Interactions between the Mas-related receptors MrgD and MrgE alter signalling and trafficking of MrgD." *Molecular pharmacology* 69:479-491.

Milligan G. (1999). "Exploring the dynamics of regulation of G protein-coupled receptors using green fluorescent protein." *British journal of pharmacology* 128:501-510.

Mohammad S, Baldini G, Granell S, Narducci P, Martelli AM, Baldini G. (2007). "Constitutive traffic of melanocortin-4 receptor in Neuro2A cells and immortalized hypothalamic neurons." *The Journal of biological chemistry* 282:4963-4974.

Musi N, Goodyear LJ. (2006). "Insulin resistance and improvements in signal transduction." *Endocrine* 29:73-80.

Narumiya S. (1999). "[Cellular functions & pharmacological manipulations of the small GTPase Rho & Rho effectors]." *Nippon yakurigaku zasshi* 114 Suppl 1:1P-5P.

Narumiya S, Ishizaki T, Uehata M. (2000). "Use and properties of ROCK-specific inhibitor Y-27632." *Methods in enzymology* 325:273-284.

Noguchi T, Kasuga M. (2006). "[Insulin action and its regulatory mechanisms]." *Nippon rinsho* 64 Suppl 9:121-125.

Onrust R, Herzmark P, Chi P, Garcia PD, Lichtarge O, Kingsley C, Bourne HR. (1997). "Receptor and betagamma binding sites in the alpha subunit of the retinal G protein transducin." *Science (New York, NY)* 275:381-384.

Pizzi S, Porzionato A, Pasquali C, Guidolin D, Sperti C, Fogar P, Macchi V, De Caro R, Pedrazzoli S, Parenti A. (2009). "Glucose transporter-1 expression and prognostic significance in pancreatic carcinogenesis." *Histology and histopathology* 24:175-185.

Pollok BA, Heim R. (1999). "Using GFP in FRET-based applications." *Trends in cell biology* 9:57-60.

Prasher DC, Eckenrode VK, Ward WW, Prendergast FG, Cormier MJ. (1992). "Primary structure of the *Aequorea victoria* green-fluorescent protein." *Gene* 111:229-233.

Rabin M, Birnbaum D, Young D, Birchmeier C, Wigler M, Ruddle FH. (1987). "Human *ros1* and *mas1* oncogenes located in regions of chromosome 6 associated with tumor-specific rearrangements." *Oncogene research* 1:169-178.

Record RD, Froelich LL, Vlahos CJ, Blazer-Yost BL. (1998). "Phosphatidylinositol 3-kinase activation is required for insulin-stimulated sodium transport in A6 cells." *The American journal of physiology* 274:E611-617.

Rens-Domiano S, Hamm HE. (1995). "Structural and functional relationships of heterotrimeric G-proteins." *Faseb J* 9:1059-1066.

Riesewijk AM, Schepens MT, Mariman EM, Ropers HH, Kalscheuer VM. (1996). "The *MAS* proto-oncogene is not imprinted in humans." *Genomics* 35:380-382.

Roettger BF, Rentsch RU, Hadac EM, Hellen EH, Burghardt TP, Miller LJ. (1995). "Insulation of a G protein-coupled receptor on the plasmalemmal surface of the pancreatic acinar cell." *The Journal of cell biology* 130:579-590.

Saklatvala J, Rawlinson L, Waller RJ, Sarsfield S, Lee JC, Morton LF, Barnes MJ, Farndale RW. (1996). "Role for p38 mitogen-activated protein kinase in platelet aggregation caused by collagen or a thromboxane analogue." *The Journal of biological chemistry* 271:6586-6589.

Santos RA, Simoes e Silva AC, Maric C, Silva DM, Machado RP, de Buhr I, Heringer-Walther S, Pinheiro SV, Lopes MT, Bader M, Mendes EP, Lemos VS, Campagnole-Santos MJ, Schultheiss HP, Speth R, Walther T. (2003). "Angiotensin-(1-7) is an endogenous ligand for the G protein-coupled receptor Mas." *Proceedings of the National Academy of Sciences of the United States of America* 100:8258-8263.

Scarselli M, Donaldson JG. (2009). "Constitutive Internalization of G Protein-coupled Receptors and G Proteins via Clathrin-independent Endocytosis." *The Journal of biological chemistry* 284:3577-3585.

Schulein R, Lorenz D, Oksche A, Wiesner B, Hermosilla R, Ebert J, Rosenthal W. (1998). "Polarized cell surface expression of the green fluorescent protein-tagged vasopressin V2 receptor in Madin Darby canine kidney cells." *FEBS letters* 441:170-176.

Shaner NC, Patterson GH, Davidson MW. (2007). "Advances in fluorescent protein technology." *Journal of cell science* 120:4247-4260.

Slack JK, Catling AD, Eblen ST, Weber MJ, Parsons JT. (1999). "c-Raf-mediated inhibition of epidermal growth factor-stimulated cell migration." *The Journal of biological chemistry* 274:27177-27184.

Sorkin A, Von Zastrow M. (2002). "Signal transduction and endocytosis: close encounters of many kinds." *Nat Rev Mol Cell Biol* 3:600-614.

Sprang SR. (1997). "G protein mechanisms: insights from structural analysis." Annual review of biochemistry 66:639-678.

Sward K, Dreja K, Susnjar M, Hellstrand P, Hartshorne DJ, Walsh MP. (2000). "Inhibition of Rho-associated kinase blocks agonist-induced Ca²⁺ sensitization of myosin phosphorylation and force in guinea-pig ileum." The Journal of physiology 522 Pt 1:33-49.

Tallant EA, Ferrario CM, Gallagher PE. (2005). "Angiotensin-(1-7) inhibits growth of cardiac myocytes through activation of the mas receptor." American journal of physiology 289:H1560-1566.

Tang X, Varella-Garcia M, Xavier AC, Massarelli E, Ozburn N, Moran C, Wistuba, II. (2008). "Epidermal growth factor receptor abnormalities in the pathogenesis and progression of lung adenocarcinomas." Cancer prevention research (Philadelphia, Pa 1:192-200.

Tanti JF, Cormont M, Gremeaux T, Le Marchand-Brustel Y. (2001). "Assays of glucose entry, glucose transporter amount, and translocation." Methods in molecular biology (Clifton, NJ 155:157-165.

Tarasova NI, Stauber RH, Choi JK, Hudson EA, Czerwinski G, Miller JL, Pavlakis GN, Michejda CJ, Wank SA. (1997). "Visualization of G protein-coupled receptor trafficking

with the aid of the green fluorescent protein. Endocytosis and recycling of cholecystokinin receptor type A." *The Journal of biological chemistry* 272:14817-14824.

Tsao P, Cao T, von Zastrow M. (2001). "Role of endocytosis in mediating downregulation of G-protein-coupled receptors." *Trends in pharmacological sciences* 22:91-96.

van 't Veer LJ, van den Berg-Bakker LA, Hermens RP, Deprez RL, Schrier PI. (1988). "High frequency of mas oncogene activation detected in the NIH3T3 tumorigenicity assay." *Oncogene research* 3:247-254.

Venter JC, Adams MD, Myers EW, Li PW, Mural RJ, Sutton GG, Smith HO, Yandell M, Evans CA, Holt RA, Gocayne JD, Amanatides P, Ballew RM, Huson DH, Wortman JR, Zhang Q, Kodira CD, Zheng XH, Chen L, Skupski M, Subramanian G, Thomas PD, Zhang J, Gabor Miklos GL, Nelson C, Broder S, Clark AG, Nadeau J, McKusick VA, Zinder N, Levine AJ, Roberts RJ, Simon M, Slayman C, Hunkapiller M, Bolanos R, Delcher A, Dew I, Fasulo D, Flanigan M, Florea L, Halpern A, Hannenhalli S, Kravitz S, Levy S, Mobarry C, Reinert K, Remington K, Abu-Threideh J, Beasley E, Biddick K, Bonazzi V, Brandon R, Cargill M, Chandramouliswaran I, Charlab R, Chaturvedi K, Deng Z, Di Francesco V, Dunn P, Eilbeck K, Evangelista C, Gabrielian AE, Gan W, Ge W, Gong F, Gu Z, Guan P, Heiman TJ, Higgins ME, Ji RR, Ke Z, Ketchum KA, Lai Z, Lei Y, Li Z, Li J, Liang Y, Lin X, Lu F, Merkulov GV, Milshina N, Moore HM, Naik AK, Narayan VA, Neelam B, Nusskern D, Rusch DB, Salzberg S, Shao W, Shue B, Sun J,

Wang Z, Wang A, Wang X, Wang J, Wei M, Wides R, Xiao C, Yan C, Yao A, Ye J, Zhan M, Zhang W, Zhang H, Zhao Q, Zheng L, Zhong F, Zhong W, Zhu S, Zhao S, Gilbert D, Baumhueter S, Spier G, Carter C, Cravchik A, Woodage T, Ali F, An H, Awe A, Baldwin D, Baden H, Barnstead M, Barrow I, Beeson K, Busam D, Carver A, Center A, Cheng ML, Curry L, Danaher S, Davenport L, Desilets R, Dietz S, Dodson K, Doup L, Ferriera S, Garg N, Gluecksmann A, Hart B, Haynes J, Haynes C, Heiner C, Hladun S, Hostin D, Houck J, Howland T, Ibegwam C, Johnson J, Kalush F, Kline L, Koduru S, Love A, Mann F, May D, McCawley S, McIntosh T, McMullen I, Moy M, Moy L, Murphy B, Nelson K, Pfannkoch C, Pratts E, Puri V, Qureshi H, Reardon M, Rodriguez R, Rogers YH, Romblad D, Ruhfel B, Scott R, Sitter C, Smallwood M, Stewart E, Strong R, Suh E, Thomas R, Tint NN, Tse S, Vech C, Wang G, Wetter J, Williams S, Williams M, Windsor S, Winn-Deen E, Wolfe K, Zaveri J, Zaveri K, Abril JF, Guigo R, Campbell MJ, Sjolander KV, Karlak B, Kejariwal A, Mi H, Lazareva B, Hatton T, Narechania A, Diemer K, Muruganujan A, Guo N, Sato S, Bafna V, Istrail S, Lippert R, Schwartz R, Walenz B, Yooseph S, Allen D, Basu A, Baxendale J, Blick L, Caminha M, Carnes-Stine J, Caulk P, Chiang YH, Coyne M, Dahlke C, Mays A, Dombroski M, Donnelly M, Ely D, Esparham S, Fosler C, Gire H, Glanowski S, Glasser K, Glodek A, Gorokhov M, Graham K, Gropman B, Harris M, Heil J, Henderson S, Hoover J, Jennings D, Jordan C, Jordan J, Kasha J, Kagan L, Kraft C, Levitsky A, Lewis M, Liu X, Lopez J, Ma D, Majoros W, McDaniel J, Murphy S, Newman M, Nguyen T, Nguyen N, Nodell M, Pan S, Peck J, Peterson M, Rowe W, Sanders R, Scott J, Simpson M, Smith T, Sprague A, Stockwell T, Turner R, Venter E, Wang M, Wen M, Wu D, Wu M, Xia A, Zandieh A, Zhu X. (2001). "The sequence of the human genome." *Science* (New York, NY 291:1304-1351).

Vlahos CJ, Matter WF, Hui KY, Brown RF. (1994). "A specific inhibitor of phosphatidylinositol 3-kinase, 2-(4-morpholinyl)-8-phenyl-4H-1-benzopyran-4-one (LY294002)." *The Journal of biological chemistry* 269:5241-5248.

Von Bohlen und Halbach O, Walther T, Bader M, Albrecht D. (2000). "Interaction between Mas and the angiotensin AT1 receptor in the amygdala." *Journal of neurophysiology* 83:2012-2021.

Wall MA, Coleman DE, Lee E, Iniguez-Lluhi JA, Posner BA, Gilman AG, Sprang SR. (1995). "The structure of the G protein heterotrimer Gi alpha 1 beta 1 gamma 2." *Cell* 83:1047-1058.

Walther T, Wessel N, Kang N, Sander A, Tschöpe C, Malberg H, Bader M, Voss A. (2000). "Altered heart rate and blood pressure variability in mice lacking the Mas protooncogene." *Brazilian journal of medical and biological research = Revista brasileira de pesquisas medicas e biologicas / Sociedade Brasileira de Biofisica* [et al 33:1-9.

Werry TD, Wilkinson GF, Willars GB. (2003). "Mechanisms of cross-talk between G-protein-coupled receptors resulting in enhanced release of intracellular Ca²⁺." *The Biochemical journal* 374:281-296.

White MF. (2006). "Regulating insulin signaling and beta-cell function through IRS proteins." *Canadian journal of physiology and pharmacology* 84:725-737.

Winzell MS, Ahren B. (2007). "G-protein-coupled receptors and islet function-implications for treatment of type 2 diabetes." *Pharmacology & therapeutics* 116:437-448.

Wood TF, Dalili S, Simpson CD, Hurren R, Mao X, Saiz FS, Gronda M, Eberhard Y, Minden MD, Bilan PJ, Klip A, Batey RA, Schimmer AD. (2008). "A novel inhibitor of glucose uptake sensitizes cells to FAS-induced cell death." *Molecular cancer therapeutics* 7:3546-3555.

Xiao Z, Zhang N, Murphy DB, Devreotes PN. (1997). "Dynamic distribution of chemoattractant receptors in living cells during chemotaxis and persistent stimulation." *The Journal of cell biology* 139:365-374.

Xu X, Quiambao AB, Roveri L, Pardue MT, Marx JL, Rohlich P, Peachey NS, Al-Ubaidi MR. (2000). "Degeneration of cone photoreceptors induced by expression of the Mas1 protooncogene." *Experimental neurology* 163:207-219.

Yang J, Holman GD. (1993). "Comparison of GLUT4 and GLUT1 subcellular trafficking in basal and insulin-stimulated 3T3-L1 cells." *The Journal of biological chemistry* 268:4600-4603.

Yoo O, Son JH, Lee DH. (2005). "4-acetoxyscirpentiol of *Paecilomyces tenuipes* inhibits Na(+)/D-glucose cotransporter expressed in *Xenopus laevis* oocytes." *Journal of biochemistry and molecular biology* 38:211-217.

Young D, Waitches G, Birchmeier C, Fasano O, Wigler M. (1986). "Isolation and characterization of a new cellular oncogene encoding a protein with multiple potential transmembrane domains." *Cell* 45:711-719.

Zaid H, Antonescu CN, Randhawa VK, Klip A. (2008). "Insulin action on glucose transporters through molecular switches, tracks and tethers." *The Biochemical journal* 413:201-215.

Zohn IE, Symons M, Chrzanowska-Wodnicka M, Westwick JK, Der CJ. (1998). "Mas oncogene signaling and transformation require the small GTP-binding protein Rac." *Molecular and cellular biology* 18:1225-1235.

Appendices

| | |
|-------------------|--|
| Appendix 1 | Composition of media |
| Appendix 2 | Composition of buffer solutions |
| Appendix 3 | Bacterial strains |
| Appendix 4 | Sequence of primers |
| Appendix 5 | Sequences of construct |
| Appendix 6 | Published abstracts |

Appendix 1 Composition of media

1. Luria-Bertani medium (LB medium)

| | |
|---------------|------|
| Tryptone | 10 g |
| Yeast Extract | 5 g |
| NaCl | 5 g |

All the components were dissolved in 900 ml pure nano water and the volume was added up to 1 liter and sterilized by autoclaving (121°C for 20 minutes, 15 lbs).

2. SOBAG plate

| | |
|---------------|-------|
| Tryptone | 20 g |
| Yeast Extract | 5 g |
| NaCl | 0.5 g |
| Bacto-agar | 15 g |

All the contents were dissolved in 900 ml pure nano water and were sterilized by autoclaving. After the medium was cooled down to about 50°C, 10 ml of sterilized 1M MgCl₂, 55.6 ml of 2 M filtered glucose and 1 ml of 100 mg/ml ampicillin were added. Each plate was poured with 10 ml of the above mixture.

3. 2 x YT medium

| | |
|---------------|------|
| Tryptone | 17 g |
| Yeast Extract | 10g |
| NaCl | 5g |

All the contents were dissolved in 900 ml pure nano water and were added up to 1 liter and sterilized by autoclaving (121°C for 20 minutes, 15 lbs).

4. IMDM full medium

17.7 g IMDM powder and 3.024 g NaHCO₃ powder were dissolved in 800 ml pure nano water. Until all the powders were dissolved, the volume was made up to 900 ml. The medium was sterilized by filtering with filter of 0.2 μM aperture. 50 ml FBS (qualified grade) and 5 ml P/S were added before use.

5. F-12 (Ham's) full medium

10.6 g F-12 powder and 1.176 g NaHCO₃ powder were dissolved in 800 ml pure nano water. Until all the powders were dissolved, pH was adjusted to around 7.2 using diluted HCl. Then the volume was made up to 900 ml. The medium was sterilized by filtering with filter of 0.2 μM aperture. 50 ml FBS (qualified grade) and 5 ml P/S were added before use.

Appendix 2 Composition of buffer solutions

1. 100 mg/ml of Ampicillin

100 mg of ampicillin was dissolved in 1 ml of pure nano water and stored at -20°C.

2. Binding buffer

1X PBS was prepared containing 0.1% SDS and 1% NP-40 in the final working solution.

3. 1X Blocking buffer

25 ml of 10X TBS was diluted into 1X TBS containing 0.05% Tween[®] 20 (Polyoxyethylene Sorbitan Monolaurate) and 5% non-fat milk. The final concentration of Tris-HCl and NaCl were 10 mM and 150 mM respectively.

4. Developing buffer

50 ml of 1 M Tris-HCl (pH 9.5), 10 ml of 5 M NaCl and 12.5 ml of 2 M MgCl₂ were added to 427.5 ml of pure nano water in a final working concentration of 100 mM Tris-HCl (pH 9.5), 100 mM NaCl and 50 mM MgCl₂.

5. 0.5 M EDTA

93.06 g di-sodium ethylene diaminetetraacetate-2H₂O (Na₂EDTA-2H₂O) was dissolved in 400 ml of pure nano water. After all the powders were dissolved, pH was adjusted to 8.0 with 10 M sodium hydroxide (NaOH). The total volume was added up to 500 ml and was sterilized by autoclaving (121°C for 20 minutes, 15 lbs).

6. 20% Glucose

20 g D-(+)-Glucose was dissolved in 90 ml pure nano water. Until all the powders were dissolved, the volume was added up to 100 ml and was sterilized by filtering with a filter of 0.2 μ M aperture.

7. Hot/Cold mixture

Certain amount of 2-deoxy-D-glucose was dissolved in KRP buffer in a stock concentration of 5 mM and was stored at 4°C. The stock concentration of 2-deoxy-D-[1-³H]-glucose was 1 μ Ci/ μ l. The final working concentration of hot/cold mixture was diluted from stock solution into 0.35 mM 2-deoxy-D-glucose/3.5 μ Ci/ml 2-deoxy-D-[1-³H]-glucose with KRP buffer just before use.

8. 1X Immunoblotting buffer

25 ml of 10X TBS was diluted into 1X TBS containing 0.05% Tween[®] 20. The final concentration of Tris-HCl and NaCl were 10 mM and 150 mM respectively.

9. 50 mg/ml Kanamycin

100 mg of kanamycin was dissolved in 2 ml of pure nano water and stored at -20°C.

10. KRP buffer

7.5972 g of NaCl, 0.37275 g of KCl and 0.1911 g of CaCl₂·2H₂O were dissolved in 500 ml of pure nano water. 0.3204 g of MgSO₄·7H₂O and 1.42 g of Na₂HPO₄ were dissolved in another 400 ml of pure nano water. Until all the powders were dissolved completely,

solution containing MgSO_4 and Na_2HPO_4 was poured slowly into the solution containing NaCl , KCl and CaCl_2 . The mixing process should be very slowly to prevent precipitants of CaSO_4 and the pH was maintained around 7.4 using 6 M HCl . Finally the total volume was made up to 1 liter. The KRP buffer was filtered to sterilize and stored at 4°C before use.

11. 5M NaCl

292.2 g sodium chloride was dissolved in 900 ml of pure nano water. The volume was made up to 1 liter and was sterilized by autoclaving.

12. 10X PBS

32 g of NaCl , 0.8 g of KCl , 5.76 g of Na_2HPO_4 and 0.96 of KH_2PO_4 was dissolved in 400 ml of pure nano water and sterilized by autoclaving (121°C for 20 minutes, 15 lbs). 1 X PBS was prepared by diluted 50 ml of 10 X PBS in 450 ml of pure nano water.

13. 1X PBS (pH 8.0)

1 X PBS was prepared by as mentioned above and pH was adjusted to 8.0 by adding 1M NaOH .

14. 1X PBS +100 mM glycine (pH 8.0)

500 ml of 1 X PBS was prepared by as mentioned above and 3.7535 g of glycine was dissolved in it. pH was adjusted to 8.0 by adding 1 M NaOH .

15. 0.3 mM Phloretin

Certain amount of phloretin was weighted and stored at 4°C. Just before use, it was dissolved in 100% of pure ethanol in a stock concentration of 100 mM and was subsequently diluted into 0.3 mM using 1X PBS. Phloretin was light-sensitive and should be kept from light by wrapping the bottle with aluminin foil.

16. 10X Reservoir buffer

288 g of glycine and 60.6 g of Tris were dissolved in 2 liters of pure nano water and stored at room temperature.

17. 1X Running buffer

100 ml of 10X Reservoir buffer was diluted in 895 ml of pure nano water and 5 ml of 20% SDS was added. The total volume was 1 liter and working concentration was 25 mM Tris, 192 mM glycine and 0.1% SDS, pH 8.3.

18. 20% SDS

100 g of sodiumdodecyl sulfate crystals (SDS) was dissolved in 400 ml of pure nano water and the total volume was added up to 500 ml.

19. 3 M sodium acetate, pH 5.2

40.824 g of sodium acetate-3H₂O (NaOAc-3H₂O) was dissolved in 80 ml of pure nano water. Until all the powders were dissolved, pH was adjusted to 5.2 and total volume was added up to 100 ml.

20. 50X TAE buffer

242 g of Tris base and 57.1 ml of glacial acetic acid and 100 ml 0.5 M EDTA (pH 8.0) was dissolved in 900 ml of pure nano water and total volume was made up to 1 liter. When used, 20 ml of 50X TAE was diluted into 980 ml of pure nano water to form a working concentration of 40 mM Tris-acetate and 1 mM EDTA.

21. 10X TBS

100 ml of Tris-HCl (pH 7.5) and 300 ml of 5 M NaCl were mixed with 600 ml of pure nano water. The final concentration of Tris-HCl and NaCl were 0.1 M and 1.5 M respectively.

22. 1X Transferring buffer

100 ml of 10X Reservoir buffer and 100 ml of pure methanol were mixed up with 800 ml of pure nano water to form a working concentration of 25 mM Tris, 192 mM glycine and 10% of methanol.

Appendix 3 Bacterial Strain

DH5 α : F- ϕ 80dlacZ Δ M15 Δ (*lacZYA-argF*) U169 *deoR*, *recA1* *endA1* *hsdR17* (*rk-* *mk+* *pho-A*, *supE44* λ - *thi-1* *gyrA96* *relA1*)

TG1: K12 Δ (*lac-pro*), *supE*, *thi*, *hsd* Δ 5/F'[*traD36*, *proAB*, *lac^f*, *lacZ* Δ M15]

Appendix 4 Sequences of primers

Rmas-EcoR I-F5

5' CCG GAA TTC ATG GAC CAA TCA AAT ATG AC 3'

Rmas-Kpn I-oligo-R1034

5' AGA ACC GCT GCC TGA ACC GCC TCC ACC ACT CGG TAC CCC TCC TCC
GAC CA 3'

oligo-EGFP-F1033

5' TCA GGC AGC GGT TCT AGC GGC GGT GGC GGA CCG GTC GCC ACC ATG
GTG AG 3'

Xba I-Not I-EGFP-R1037

5' TGA TCT AGA GTC GCG GCC GCT TTA CTT GTA 3'

Appendix 5 Sequences of constructs

>mas-oligo-GFP encoding mas-(Gly₁₀Ser₅)-GFP

atggaccaatcaaatatgacatcctttgctgaggagaaagccatgaatacctccagcaga
M D Q S N M T S F A E E K A M N T S S R
aatgcctccctggggacttcacaccacccattcccatagtgactgggtcatcatgagc
N A S L G T S H P P I P I V H W V I M S
atctctcctctcggctttgtgggagaacgggatcctcctctgggtcctttgcttccggatg
I S P L G F V E N G I L L W F L C F R M
aggagaaatcccttcacgggtctatatcaccacttgtccattgctgacatctccctcctg
R R N P F T V Y I T H L S I A D I S L L
ttctgtatTTTTattctgtccatcgactatgcttttagactatgaactctcttctggccat
F C I F I L S I D Y A L D Y E L S S G H
tactacacaatcgtgacggttatcgggtgacttttctatttggtacaacacaggcctctat
Y Y T I V T L S V T F L F G Y N T G L Y
ctgctgacagccatcagtgtggagagatgcctttcggtcctctaccccatctggtacaga
L L T A I S V E R C L S V L Y P I W Y R
tgtcaccgccccaaagcaccagtcggcattcgtctgtgccctcctgtgggcactttcatgc
C H R P K H Q S A F V C A L L W A L S C
ttggtgaccaccatggagtagtcatgtgtattgacagcggagaagagagtcactctcag
L V T T M E Y V M C I D S G E E S H S Q
agtgactgtcgggcggtcatcatcttcatagccatcctcagcttcttgggtcttcaactcgg
S D C R A V I I F I A I L S F L V F T P
ctcatgttagtgtccagcaccatcttgggtggggaagatacggagaacacatgggcctcc
L M L V S S T I L V V K I R K N T W A S

cattcttcgaagctgtacatcgatcatcatggtcaccattatcatattcctcatcttcgcc
H S S K L Y I V I M V T I I I F L I F A
atgcccatgcgggtcctctacctgttattacgagtactggccaacctttgggaacctg
M P M R V L Y L L Y Y E Y W S T F G N L
cataacatctccttgcttttctccaccatcaatagcagcgccaacctttcatctacttt
H N I S L L F S T I N S S A N P F I Y F
tttgtgggcagcagtaagaagaagcgcttcagggagtccttaaaagtggcctgaccaga
F V G S S K K K R F R E S L K V V L T R
gctttcaaagacgagatgcaacctagggcgccaggagggaatggcaacactgtatccatt
A F K D E M Q P R R Q E G N G N T V S I
gagactgtggtcggaggaggggtaccgagtggtggaggcggttcaggcagcggttctagc
E T V V G G G V P S G G G G S G S G S S
ggcgggtggcggaccggtcgccaccatggtgagcaagggcgaggagctgttcaccggggtg
G G G G P V A T M V S K G E E L F T G V
gtgcccatcctggtcgagctggacggcgacgtaaacggccacaagttcagcgtgtccggc
V P I L V E L D G D V N G H K F S V S G
gagggcgagggcgatgccacctacggcaagctgacctgaagttcatctgcaccaccggc
E G E G D A T Y G K L T L K F I C T T G
aagctgcccgtgccctggcccaccctcgtagccacctgacctacggcgtgcagtgcttc
K L P V P W P T L V T T L T Y G V Q C F
agccgctaccccgaccacatgaagcagcagacttcttcaagtccgccatgcccgaaggc
S R Y P D H M K Q H D F F K S A M P E G
tacgtccaggagcgcaccatcttcttcaaggacgacggcaactacaagaccgcgcccag
Y V Q E R T I F F K D D G N Y K T R A E
gtgaagttcgagggcgacaccctgggtgaaccgcatcgagctgaagggcatcgacttcaag

V K F E G D T L V N R I E L K G I D F K
gaggacggcaacatcctggggcacaagctggagtacaactacaacagccacaacgtctat
E D G N I L G H K L E Y N Y N S H N V Y
atcatggccgacaagcagaagaacggcatcaaggtgaacttcaagatccgccacaacatc
I M A D K Q K N G I K V N F K I R H N I
gaggacggcagcgtgcagctcgccgaccactaccagcagaacacccccatcggcgacggc
E D G S V Q L A D H Y Q Q N T P I G D G
cccgtgctgctgcccgacaaccactacctgagcaccagtcgcacctgagcaaagacccc
P V L L P D N H Y L S T Q S A L S K D P
aacgagaagcgcgatcacatgggtcctgctggagttcgtgaccgccgccgggatcactctg
N E K R D H M V L L E F V T A A G I T L
gaaatggacatggacgagctgtacaagtaa
E M D M D E L Y K -

Appendix 6 Published abstract

Receptor activity of GPCR mas is suppressed by C-terminal GFP tagging

J.X. Sun¹, S.S.T. Lee¹, W.H. Ko², W.T. Cheung¹

¹*Department of Biochemistry, ²Department of Physiology, The Chinese University of Hong Kong, Shatin, New Territories, Hong Kong, China.*

Orphan G protein-coupled receptor (GPCR) mas was initially isolated from a human epidermal carcinoma. Previous study from our lab has identified a surrogate ligand MBP7 (mas binding peptide 7) for mas, and indicated GFP tagging may affect the receptor activity of mas [Bikkavilli RK, et. al. (2006) *Biochem Pharmacol.* 71(3): 319-337]. To further functionally characterize receptor activity of mas, we established three stable CHO cell lines expressing native mas, mas-GFP and mas-(Gly₁₀Ser₅)-GFP. Phages expressing a surrogate peptide ligand for mas displayed punctate binding and were internalized in all the three cell lines expressing native mas and GFP-tagged variants. However, number of phages being internalized in cells expressing mas-GFP was substantially less than that of cells expressing mas-(Gly₁₀Ser₅)-GFP and native mas. In parallel, biotinylation experiment quantitatively showed that the extent of mas-(Gly₁₀Ser₅)-GFP internalization was higher than that of mas-GFP. Consistent with internalization assay, calcium mobilization stimulated by MBP7 was also different in cell lines expressing native mas and GFP tagged variants. In cells expressing native mas, MBP7 induced a rapid increase of calcium and then the cellular calcium level returned to a basal level within five minutes. Instead, a sustained high level of intracellular calcium was observed in cells expressing mas-(Gly₁₀Ser₅)-GFP. By contrast, only a transient and delayed rising of intracellular calcium

level was detected in cells expressing mas-GFP. These results suggested that C-terminal GFP-tagging reduced the receptor activity of mas.

Poster presented at

2008 AACR Annual Meeting in San Diego, CA, USA

April 12-16, 2008